

LSE AND MSE OPTIMUM DECONVOLUTION

A THESIS SUBMITTED TO
THE GRADUATE SCHOOL OF NATURAL AND APPLIED SCIENCES
OF
MIDDLE EAST TECHNICAL UNIVERSITY

BY

METİN AKTAŞ

IN PARTIAL FULFILLMENT OF THE REQUIREMENTS FOR THE DEGREE OF
MASTER OF SCIENCE
IN
ELECTRICAL AND ELECTRONICS ENGINEERING

JULY 2004

Approval of the Graduate School of Natural and Applied Sciences

Prof. Dr. Canan Özgen
Director

I certify that this thesis satisfies all the requirements as a thesis for the degree of Master of Science.

Prof. Dr. Mübeccel Demirekler
Head of Department

This is to certify that we have read this thesis and that in our opinion it is fully adequate, in scope and quality, as a thesis for the degree of Master of Science.

Assoc. Prof. Dr. T. Engin Tuncer
Supervisor

Examining Committee Members

Prof. Dr. Buyurman Baykal	METU	_____
Assoc. Prof. Dr. T. Engin Tuncer	METU	_____
Assoc. Prof. Dr. Tolga Çiloğlu	METU	_____
Assoc. Prof. Dr. Aydın Alatan	METU	_____
Asst. Prof Dr.Yakup Özkazañ	Hacettepe Uni.	_____

I hereby declare that all information in this document has been obtained and presented in accordance with academic rules and ethical conduct. I also declare that, as required by these rules and conduct, I have fully cited and referenced all material and results that are not original to this work.

Name, Last name : Metin Aktaş

Signature :

ABSTRACT

LSE AND MSE OPTIMUM DECONVOLUTION

Aktaş, Metin

MSc., Department of Electrical and Electronics Engineering

Supervisor: Assoc. Prof. Dr. T.Engin Tuncer

July 2004, 84 pages

In this thesis, we considered the deconvolution problem when the channel is known a priori. LSE and MSE optimum solutions are investigated with deterministic and statistical approaches. We derived closed form LSE expressions and investigated the factors that affect the FIR inverse filters. It turns out that, minimum LSE can be obtained when the system zeros are distributed homogeneously on the z-plane. We proposed partition-based FIR-IIR inverse filters. The selection of FIR and IIR parts is based on partitioning the channel zeros into two regions and using the specified channel zeros to design the best delay FIR and all pole IIR inverse filters. Three methods for partitioning are presented, namely unit circle-based, ring-based and optimum-partitioning. It turns out that ring-based and optimum-partitioning FIR-IIR inverse filter performs better than the best delay FIR inverse filter for the same complexity by about 4-5 dB. For noisy observations, it is shown that, noise should also be considered in the delay selection and partitioning. We extended our results for the design of MSE optimum statistical inverse filters. It is shown that best delay FIR-IIR inverse filters are less sensitive to the estimation errors compared to the IIR Wiener filters and they perform better than the FIR Wiener filters. Furthermore, they are always causal and stable making them suitable for real-time implementations. When the statistical and deterministic filters are compared, it is shown that for low SNR statistical filters perform better by about 1-2 dB, while deterministic filters perform better by about 0.5-1 dB for high SNR.

Keywords: Deconvolution, inverse filter, FIR, IIR

ÖZ

LSE VE MSE ENİYİ TERS EVRİŞİM

Aktaş, Metin

Yüksek Lisans, Elektrik ve Elektronik Mühendisliği Bölümü

Tez Yöneticisi: Doç. Dr. T.Engin Tuncer

Temmuz 2004, 84 sayfa

Bu tezde, kanalın önceden bilindiği durumlarda ters evrişim problemini inceledik. Gerekirci ve istatistiksel yaklaşımlarla LSE ve MSE eniyi çözümler incelenmiştir. Kapalı formda LSE ifadelerini çıkarttık ve FIR ters süzgezi etkileyen etmenleri inceledik. En küçük LSE'nin sistem sıfırları z-düzleminde tektürel olarak dağıldığında elde edilebildiği görülmüştür. Bölüntüleme tabanlı FIR-IIR ters süzgeçleri önerdik. FIR ve IIR parçalarının seçimi kanal sıfırlarının iki bölgeye parçalanması ve bu kanal sıfırlarının eniyi gecikmeli FIR ve tüm kutuplu IIR ters süzgeçlerin tasarlanması için kullanılması temeline dayanmaktadır. Bölüntüleri elde etmek için üç yöntem sunulmuştur, bunlar birim çember tabanlı, halka tabanlı ve eniyi bölüntülemedir. Halka tabanlı ve eniyi bölüntülemeli FIR-IIR ters süzgeçlerin, aynı karmaşıklığıdaki eniyi gecikmeli FIR ters süzgece göre yaklaşık 4-5 dB daha iyi başarımlar sergilediği ortaya çıkmıştır. Gürültülü gözlemler için gürültünün de gecikme seçiminde ve parçalamada hesaba katılması gerektiği gösterilmiştir. Bu sonuçları istatistiksel eniyi MSE ters süzgeç tasarımları için genişlettik. Eniyi gecikmeli FIR-IIR ters süzgeçlerin, kestirim hatalarına IIR Wiener süzgeçlerden daha az hassas oldukları ve FIR Wiener süzgeçten daha iyi başarımlar sergiledikleri gösterilmiştir. Ayrıca bu süzgeçlerin her zaman nedensel ve kararlı olmaları, onları gerçek zamanlı uygulamalar için uygun kılmaktadır. İstatistiksel ve gerekirci süzgeçler karşılaştırıldığında, düşük sinyal gürültü oranında istatistiksel süzgeçler yaklaşık 1-2 dB daha iyi başarımlar sergilerken gerekirci süzgeçlerin yüksek sinyal gürültü oranında yaklaşık 0.5-1 dB daha iyi başarımlar sergilediği gösterilmiştir.

Anahtar Kelimeler: Ters evrişim, ters süzgeç, FIR, IIR

ACKNOWLEDGEMENTS

I would like to thank Assoc. Prof. Dr. T. Engin Tuncer, for his help, professional advice and valuable supervision during the development of this thesis. This thesis would not be completed without his guidance and support.

Thanks to TÜBİTAK BAYG (Bilim Adamı Yetiştirme Grubu) for their financial supports during this thesis.

Special thanks to my parents and my friend Hakan Y. Gürsan for their great encouragement and continuous moral support.

TABLE OF CONTENTS

ABSTRACT	iv
ÖZ	v
ACKNOWLEDGMENTS	vi
TABLE OF CONTENTS	vii
CHAPTER	
1. INTRODUCTION	1
2. INVERSE FILTERS FOR NOISELESS OBSERVATIONS	6
2.1 Best Delay FIR Inverse Filters	7
2.1.1 Factors that Affect the LSE of FIR Inverse Filters	11
2.2 IIR Inverse Filters	17
2.3 Partition-Based FIR-IIR Inverse Filters	19
2.3.1 Unit Circle-Based Partitioning	20
2.3.2 Ring-Based Partitioning	22
2.3.3 Optimum-Partitioning	26
3. INVERSE FILTERS FOR NOISY OBSERVATIONS	32
3.1 Noise Considered Deterministic Inverse Filters	32
3.1.1 Noise Considered Deterministic FIR Inverse Filters	33
3.2 MSE Optimum Statistical Inverse Filters	36
3.2.1 MSE Optimum Best Delay FIR Deconvolution Filters	37

3.2.2 Best Delay FIR-IIR Partition-Based Deconvolution Filters	39
3.2.3 IIR Wiener Filters	42
4. PERFORMANCE EVALUATIONS	44
4.1 Deterministic Inverse Filters	45
4.1.1 Noiseless Observations	45
4.1.2 Noisy Observations	49
4.2 Statistical Inverse Filters	54
4.3 Noise Considered Deterministic versus Statistical Inverse Filters	58
5. CONCLUSION	60
REFERENCES	63
APPENDICES	
A.	66
A.i Properties of B_N	66
A.ii Iterative Procedure	76
B.	82

LIST OF TABLES

Table

2.1 The effect of delay on LSE	8
2.2 The number of partitioning cases	27
3.1 Effect of delay on LSE and MSE	34

LIST OF FIGURES

Figure		
2.1	System structure of inverse filter design problem for noiseless observations	7
2.2	The effect of inverse filter length on LSE for first order channel	13
2.3	The effect of channel zero position on LSE for first order channel and $N=8$	14
2.4	Overall system zeros for FIR inverse filter with $N=32$ and channel with $L=8$ \square represents channel zero, o represents inverse filter zero	15
2.5	Zero positions of channel with $L=2$ for Example 2.1	16
2.6	LSE values for different distance between two channel zeros	17
2.7	Pole-zero plots for (a) FIR and (b) unit circle-based FIR-IIR inverse filters when $L=8$, $N=16$. o , \square and x represent inverse filter zero, channel zero and IIR pole respectively	22
2.8	Inner and outer radiuses and ring region inside the unit circle for ring-based partitioning	23
2.9	Pole-zero plots for (a) FIR and (b) ring-based FIR-IIR inverse filters when $L=8$, $N=16$. o , \square and x represent inverse filter zero, channel zero and IIR pole respectively	24
2.10	Zero plots of the channel and FIR inverse filter for $L=8$ and $N=16$. o and \square represent inverse filter zero and channel zero respectively	25
2.11	Zero plots of the selected channel zeros for (a) the ring-base (outer radius is one) and (b) optimum-partitioning case when $L=12$, $N=16$. o , \square and x represent inverse filter zero, channel zero and IIR pole respectively	28
2.12	LSE performance of the deconvolution filters for different inverse filter lengths, (a) $L=4$, (b) $L=8$, (c) $L=12$, (d) $L=16$	30

2.13	Inner and outer ring radiuses for the LSE case, (a) $L=4$, (b) $L=8$, (c) $L=12$, (d) $L=16$	31
3.1	System structure of inverse filter design problem for noisy observations	33
3.2	The pole-zero plots of FIR-IIR inverse filter. (a) ring-based for SNR=0 dB, (b) ring-based for SNR=20 dB, (c) optimum-partitioning for SNR=0 dB, (d) optimum-partitioning for SNR=20 dB. o represents channel zero and x represents pole of inverse filter	35
4.1	LSE performance of best and $(N+L)/2$ delay FIR inverse filters when $L=8$ (a) Uniform distributed complex channel, (b) Uniform distributed real channel, (c) Gaussian distributed complex channel, (d) Gaussian distributed real channel	46
4.2	LSE performances of the inverse filters for different channel types, (a) uniform distributed real, (b) Gaussian distributed real, (c) uniform distributed complex, (d) Gaussian distributed complex channel	48
4.3	Inner and outer ring radiuses of ring-based FIR-IIR inverse filter for different channel types, (a) uniform distributed real, (b) Gaussian distributed real, (c) uniform distributed complex, (d) Gaussian distributed complex channel	49
4.4	MSE performance of best and arbitrary delay FIR inverse filters designed with deterministic approach when $L=8$ and $N=32$. (a) Gaussian distributed complex channel, (b) Gaussian distributed real channel, (c) Uniform distributed complex channel, (d) Uniform distributed real channel	51
4.5	MSE performances of LSE optimum deterministic inverse filters when $N=24$, (a) $L=8$, (b) $L=12$	53
4.6	MSE performances of noise considered deterministic inverse filters when $N=24$, (a) $L=8$, (b) $L=12$	53
4.7	Inner and outer radiuses of ring-based FIR-IIR inverse filter for LSE optimum deterministic method when $N=24$, (a) $L=8$, (b) $L=12$	54
4.8	Inner and outer radiuses of ring-based FIR-IIR inverse filter for noise considered deterministic method when $N=24$, (a) $L=8$, (b) $L=12$	54
4.9	MSE performance of best and arbitrary delay FIR inverse filters designed with statistical approach when $L=8$ and $N=32$. (a) Gaussian distributed complex channel, (b) Gaussian distributed real channel, (c) Uniform distributed complex channel, (d) Uniform distributed real channel	56
4.10	MSE performances of inverse filters for statistical method when the correlation estimates are used. $N=24$, (a) $L=8$, (b) $L=12$	57

4.11	Inner and outer radiuses of ring-based FIR-IIR inverse filter for statistical method when the correlation estimates are used. $N=24$, (a) $L=8$, (b) $L=12$	57
4.12	MSE performances of inverse filters for statistical method when true correlations are used. $N=24$, (a) $L=8$, (b) $L=12$	58
4.13	Inner and outer radiuses of ring-based FIR-IIR inverse filter for statistical method when the true correlations are used. $N=24$, (a) $L=8$, (b) $L=12$...	58
4.14	MSE performances of FIR, FIR-IIR optimum-partitioning inverse filters for statistical and deterministic methods when $N=24$, (a) $L=8$, (b) $L=12$	59

CHAPTER 1

INTRODUCTION

Telecommunication is based on transmitting information between two points, namely the source and the receiver. In modern communication systems, information is carried by many types of signals in the form of electrical, electromagnetic, acoustic or so on. During the transmission, these signals travel in a medium such as cable, air, water, ground, etc. These mediums are commonly called as channel and can be modeled as a linear filter. The channel can be expressed in frequency domain as,

$$H(f) = |H(f)|e^{j\theta(f)}$$

where $|H(f)|$ is the amplitude response characteristic and $\theta(f)$ is the phase response characteristic. A channel is said to be nondistorting or ideal if the amplitude response $|H(f)|$ is constant for all frequencies and $\theta(f)$ is a linear function of frequency. On the other hand, if $|H(f)|$ is not constant for all frequencies, we say that the channel distorts the transmitted signal in amplitude and if $\theta(f)$ is not a linear function of frequency, we say that the channel distorts the signal in phase.

The signal is not only distorted by the channel, but it is also contaminated along the path by undesirable signals lumped under the broad term noise which are unpredictable signals. In communication systems, the noise is tried to be modeled as random variables. Depending on spectral characteristics, noise can be classified as white or colored noise. The noise power for all frequencies is assumed to be constant for the white noise. On the other hand for the colored noise, the noise power concentrates on some frequency range. The choice of which noise model to use depends on application. In this thesis we will use the white noise model.

All of these undesired distortions should be minimized or eliminated, if possible, to reconstruct the original source signal in the receiver. Inverse filters are used in the receiver part to achieve this goal. In this respect, inverse filtering is closely related to the deconvolution and equalization problems. Deconvolution is the process of finding either the input sequence or channel characteristics when the output sequence and either one of the channel characteristics or input sequence are given. On the other hand, input sequence is found from the output in equalization problem. Both deconvolution and equalization problems can be analyzed for noisy and noiseless observations. In addition, deterministic and statistical problem settings can be investigated. Deconvolution problem is investigated in time [1], frequency [2] and wavelet domains [3, 4]. These types of problems find applications in communications, radar and sonar systems, astrophysics, seismology and so on.

Inverse filter design for deconvolution problem has been widely investigated. At first glance, the solution to the deconvolution problem seems to be straightforward. For a given channel filter, $H(z)$, find an inverse filter $1/H(z)$. It turns out that the solution is not so simple because for an arbitrary $H(z)$, $1/H(z)$ may not be causal and stable. Therefore $1/H(z)$ is mostly suitable for minimum-phase systems. Furthermore direct inversion is not recommended when the channel has spectral nulls. This situation is equivalent to stating that the inversion problem is ill-posed. That is, the inverse filter is asked to reproduce components of the channel input that are unobservable at the channel output or are obscured by noise. This leads to noise amplification.

Generalized inverse or Pseudoinverse solution [5, 6] is commonly used instead of direct inversion for an arbitrary channel. The pseudoinverse solution is the result of an optimization operation that seeks to minimize the least squares error [7, 8]. Any spectral loss in the signal caused by the channel is directly translated into a corresponding decrease in the minimum eigenvalue, λ_{\min} , of the received signal. If λ_{\min} becomes small, but nonzero, pseudoinverse solution becomes ill-conditioned and inversion leads to noise enhancement at the receiver output and to noise sensitivity in the filter coefficient solution. An alternative to the pseudoinverse is to use regularized or smoothing inverse techniques [5, 9, 10, 11, 12] wherein the eigenmodes are weighted prior to inversion. These methods attempt to force smoothness

on the solution of a least squares error problem and lead to a tradeoff between the noise immunity of the inverse filter weights and the signal fidelity at the inverse filter output.

The optimum solution for deconvolution problem is the IIR Wiener filter [5, 8, 13]. Wiener filtering combines inverse filtering with a priori statistical knowledge about the noise and the input signal [14]. “The Wiener filters attempt to minimize the noise amplification obtained in a direct inverse by providing a taper determined by the statistics of the signal and noise process under consideration [5].” In practice, the power spectra of the noise and desired signal might not be known. In this condition spectral estimation techniques [15] are used, but these filters are sensitive to the estimation errors [16]. Furthermore, the main drawback of IIR Wiener filter is that, it is either noncasual or unstable and therefore it is not very suitable for real time sample based processing. Using FIR Wiener filter [13] or extracting the casual part of the IIR Wiener filter [17] overcomes these problems with higher mean square error (MSE).

Adaptive filters can also be used in inverse filtering problem. These filters start from some predetermined set of initial conditions and recursively update its coefficients, unlike the nonrecursive filters described above. The advantage of adaptive filters is “to perform satisfactorily in an environment where complete knowledge of the relevant signal characteristics is not available” [7]. On the other hand, it requires a convergence time to achieve the desired performance. Some of the adaptive algorithms are, least mean squares (LMS), recursive least squares (RLS) and block-iterative normalized LMS (BINLMS) [7, 14]. The choice of which adaptive algorithm to use is application-dependent and determined by considering the convergence time and stability of the filter.

In this thesis, we will investigate the nonrecursive deconvolution problem when the channel is known a priori. We will divide the problem into two parts. In the first part, we will investigate the deterministic problem where there is no noise in the observations. In the second part, we will look at a more general and practical problem where the observations are corrupted by noise. Deterministic and statistical solutions will be investigated for the noisy observations.

The deterministic setting of deconvolution for noiseless observations requires the design of least squares inverse filters [7, 8]. This problem is analyzed in detail and the design of such filters is well known [18]. It has been shown that the choice of system delay plays an important role for decreasing the least squares error (LSE) [8, 17]. Therefore best delay LSE optimum FIR inverse filter is one of the most effective solutions for deconvolution operation. In this thesis, we will use an efficient approach for the design of best delay inverse filters proposed in [19]. The closed form LSE expressions for the FIR inverse filters will be derived and the factors that affect the LSE of FIR inverse filter will be investigated. Then IIR inverse filters will be discussed. IIR inverse filters are more powerful tools for deconvolution problem than the FIR inverse filters when the channel is minimum-phase. But for nonminimum-phase channels they suffer from the stability problem.

In this thesis, we will propose partition-based FIR-IIR inverse filters with best delay. In general, FIR-IIR inverse filters are hybrid filters with an FIR and all pole IIR part. IIR part is the inverse filter for the channel zeros which fall into a selected region inside the unit circle. FIR part corresponds to the best delay LSE optimum inverse filter of the channel zeros outside the selected region. These filters use the advantages of both IIR and FIR deconvolution filters and it turns out that they perform significantly better than purely FIR filters. We will investigate three approaches for the partitioning of channel zeros to construct FIR and IIR parts. The simplest one is unit circle-based partitioning in which, IIR part is constructed from the minimum-phase part of the channel filter and the FIR part correspond to the inverse filter of maximum-phase part. The second one is ring-based partitioning [26], which divides the z -plane into two parts by a ring inside the unit circle. The ring is defined by the inner and outer radiuses. In this case, optimum inner and outer ring radiuses are found jointly in order to get the minimum LSE. In the optimum-partitioning, we consider all the possible channel zero combinations inside the unit circle and select group of zeros, which return the minimum LSE. It turns out that ring-based approach is suboptimum compared to the optimum-partitioning. However the difference between these two approaches is very small when the overall LSE is considered.

We will extend the results for LSE designs and obtain the MSE solutions for the proposed deconvolution filters. We will also look at the performance of deterministic inverse filters for noisy observations. The deterministic method is the same as used in LSE designs, but in this case the noise also affects the partitioning and delay selection. In the statistical approach we use autocorrelation functions of input and noise sequences in the design procedure. For this case, we will first consider the MSE optimum FIR best delay deconvolution filter formulation. These filters are the FIR counterparts of the IIR Wiener deconvolution filters with best delay property [24, 25]. Then we will present the partition-based FIR-IIR best delay MSE optimum deconvolution filters. Three different partitioning procedures will be investigated as in LSE design. We will compare these filters with the FIR and IIR Wiener deconvolution filters. It turns out that FIR-IIR partition-based inverse filters perform better than the FIR Wiener deconvolution filters. Furthermore, they are less sensitive to the estimation errors than the IIR Wiener filters. Another advantage of these filters is, they are casual and can be used in real-time implementations as opposed to the IIR Wiener filters.

The organization of the thesis is as follows. In Chapter II, we will present LSE optimum designs for FIR and FIR-IIR deconvolution filters. Also we will derive the closed form LSE expressions for the FIR inverse filter and show the factors that affect the LSE. In Chapter III, MSE designs for FIR and FIR-IIR deconvolution filters will be given. We will compare the performances of proposed inverse filters for different channel characteristics in chapter IV. Chapter V will present a conclusion about the proposed inverse filters.

CHAPTER 2

INVERSE FILTERS FOR NOISELESS OBSERVATIONS

In this chapter, we will consider the design of deterministic inverse filters for the deconvolution problem. In this context, we will look at the least squares optimum FIR inverse filters first. It has been shown that, deconvolution delay plays an important role on LSE of FIR inverse filters in different works [8]. In this chapter, we will consider the best delay design and show the effect of delay on LSE. We will give an effective and a simple procedure for obtaining best delay as proposed in [19]. Also we will derive the closed form LSE expressions in order to show the other factors that affect the LSE of FIR inverse filters. IIR inverse filters can also be used in deconvolution problem. They are more powerful tools when compared with FIR inverse filters when the channel is minimum-phase. They perfectly deconvolve the minimum-phase channels. On the other hand, they have stability problems for nonminimum-phase channels. We will combine these filter types and propose a new inverse filter called FIR-IIR which is the hybrid filter composed of best delay FIR inverse filter and the all pole IIR inverse filter. The most critical point is the selection of FIR and IIR parts. We will introduce three types of partitioning procedures, namely unit circle-based partitioning, ring-based partitioning and optimum-partitioning.

LSE inverse filter design for the deconvolution problem will be investigated by using the system structure shown in Figure 2.1. $\delta(n)$ is used as an input to eliminate the input signal dependence of the system performance; only the channel and inverse filter impulse responses will affect the overall performance.

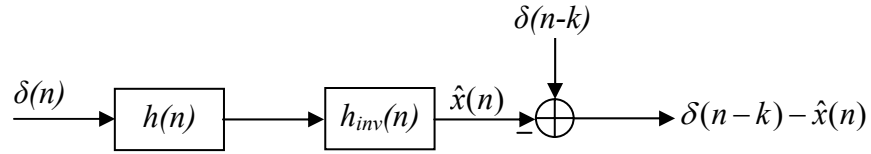


Figure 2.1 System structure of inverse filter design problem for noiseless observations.

2.1 Best Delay FIR Inverse Filters

FIR (Finite Impulse Response) inverse filter design problem is well known. The basic equality that should be considered in FIR inverse filter design is given as follows,

$$h(n) * h_{inv}^{FIR}(n) = \delta(n - k) \quad (1)$$

where $h(n)$ and $h_{inv}^{FIR}(n)$ are the impulse responses of the channel and FIR inverse filter respectively and k is the convolution delay. Since both channel and the inverse filter are the FIR filters, the possible convolution delay is in the range of $[0, L+N-1]$ where L is the channel order and N is the inverse filter length. Equation (1) is the desired result, but it is not possible to obtain such an exact result by using finite number of coefficients. When an FIR inverse filter is used, equation (1) is not satisfied perfectly. There is a nonzero LSE term, which should be minimized to obtain the optimum inverse filter,

$$E_{LSE} = \sum_n \left| \delta(n - k) - h(n) * h_{inv}^{FIR}(n) \right|^2 \quad (2)$$

Equation (1) can also be written in matrix form as,

$$\mathbf{H}\mathbf{h}_{inv}^{FIR} = \mathbf{d} \quad (3)$$

where \mathbf{H} is the Toeplitz channel convolution matrix with the size of $(N+L) \times N$ and \mathbf{d} is the desired vector, which contains 1 at k^{th} location and all the other elements are zero with the size of $(N+L) \times 1$ such as,

$$\mathbf{H} = \begin{bmatrix} h_0 & h_1 & \cdots & h_L & 0 & \cdots & 0 \\ 0 & h_0 & \cdots & h_{L-1} & h_L & \cdots & 0 \\ \vdots & \vdots & \vdots & \vdots & \vdots & \vdots & \vdots \\ 0 & 0 & \cdots & h_0 & h_1 & \cdots & h_L \end{bmatrix}^T \quad (4)$$

$$\mathbf{d} = [0 \ \cdots \ 0 \ 1 \ 0 \ \cdots \ 0]^T \quad (5)$$

where h_i terms are the coefficients of channel filter. Then the inverse filter can be found from (3) as,

$$\mathbf{h}_{inv}^{FIR} = \mathbf{H}^\dagger \mathbf{d} \quad (6)$$

where,

$$\mathbf{H}^\dagger = (\mathbf{H}^H \mathbf{H})^{-1} \mathbf{H}^H \quad (7)$$

is the pseudoinverse [7] of \mathbf{H} .

The effect of delay on LSE can be seen in Table 2.1, where the LSE corresponding to all the possible delays are given for the arbitrary third order channel, $h(n) = 0.33\delta(n) + 0.13\delta(n-1) + 1.32\delta(n-2) + 1.22\delta(n-3)$, and the FIR inverse filter with length of 4.

Table 2.1 The effect of delay on LSE

Delay (k)	LSE (dB)
0	-4.8473
1	-5.7394
2	-7.0573
3	-7.0858
4	-7.4318
5	0.9685
6	-0.1891

As it can be seen from Table 2.1, delay selection seriously affects the LSE. The difference between the maximum and minimum LSE values is very large,

approximately 8.4 dB. So in FIR inverse filter design, best delay selection is an important problem.

The best delay can be found in two ways. In the first one, for all the possible delays, desired vector \mathbf{d} is constituted as in (5) and the inverse filter is obtained from the equation (6) to calculate the LSE as in (2). After finding all the LSE values corresponding to the possible delays, selecting the minimum one gives us the inverse filter with best delay. In the second case, best delay is found by using rows of \mathbf{H} matrix as proposed in [19]. Once the best delay is found, desired vector \mathbf{d} is determined and the inverse filter is obtained. So the design process seems to be more efficient in the second case, because it does not compute the inverse filter for all the possible delays. It uses Singular Value Decomposition (SVD) [7] of the Toeplitz channel convolution matrix, \mathbf{H} , namely,

$$\mathbf{H} = \mathbf{U} \begin{bmatrix} \boldsymbol{\Sigma} & \mathbf{0} \\ \mathbf{0} & \mathbf{0} \end{bmatrix} \mathbf{V}^H \quad (8)$$

If we use the same error expressions as in [7] for LSE,

$$E_{LSE} = \mathbf{d}^H (\mathbf{d} - \mathbf{H}\mathbf{h}_{inv}^{FIR}) = \mathbf{d}^H \mathbf{U} (\mathbf{U}^H \mathbf{d} - \mathbf{U}^H \mathbf{H} \mathbf{V} \mathbf{V}^H \mathbf{h}_{inv}^{FIR}) \quad (9)$$

The above error expression is obtained from the counterpart of the orthogonality principle and is based on the orthogonality of the left and right singular matrices \mathbf{U} and \mathbf{V} . This expression is especially useful for the overdetermined matrices like \mathbf{H} .

Let us define,

$$\mathbf{V}^H \mathbf{h}_{inv}^{FIR} = \mathbf{b} = \begin{bmatrix} \mathbf{b}_1 \\ \mathbf{b}_2 \end{bmatrix} \quad (10)$$

and

$$\mathbf{U}^H \mathbf{d} = \mathbf{c} = \begin{bmatrix} \mathbf{c}_1 \\ \mathbf{c}_2 \end{bmatrix} \quad (11)$$

where, \mathbf{b}_1 and \mathbf{c}_1 are $N \times 1$ vectors. LSE can be written as,

$$E_{LSE} = \mathbf{d}^H \mathbf{U} \begin{bmatrix} \mathbf{c}_1 - \boldsymbol{\Sigma} \mathbf{b}_1 \\ \mathbf{c}_2 \end{bmatrix} \quad (12)$$

E_{LSE} is minimized when $\mathbf{c}_1 = \Sigma \mathbf{b}_1$. Therefore, LSE for the overdetermined set of equations is given as,

$$E_{LSE} = \mathbf{d}^H \mathbf{U} \bar{\mathbf{c}}_2 \quad (13)$$

where $\bar{\mathbf{c}}_2$ has the following form,

$$\bar{\mathbf{c}}_2 = [0 \quad \cdots \quad \bar{u}_{k,N} \quad \bar{u}_{k,N+1} \quad \cdots \quad \bar{u}_{k,N+L-1}]^H \quad (14)$$

and

$$\mathbf{d}^H \mathbf{U} = [0 \quad \cdots \quad 0 \quad 1 \quad 0 \quad \cdots \quad 0] \begin{bmatrix} \bar{\mathbf{u}}_0 \\ \bar{\mathbf{u}}_1 \\ \vdots \\ \bar{\mathbf{u}}_{N+L-1} \end{bmatrix} = \bar{\mathbf{u}}_k \quad (15)$$

where $\bar{\mathbf{u}}_i$ are the row vectors of \mathbf{U} . Therefore, LSE for a delay of k can be written as,

$$E_{LSE}^k = \sum_{i=N}^{N+L-1} |\bar{u}_{k,i}|^2 \quad (16)$$

Above equation is nothing but the magnitude squared sum of the elements in the k^{th} row of the left singular matrix \mathbf{U} . Best delay for a given channel \mathbf{h} is found as the index of the row which gives the minimum LSE, i.e.,

$$k_{opt} = \arg \min_k (E_{LSE}^k) \quad (17)$$

It turns out that best delay k_{opt} for a minimum-phase channel is zero while it is $N+L-1$ for a maximum-phase channel. In general, best delay is between these two extreme cases, namely $0 \leq k_{opt} \leq N+L-1$. Once the best delay is found, desired vector \mathbf{d} is determined and the LSE inverse filter is found as,

$$\mathbf{h}_{inv}^{FIR} = \sum_{i=0}^{N-1} \frac{1}{\sigma_{c,i}^2} \mathbf{v}_i \mathbf{v}_i^H \mathbf{H}^H \mathbf{d} \quad (18)$$

where $\sigma_{c,i}$'s are the singular values and \mathbf{v}_i 's are the right singular vectors of \mathbf{H} . Above design procedure is direct and simple. Instead of designing the inverse filter for all possible delays and computing the LSE, we can find the optimum delay and inverse filter by a simple procedure. Note that equation (18) is exactly the same as

equation (6). However equation (18) is more efficient since there is no matrix inversion as in (6). This is especially important when the filter length is large.

2.1.1 Factors that Affect the LSE of FIR Inverse Filters

Apart from convolution delay, there are additional factors that affect the LSE performance of FIR inverse filter. The factors that will be investigated in this section are the inverse filter length, the position of channel zeros on the z-plane and the channel zero distribution. In the following part, we will derive the closed form LSE expressions as a function of channel coefficients and the inverse filter length, N , to understand the dependencies of LSE performance on these factors more clearly.

LSE optimum inverse filter \mathbf{h}_{inv}^{FIR} is found from equation (6), but this filter can not result desired response, \mathbf{d} , after deconvolution operation. The actual response can be expressed as,

$$\mathbf{d}_{actual} = \mathbf{H}\mathbf{h}_{inv}^{FIR} = \mathbf{H}\mathbf{H}^\dagger \mathbf{d} \quad (19)$$

The error term between the desired and actual responses can be written as,

$$\mathbf{e} = \mathbf{d} - \mathbf{d}_{actual} = \mathbf{B}\mathbf{d} \quad (20)$$

where

$$\mathbf{B} = \mathbf{I} - \mathbf{H}\mathbf{H}^\dagger \quad (21)$$

LSE can be found by using equation (20) as,

$$\begin{aligned} LSE &= \mathbf{e}^H \mathbf{e} \\ &= \mathbf{d}^H \mathbf{B}^H \mathbf{B} \mathbf{d} \\ &= \mathbf{d}^H \mathbf{B} \mathbf{d} \end{aligned} \quad (22)$$

The last equality comes from Property 1 and Property 3 in Appendix A.

Let the optimum delay for FIR inverse filter be k , so the desired response can be written as given in (5). Then LSE expression in (22) can be simplified as,

$$LSE = \mathbf{d}^H \left[b_{1,k} \quad \dots \quad b_{(k-1),k} \quad b_{k,k} \quad b_{(k+1),k} \quad \dots \quad b_{(N+L),k} \right]^T \quad (23)$$

where $b_{j,k}$ term represents the elements in the k^{th} column of matrix \mathbf{B} . Then LSE expression becomes,

$$LSE = b_{k,k} = \mathbf{B}(k,k) \quad (24)$$

This equation tells us that the minimum LSE is the k^{th} element in the diagonal of matrix \mathbf{B} . By using this result, we derived the LSE for the FIR inverse filter when the channel order is one. It is given as,

$$\begin{aligned} LSE &= \frac{|a|^{2N}}{1+|a|^2+|a|^4+\dots+|a|^{2N}} & \text{for } |a| < 1 \\ LSE &= \frac{1}{1+|a|^2+|a|^4+\dots+|a|^{2N}} & \text{for } |a| > 1 \end{aligned} \quad (25)$$

where a is the zero of the channel filter. Note that, since the first order channel is either minimum-phase or maximum-phase, the best delay can be either 0 or N . So there are two LSE expressions for the first order channel regardless of inverse filter length, N . The proof of equation (25) is given in Appendix A. For the higher order channel filters, LSE formulas can also be derived by using equations (21) and (24) as well. But unfortunately LSE formulas for higher order channels are more complicated and can not be generalized with respect to N . Furthermore, since the possible delays are in the range of $[0, N+L-1]$, $N+L$ many LSE formulas should be derived. In Appendix B, LSE formulas are given for second order channel with $N=2$ and $N=3$.

When equation (25) is investigated, the effects of inverse filter length and position of channel zero on the LSE can be seen easily. Increasing inverse filter length decreases the LSE as it can be seen from Figure 2.2, where equation (25) is evaluated for $a=0.95$ and $a=1.08$ corresponding to the minimum and maximum-phase channels respectively. When the inverse filter length, N , is small, LSE is more sensitive to a change in N . Furthermore, LSE values for minimum-phase and maximum-phase channels in this example are different. This fact states that, the position of channel zero also affects the LSE and this effect is shown in Figure 2.3, which is obtained from equation (25) for $N=8$. As it is seen, LSE increases as the channel zero gets closer to the unit circle and it decreases when the zero is away

from unit circle. Thus the error contribution of the channel zeros close to the unit circle is larger than the ones far away from the unit circle.

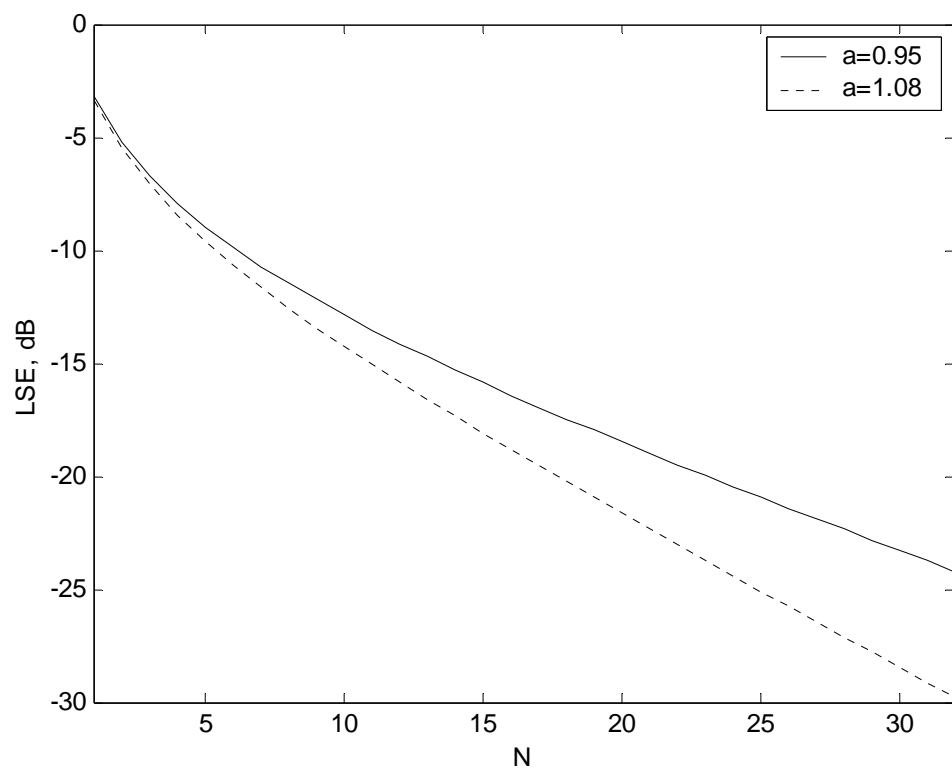


Figure 2.2 The effect of inverse filter length on LSE for first order channel.

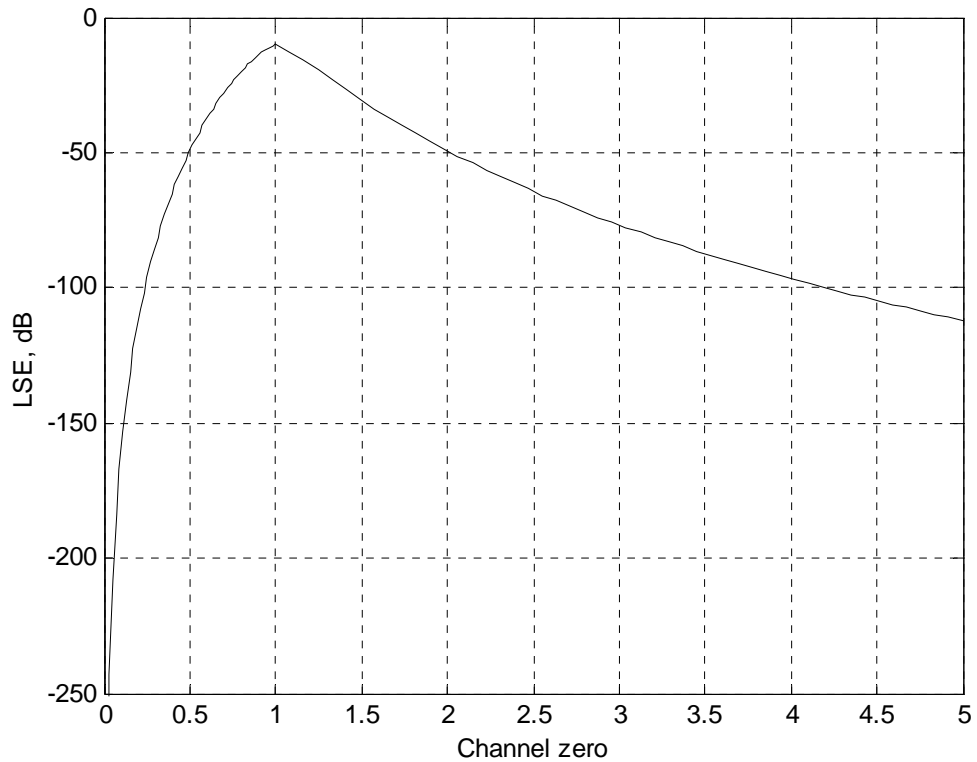


Figure 2.3 The effect of channel zero position on LSE for first order channel and $N=8$.

In the following part, we will look at the inverse filtering procedure of FIR filters in z -domain to show the effect of channel zero distribution on LSE.

FIR channel zeros produce spectral deeps in frequency domain and causes a distortion in the transmitted signal. This distortion effect increases when the channel zero comes closer to the unit circle. The aim of the inverse filter is to eliminate the undesired effects of these channel zeros. In ideal inverse filtering, there should be no system (cascaded channel and inverse filter) zero on the z -plane. But in the FIR case, since both channel and inverse filter are all zero filters, there are always zeros on the z -plane. Therefore, the locations of system zeros become an important point in inverse filtering.

When the distribution of overall system zeros on the z -plane are considered, it is obvious that isolated zeros cause more distortion or larger LSE compared to homogeneously distributed zeros. In fact, homogeneous distribution corresponds to locating each spectral deep side by side with equal distance and obtaining a flat

spectrum. Therefore, locating FIR inverse filter zeros in such a way that they produce a homogenous distribution when combined with channel zeros, seems to be the best solution for inverse filtering procedure. Figure 2.4 shows the overall system zero distribution for the best delay FIR inverse filter with length of 32 and the channel with order of 8. The homogeneous distribution can be observed in this figure. It should be noted that, the number of inverse filter zeros around the channel zeros is varying with the positions of channel zeros. In fact, the inverse filter zeros concentrate around the channel zeros close to the unit circle. This observation states that more inverse filter zeros are used for channel zeros with large error contribution.

Inverse filtering procedure can explain the effect of channel zero distribution on LSE. When two channel zeros are close to each other on the z-plane, producing a homogeneous distribution needs more inverse filter zeros or a large LSE is produced for the same inverse filter length. The effect of closeness of two channel zeros can be seen by investigating the following example.

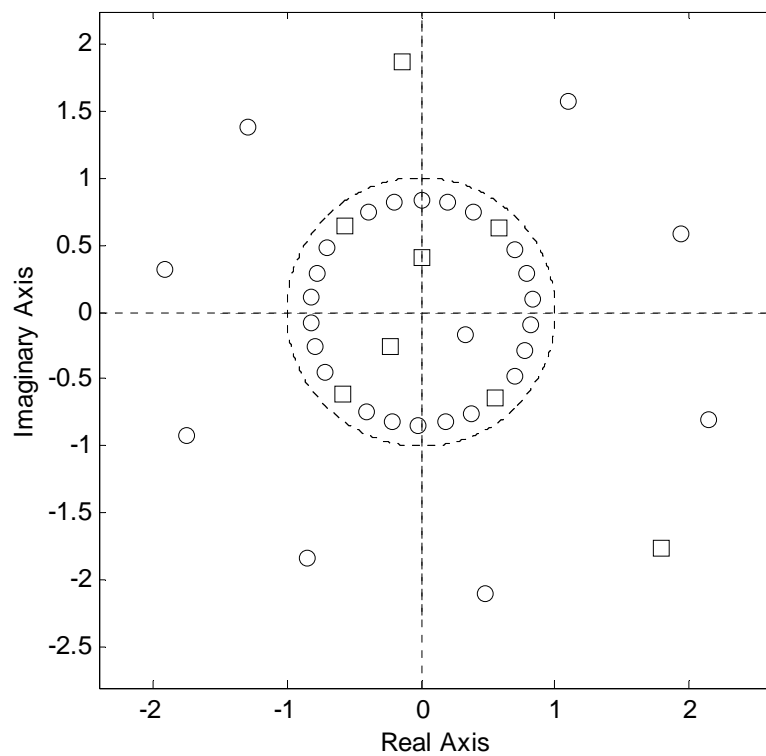


Figure 2.4 Overall system zeros for FIR inverse filter with $N=32$ and channel with $L=8$. \square represents channel zero, \circ represents inverse filter zero.

Example 2.1: We have chosen a single channel with $L=2$, such that both channel zeros are located on the same radius, which is 0.8. The distance between these channel zeros are changed by moving one of them on the same radius while the other one is fixed. The process can be seen in Figure 2.5. Then at each channel zero positions, LSE is found for the best delay FIR inverse filter, whose length is chosen as 7. So LSE is obtained as a function of the channel zero positions with respect to each other, which is shown in Figure 2.6. The channel zero positions with respect to each other are illustrated as an angular difference between these zeros. As it is seen, LSE is the maximum when two zeros coincide and decreases when they go far away from each other. But it has some fluctuations. If the minimum points of these fluctuations are investigated, it can be seen that, these are approximately the multiples of 45° . In fact, since there are 8 zeros in the overall system, this is the angular difference between each zero when the homogenous distribution is achieved.

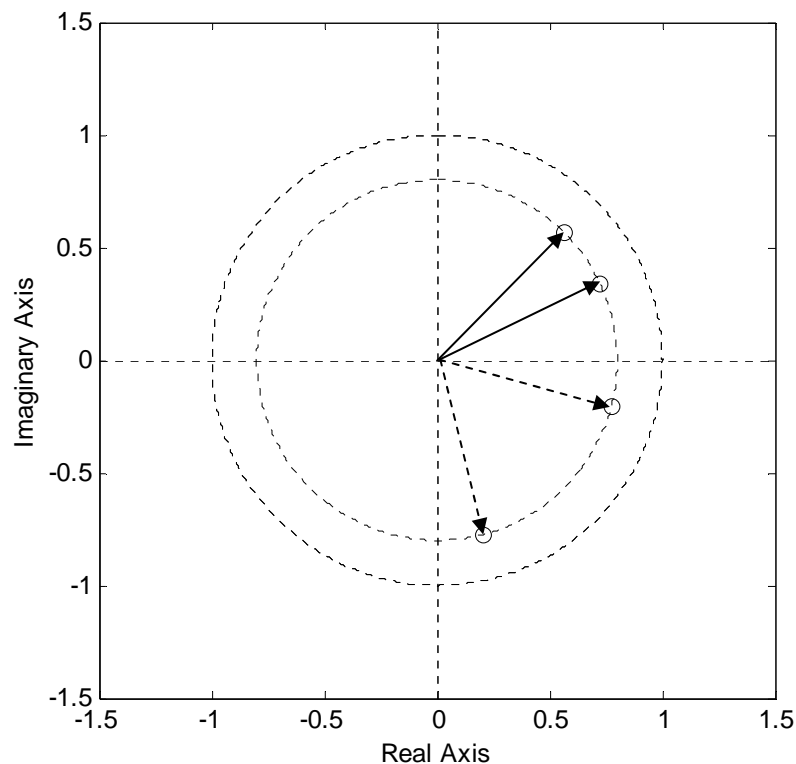


Figure 2.5 Zero positions of channel with $L=2$ for Example 2.1.

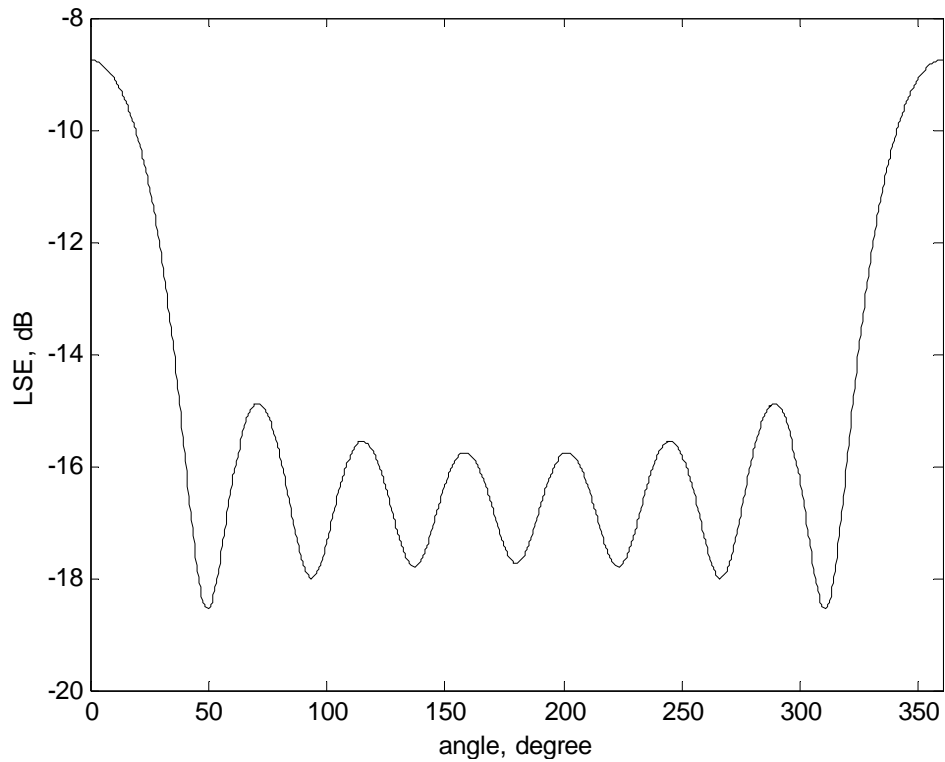


Figure 2.6 LSE values for different distance between two channel zeros.

As a result, FIR inverse filter design is a simple procedure but many factors should be considered in order to fully understand the deconvolution operation. For a given channel, selecting an appropriate inverse filter length and convolution delay are the most critical points to obtain an LSE optimum inverse filter. Channel zero positions and distributions also affect the LSE performance significantly.

2.2 IIR Inverse Filters

IIR (Infinite Impulse Response) filter is the all pole filter and uses poles, which are in a way the opposite of the zeros, to make the filtering operation. It operates in a recursive manner. When the inverse filter is expressed as a nonrecursive filter, it contains infinite number of filter coefficients. So it is a more powerful tool for the inverse filtering operation than the FIR filter. But it has some

limitations. It should be used for minimum-phase channels because of the stability problem, while there is no such a problem in FIR inverse filter.

Investigating a first order channel can help us to understand the advantage and disadvantage of these two types of inverse filters. Let a be the channel zero. Then the channel can be expressed in z-domain and time domain as,

$$H(z) = 1 - az^{-1} \quad h(n) = \delta(n) - a\delta(n-1) \quad (26)$$

The IIR inverse filter for this channel can be written as,

$$H_{inv}^{IIR}(z) = \frac{1}{1 - az^{-1}} \quad h_{inv}^{IIR}(n) = a^n u(n) \quad (27)$$

where $u(n)$ is the unit step function. Note that the time domain coefficients in equation (27) exponentially increase with time, n , when the channel zero is located outside the unit circle, namely $|a| > 1$. In this condition IIR inverse filter is said to be unstable. For stability, channel zero should be located inside the unit circle. If this is the case, then IIR inverse filter is the perfect filter with no error.

Equation (27) can also be written as,

$$\begin{aligned} H_{inv}^{IIR}(z) &= 1 + az^{-1} + a^2 z^{-2} + \dots + a^{N-1} z^{-N+1} + \dots \\ h_{inv}^{IIR}(n) &= \delta(n) + a\delta(n-1) + a^2 \delta(n-2) + \dots + a^{N-1} \delta(n-N+1) + \dots \end{aligned} \quad (28)$$

As it can be seen from equation (28), when the IIR filter is expressed as an all zero filter, it uses infinite number of filter coefficients to achieve the desired response. On the other hand in the FIR case, we have limited number of coefficients to use in inverse filtering. Truncating equation (28) and taking the first N coefficients is the simplest way to obtain the FIR inverse filter such as,

$$H_{inv}^{FIR}(z) = 1 + az^{-1} + a^2 z^{-2} + \dots + a^{N-1} z^{-N+1} \quad (29)$$

This may not be the inverse filter with minimum LSE but it gives the idea about why FIR filter produces LSE. It uses finite number of filter coefficients instead of infinite number of filter coefficients as in IIR filter. On the other hand, although FIR filter produces larger LSE, it can be used for any channel filter, while in the IIR inverse filter case, we need to have a minimum-phase channel. It is possible to combine the FIR and IIR inverse filters in order to fully take the advantage of both approaches. In the following section, we will extend this idea and

introduce a new inverse filter design method, which is called partition-based FIR-IIR inverse filtering.

2.3 Partition-Based FIR-IIR Inverse Filters

In general, FIR-IIR inverse filters are hybrid filters composed of best delay FIR and all pole IIR inverse filters. Thus the advantages of both filter types can be combined in inverse filtering operation. The most critical point in the design is the selection of FIR and IIR parts. Selection procedure is based on partitioning of channel zeros into two regions. IIR part is the inverse filter for the channel zeros that fall into one of the regions, while the FIR part corresponds to the best delay LSE optimum inverse filter of the channel zeros outside the first region. It is important to note that, the region used for IIR part should not contain any channel zero outside the unit circle because of the stability problem. Another important point in the FIR-IIR inverse filter design is the filter orders. For the fair comparison with the FIR inverse filter, the selection of FIR and IIR parts is performed such that the complexity of the FIR-IIR inverse filter is equal to the complexity of the FIR inverse filter. The order of the FIR-IIR inverse filter can be defined as the summation of the FIR part and IIR part orders. Therefore, we decrease the length of the FIR part of the FIR-IIR inverse filter by one for every pole in IIR part. In the following part, we will give the design procedure of FIR-IIR inverse filters.

Let us assume that, the channel filter $H(z)$ is partitioned into two regions such that one of them is inside the unit circle. After partitioning, the channel filter can be written as,

$$H(z) = H_1(z)H_2(z) \quad (30)$$

where $H_1(z)$ is the part of the channel filter composed of zeros taken from the region inside the unit circle. $H_2(z)$ is composed of the channel zeros inside the other region. These channel filter parts are used to obtain the IIR and FIR parts of the FIR-IIR inverse filter. IIR part is obtained from $H_1(z)$ by simply inverting it such as,

$$H_{1,inv}^{IIR}(z) = \frac{1}{H_1(z)} \quad (31)$$

Since $H_1(z)$ is defined inside the unit circle, there is no stability problem. The FIR part is obtained from $H_2(z)$ by applying best delay FIR inverse filter design procedure. Then, the FIR-IIR inverse filter is defined as the combination of these inverse filters such as,

$$H_{inv}^{FIIR}(z) = \frac{1}{H_1(z)} H_{2,inv}^{FIR}(z) \quad (32)$$

The system response after deconvolution can be expressed as,

$$H(z)H_{inv}^{FIIR}(z) = H_2(z)H_{2,inv}^{FIR}(z) \quad (33)$$

As it is seen from (33), IIR part completely eliminates the effects of channel filter part, $H_1(z)$ and the overall system reduces to the deconvolution of reduced channel filter, which is $H_2(z)$.

The FIR-IIR filter structure can be constructed in different ways depending on partitioning procedure. In the following subsections, we will present three types of partitioning, namely unit circle-based partitioning, ring-based partitioning and optimum-partitioning.

2.3.1 Unit Circle-Based Partitioning

In unit circle-based partitioning procedure, the regions are defined as the minimum and maximum-phase parts of the channel filter. Then, FIR-IIR inverse filter is constructed such that, IIR part is obtained from the minimum phase part of the channel filter while the maximum phase part is used for FIR part design. Since IIR part is a perfect inverse filter with no error, eliminating the effects of all the channel zeros inside the unit circle with this partitioning seems to be reasonable. But unfortunately, such a simple partitioning procedure is not the optimum one and it is not guaranteed to be always better than the completely FIR inverse filter. In some cases it may produce higher LSE than the FIR inverse filter.

The main reason for such an FIR-IIR inverse filter performance is that, unit circle-based partitioning procedure does not take into account the position of the channel zeros and the length of the FIR part, which are the parameters that affect the LSE of FIR inverse filter mentioned before. As equation (33) states, the overall error of the FIR-IIR inverse filter comes from the FIR part. Since the length of the FIR part is decreased by one for every pole of the IIR part, in some cases the length of the FIR part may become so small that the error of the FIR part exceeds the error of the completely FIR inverse filter. Such a case arises especially when there are many channel zeros close to the origin. As it can be seen from Figure 2.4, FIR inverse filter uses a small number of inverse filter zeros for the channel zeros close to the origin. It saves its zeros for the channel zeros close to the unit circle. But since unit circle-based partitioning procedure does not take into account these facts, it also uses poles for channel zeros close to the origin although it may be unnecessary in some cases. Thus less inverse filter zeros are remained for the channel zeros outside the unit circle. Therefore, even though there is no error term that comes from the channel zeros inside the unit circle, the overall LSE of unit circle based FIR-IIR inverse filter may exceed the LSE of the completely FIR inverse filter. Figure 2.7 illustrates such a case in which channel order is selected as $L=8$ and the inverse filter length as $N=16$. As it is seen, there are 6 channel zeros inside the unit circle and FIR inverse filter uses only 3 of its zeros for these channel zeros to compensate their effects on LSE. The other 12 inverse filter zeros are used for the remaining two channel zeros outside the unit circle. These observations tell us that, the error contribution of the channel zeros outside the unit circle is much greater than the ones inside the unit circle.

As it is seen from Figure 2.7(b), 6 poles are used for the unit circle-based FIR-IIR inverse filtering and the effects of channel zeros inside the unit circle are completely eliminated. Therefore, the number of inverse filter zeros that can be used for the remaining channel zeros reduces to 8. But, since these channel zeros have large error contribution, 8 inverse filter zeros are not enough to obtain the better LSE performance than the FIR inverse filter. In fact, for this example the LSE of the FIR inverse filter is -14.77 dB while it is -12.15 dB for the unit circle-based FIR-IIR.

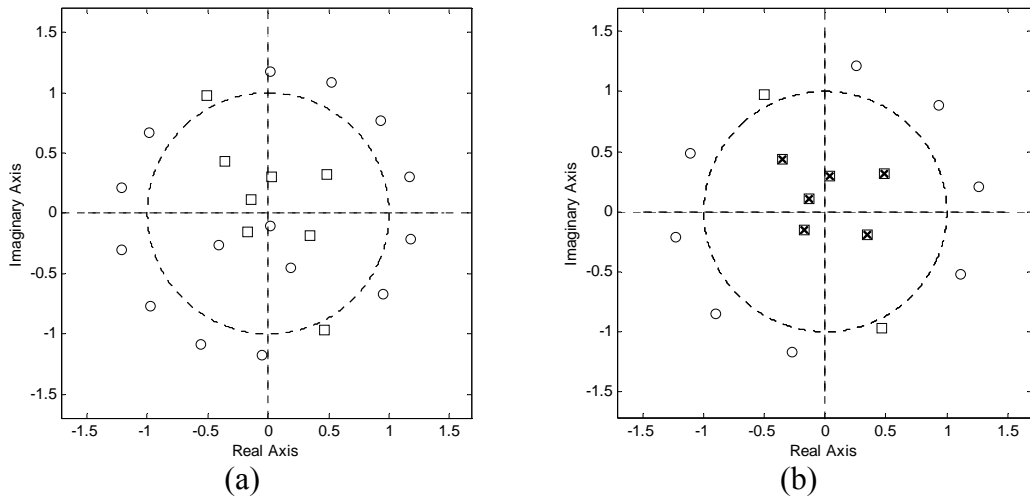


Figure 2.7 Pole-zero plots for (a) FIR and (b) unit circle-based FIR-IIR inverse filters when $L=8$, $N=16$. o, \square and x represent inverse filter zero, channel zero and IIR pole respectively.

2.3.2 Ring-Based Partitioning

Ring-based partitioning procedure divides the z-plane into two parts by a ring region inside the unit circle. The ring region is defined between the inner and outer radiuses inside the unit circle as can be seen in Figure 2.8. The IIR and FIR parts of the FIR-IIR inverse filter are designed by considering the channel zeros inside and outside the defined ring region respectively. The ring-based partitioning procedure uses a tradeoff between FIR part length and the error contribution of channel zeros inside the unit circle. It tries to use the poles in an economical way in order not to decrease the FIR part length so much. So it uses poles to eliminate the effects of channel zeros with a large error contribution inside the unit circle and leaves the channel zeros with a small error contribution to the FIR part. Thus it has a better performance than the unit circle-based partitioning.

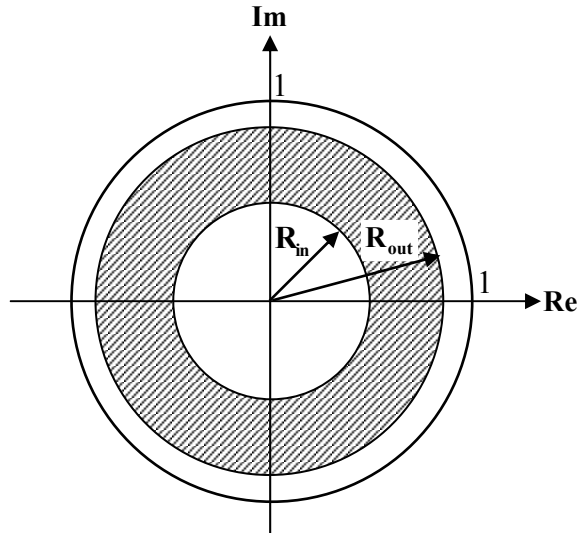


Figure 2.8 Inner and outer radiuses and ring region inside the unit circle for ring-based partitioning.

Effectiveness of ring-based partitioning can be seen in Figure 2.9, where channel order is 8 and the inverse filter length is 16. As it is seen from Figure 2.9(a), inside the unit circle inverse filter uses 9 zeros, all of which are for three channel zeros close to the unit circle. No inverse filter zeros are used for the other channel zeros inside the unit circle. The remaining inverse filter zeros are used for the channel zeros outside the unit circle. On the other hand, as it is seen from Figure 2.9(b), using only 3 poles instead of 9 zeros for the channel zeros inside the unit circle, not only eliminates the effects of these zeros completely but also saves inverse filter zeros for the remaining channel zeros. So the overall LSE is decreased. In fact, LSE values for FIR and ring-based FIR-IIR inverse filters are -15.74 dB and -21.46 dB respectively, while it is -20.76 dB for unit circle-based FIR-IIR.

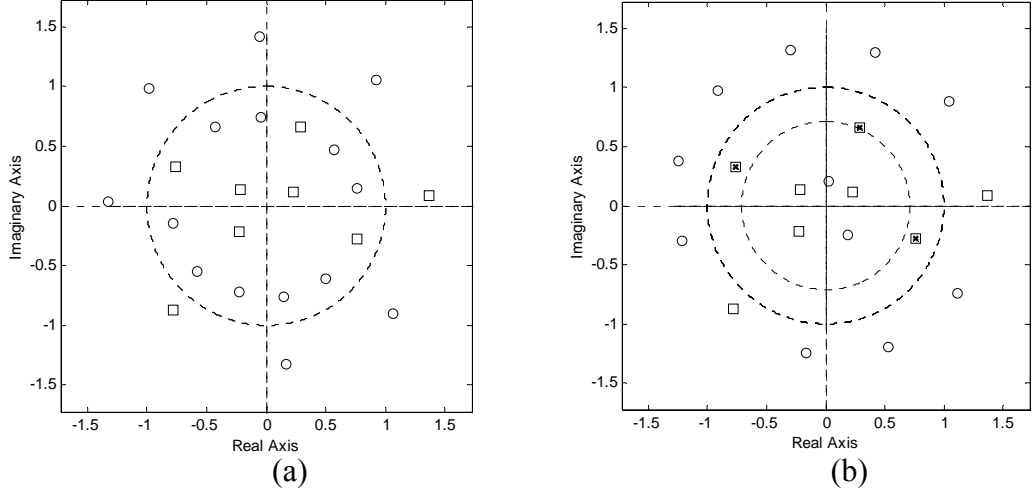


Figure 2.9 Pole-zero plots for (a) FIR and (b) ring-based FIR-IIR inverse filters when $L=8$, $N=16$. o, \square and x represent inverse filter zero, channel zero and IIR pole respectively.

The most critical point in ring-based partitioning is to find the optimum inner and outer radiuses; R_{in} , R_{out} and they are found jointly in order to get the minimum LSE. Once these radiuses are found, the channel zeros inside the ring are identified and the IIR part of the FIR-IIR inverse filter is determined. The procedure for finding the optimum ring radiuses is simple. Assume that P distinct channel zeros are inside the unit circle. They are given as $z_i = r_i e^{j\theta_i}$ ($i=1,2,\dots,P$) and they are ordered according to r_i ,

$$r_0 = 1 > r_1 > \dots > r_P > r_{P+1} = 0 \quad (34)$$

For each outer radius $R_{out}=r_i$, ($i=0,1,\dots,P$), we consider an inner radius $R_{in}=r_j$, ($j=P+1,P,\dots,i+2$). We identify the channel zeros inside the ring for each of the above cases and select the optimum radius pair by considering the minimum LSE. Unfortunately, since the LSE formulas are nonlinear with respect to N , L and distribution of channel zeros and also so complicated, we must design the inverse filter for each radius pair to find the LSE. The number of possible cases including $R_{out}=R_{in}$ is $P(P+1)/2+1$. Note that when $R_{out}=R_{in}$, we have an FIR inverse filter instead of an FIR-IIR inverse filter. This condition can occur when no ring region can be defined to make the FIR-IIR better than the FIR inverse filter. Figure 2.10

illustrates an example that shows this condition, where the channel order and inverse filter length are selected as $L=8$ and $N=16$ respectively. As it is seen, since the channel zeros closest to the unit circle are located outside the unit circle, the most of the inverse filter zeros are used for these channel zeros. Only 3 inverse filter zeros are used to compensate the effects of channel zeros inside the unit circle. So, using a pole for any channel zero inside the unit circle will not improve the performance, because the number of inverse filter zeros will be decreased by one and the channel zeros outside the unit circle will produce larger LSE. Therefore using FIR inverse filter instead of ring-based FIR-IIR inverse filter for this channel is more suitable.

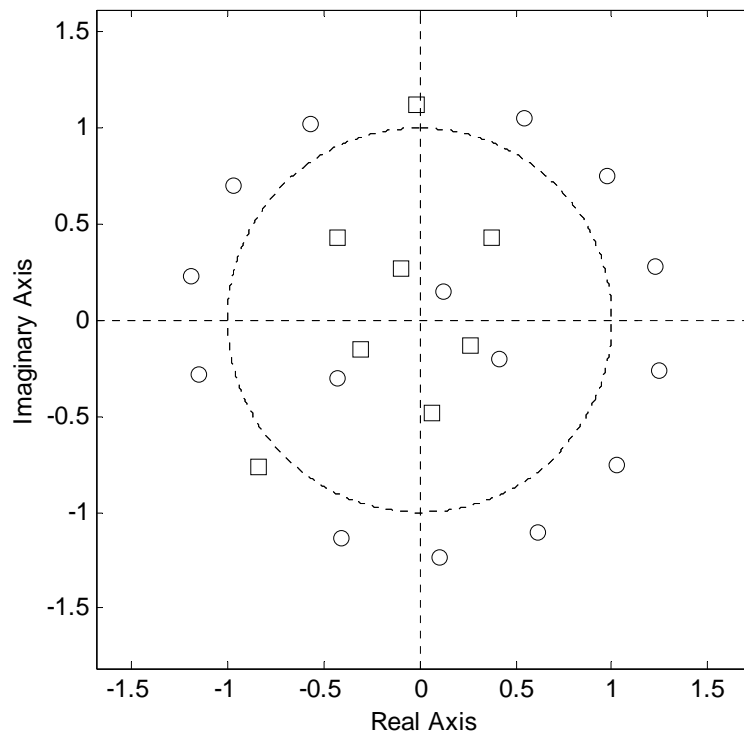


Figure 2.10 Zero plots of the channel and FIR inverse filter for $L=8$ and $N=16$. \circ and \square represent inverse filter zero and channel zero respectively.

Ring-based partitioning has some limitations in the LSE performance improvement. It performs partitioning by considering two main parameters, namely inner and outer radiuses. Therefore, it can not distinguish the channel zeros on the

same radius. It puts all of these zeros together either inside or outside the ring region. Also, ring-based partitioning procedure can not exclude any channel zero from the defined ring region to use it in FIR part design. It is critical especially when there are two channel zeros close to each other. As a result, in some special cases ring-based partitioning FIR-IIR inverse filter may not give the possible minimum LSE. To achieve this value optimum-partitioning procedure will be proposed in the following subsection.

2.3.3 Optimum-Partitioning

In optimum-partitioning, all the possible combinations of channel zeros inside the unit circle are found and for each of such zero groupings the LSE is determined. The advantage of the optimum-partitioning is that we have more degree of freedom to select the FIR and IIR parts than ring-based approach. In this case, we do not restrict the IIR part between two radiuses; it can be an arbitrary region. So optimum-partitioning can separate the channel zeros close to each other or on the same radius by putting some of them to IIR part and the other to the FIR part. By this way, it helps the FIR part to produce an effective homogeneous distribution with small number of inverse filter zeros. Thus a lower LSE can be obtained when compared with the ring-based approach.

On the other hand this process can require significant computational power when there are several zeros inside the unit circle. For the same assumption as in ring-based partitioning, we need to consider 2^P cases of zero groupings to find the optimum-partitioning. As the number of channel zeros inside the unit circle increases, computational load of the optimum-partitioning approach increases exponentially. Table 2.2 compares the ring-based and optimum-partitioning design approaches in terms of the number of cases they should consider to obtain an optimum solution. It turns out that ring-based approach is always more efficient than the optimum-partitioning case for a given channel with P zeros inside the unit circle.

Table 2.2 The number of partitioning cases

P	Optimum-partitioning	Ring-based
2	4	4
3	8	7
4	16	11
5	32	16
6	64	22
7	128	29
8	256	37

The LSE performances of ring-based partitioning and optimum-partitioning FIR-IIR inverse filters will be investigated in the following example.

Example 2.2: We have chosen a single channel with $L=12$ and the optimum FIR and IIR parts of FIR-IIR inverse filter are found for both ring-based and optimum-partitioning approaches. The corresponding poles and zeros for ring-based and optimum-partitioning approaches are shown in Figure 2.11(a) and (b) respectively. Figure 2.11(a) also shows the ring region. As it is seen ring-based approach selects all the channel zeros inside the ring region to construct IIR part, while optimum-partitioning selects some of them for the IIR part and uses the others for the FIR part to achieve effective homogeneous zero distribution. In this case, the LSE is found as -9.7 dB and -10.59 dB for the ring-based and optimum-partitioning approaches respectively. If the best delay FIR inverse filter is used, -9.21 dB is obtained for the LSE.

As a result, the LSE performances of FIR-IIR inverse filters depend heavily on partitioning approaches. Unit circle-based partitioning is a simple procedure but since it does not take into account the channel zero distribution and the FIR part length, its performance is limited for a given channel. Ring-based and optimum-partitioning approaches try to make an optimization with the parameters that unit circle-based approach does not have. As it is seen from Figure 2.11, the difference between the ring-based and optimum-partitioning case is more obvious when there are zeros close to each other. In this case, optimum-partitioning has the freedom to choose the appropriate zero and in this way it helps the FIR part for producing an effective homogenous zero distribution. But the ring-based approach can only select

a ring region to have the minimum LSE. In summary, ring-based design is suboptimum but its design process is more efficient than the optimum-partitioning. Furthermore the difference between the two designs can be observable only for some special channels.

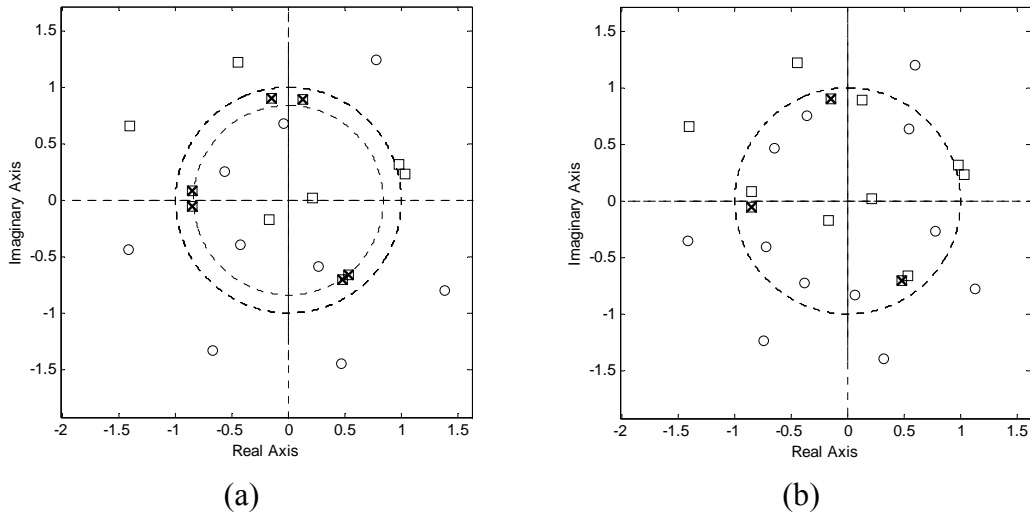


Figure 2.11 Zero plots of the selected channel zeros for (a) the ring-base (outer radius is one) and (b) optimum-partitioning case when $L=12$, $N=16$. o, \square and \times represent inverse filter zero, channel zero and IIR pole respectively.

The LSE performances of inverse filters for noiseless observation described above have been investigated in the following example.

Example 2.3: We have generated channels which have zeros uniformly distributed over the $[0, 2]$ radius. 100 trials are done with different channels. At each case, optimum ring radiuses and optimum-partitioning are found. In addition, best delays for both FIR and FIR-IIR filters are found separately. Figure 2.12 shows the LSE performances of FIR, FIR-IIR unit circle, FIR-IIR ring-based and FIR-IIR optimum-partitioning filters for different channel orders. Figure 2.12 a, b, c and d show the performances for $L=4$, $L=8$, $L=12$ and $L=16$ respectively. For small channel order, FIR-IIR unit circle filter have the same performance as the optimum FIR-IIR inverse filter. As the channel order increases, the difference becomes more

obvious. However, there is no significant difference between the ring-based FIR-IIR and optimum-partitioning FIR-IIR filters. Both of these filters are better than the FIR inverse filters by about 4-5dB. These simulations effectively show the performance gain, when the proposed FIR-IIR inverse filters are used. Figure 2.13 shows the average of the selected inner and outer ring radiuses for the channels in this example. These plots can be taken as a basis when someone is satisfied with a suboptimum but a quick solution to the design problem. The outer ring radius for different channel orders is about one while the inner radius is large for small N and it gets closer to zero as N becomes large. This figure shows that the use of the IIR part is less favoured when the channel order L is comparable with the inverse filter length N .

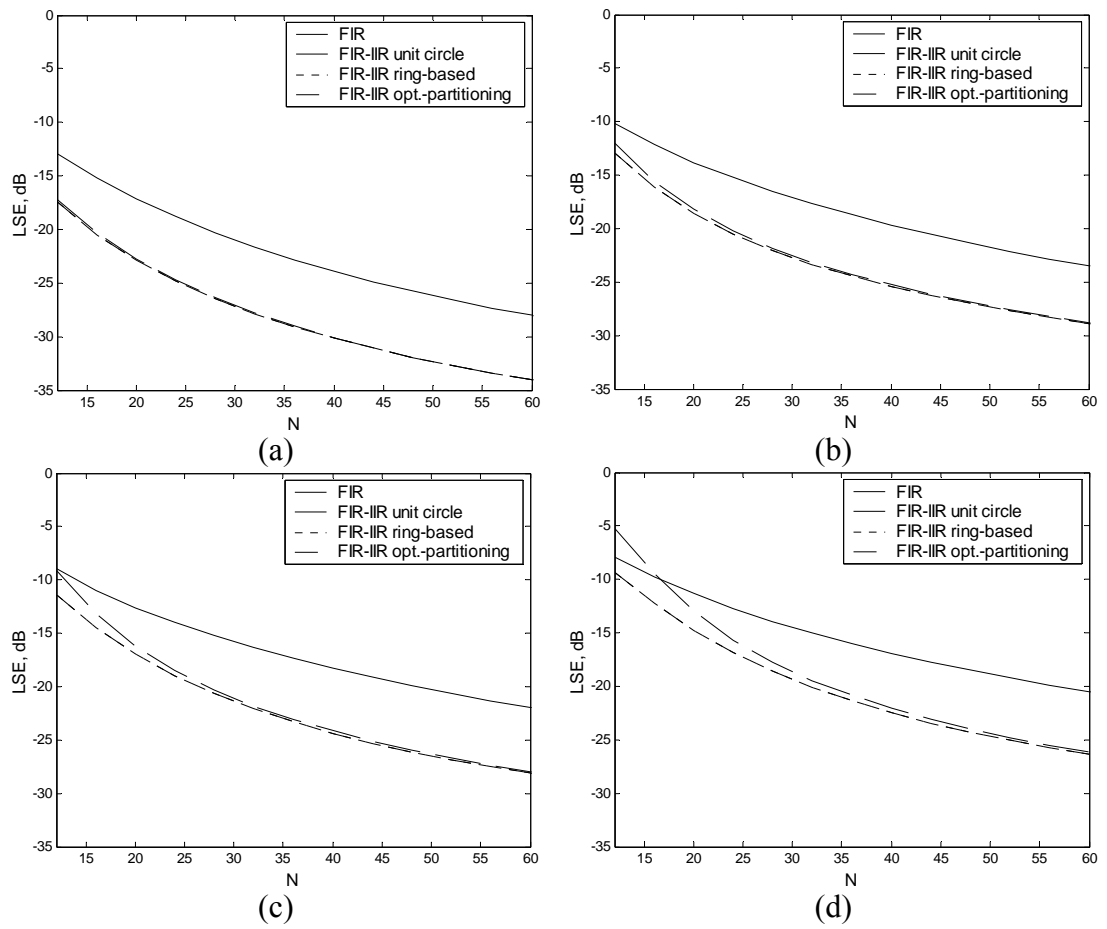


Figure 2.12 LSE performance of the deconvolution filters for different inverse filter lengths, (a) $L=4$, (b) $L=8$, (c) $L=12$, (d) $L=16$.

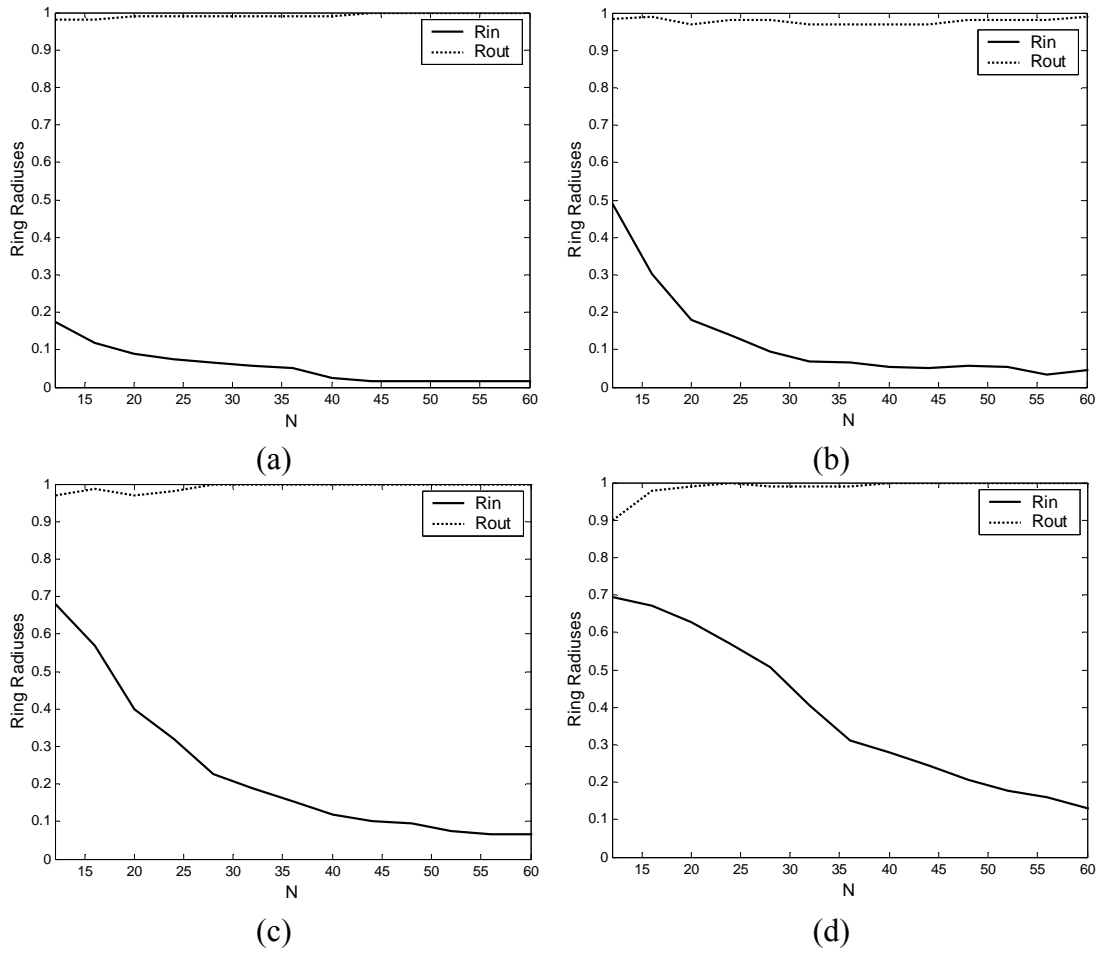


Figure 2.13 Inner and outer ring radiuses for the LSE case, (a) $L=4$, (b) $L=8$, (c) $L=12$, (d) $L=16$.

CHAPTER 3

INVERSE FILTERS FOR NOISY OBSERVATIONS

In this chapter, we will investigate the design problem of inverse filters when there is noise in the system with the system structure shown in Figure 3.1. In this case the overall error depends on both LSE obtained for noiseless observations and the output noise power. Especially for low SNR, output noise power plays an important role on the performance of inverse filter design. Two types of solutions will be presented, namely deterministic and statistical. Deterministic solution can be used in either LSE sense or directly by considering the effects of noise to choose the best delay and partition. LSE optimum deterministic inverse filter design for noisy observations is the same as for noiseless observations; no operation is done for noise sequence. In the second case, best delay selection and the partitioning are performed by considering the noise sequence. In the following section we will show the effect of noise power on the delay selection and partitioning. The performance of LSE optimum deterministic inverse filters for noisy observations will be investigated in chapter 4.

As a third solution, statistical inverse filters will also be investigated [20]. They use autocorrelation functions of input and noise sequences to minimize the MSE. In fact they are called MSE optimum inverse filters. In this chapter we will present MSE optimum FIR and partition-based FIR-IIR inverse filters and review the IIR Wiener filter.

3.1 Noise Considered Deterministic Inverse Filters

In the following section we will start with the deterministic FIR inverse filter and show the effect of noise on best delay selection. Then, we will present partition-

based FIR-IIR inverse filter and show the effect of noise on the partitioning.

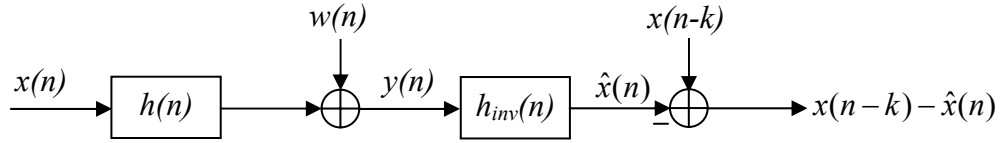


Figure 3.1 System structure of inverse filter design problem for noisy observations.

3.1.1 Noise Considered Deterministic FIR Inverse Filters

The design procedure of noise considered deterministic FIR inverse filters is the same as LSE optimum ones with the exception of noise effect on best delay selection. The effect of noise can be seen in the following example.

Example 3.1: We have chosen an arbitrary unit norm channel such as $h(n) = 0.44\delta(n) + 0.57\delta(n-1) + 0.60\delta(n-2) + 0.36\delta(n-3)$. Then, LSE optimum and noise considered FIR inverse filters are obtained. The LSE and MSE values corresponding to all the possible delays are given in Table 3.1. The noise sequence is chosen such that SNR=0 dB for the noise considered design. As it is seen the best delay is 5 for LSE optimum filter, while it is 2 for the other. If the delay found for LSE optimum inverse filter is considered to be used in noise considered inverse filter, it results a large MSE. Therefore in noise considered FIR inverse filter design, best delay should be found by taking into account the noise. Unfortunately, since noise considered design depends on not only the channel Toeplitz matrix, \mathbf{H} , but also the noise sequence, a simple delay selection procedure described in section 2.1 can not be used. Finding the best delay requires designing the inverse filters for all the possible delays and computing the MSE.

Table 3.1 Effect of delay on LSE and MSE

Delay	LSE (dB)	MSE (dB)
0	-2.7564	5.6440
1	-3.8101	3.7838
2	-2.7327	0.0646
3	-2.3504	1.1726
4	-4.1631	4.1678
5	-5.6105	6.8667
6	-5.5167	7.2934

3.1.2 Noise Considered Partition-Based FIR-IIR Inverse Filters

In FIR-IIR inverse filter design for noisy observations, the selection of appropriate partitioning is again the most critical point as it is in noiseless case. Again the partitioning can be performed by either ring-based or optimum-partitioning approaches. But in this case output noise power should also be considered for the selection of appropriate FIR and IIR parts. The effect of noise power on partitioning can be understood by considering the poles of IIR part.

Poles in FIR-IIR inverse filter produce spectral peaks in frequency domain and they can completely eliminate the spectral deeps produced by channel zeros. But on the other hand, they also increase the output noise power. The output noise power level increases when the poles come closer to the unit circle. Note that, the channel zeros close to the unit circle have large error contribution and using poles for these zeros inside the unit circle is suitable for noiseless case. But for noisy case, this solution may not give the desired performance depending on SNR; it leads to noise amplification. So a tradeoff should be performed between LSE and output noise power to achieve the best performance for noisy observations. The following example shows the effect of noise power on partitioning for ring-based and optimum-partitioning approaches.

Example 3.1: We have chosen a single channel with $L=8$ and the inverse filter with $N=16$. In order to show the effect of noise on the FIR-IIR inverse filter design, the design process is performed for SNR=0 dB and SNR=20 dB. Both ring-

based and optimum-partitioning is used in the design. The selected channel zeros (crossed) for each design can be seen in Figure 3.2.

For ring-based design, when SNR=0 dB, it can be seen that the innermost and outermost channel zeros inside the unit circle are located outside the ring region. On the other hand when SNR=20 dB, the outermost channel zero enters the ring region while the innermost three channel zeros are taken out from the ring region. A similar situation arises for optimum-partitioning design.

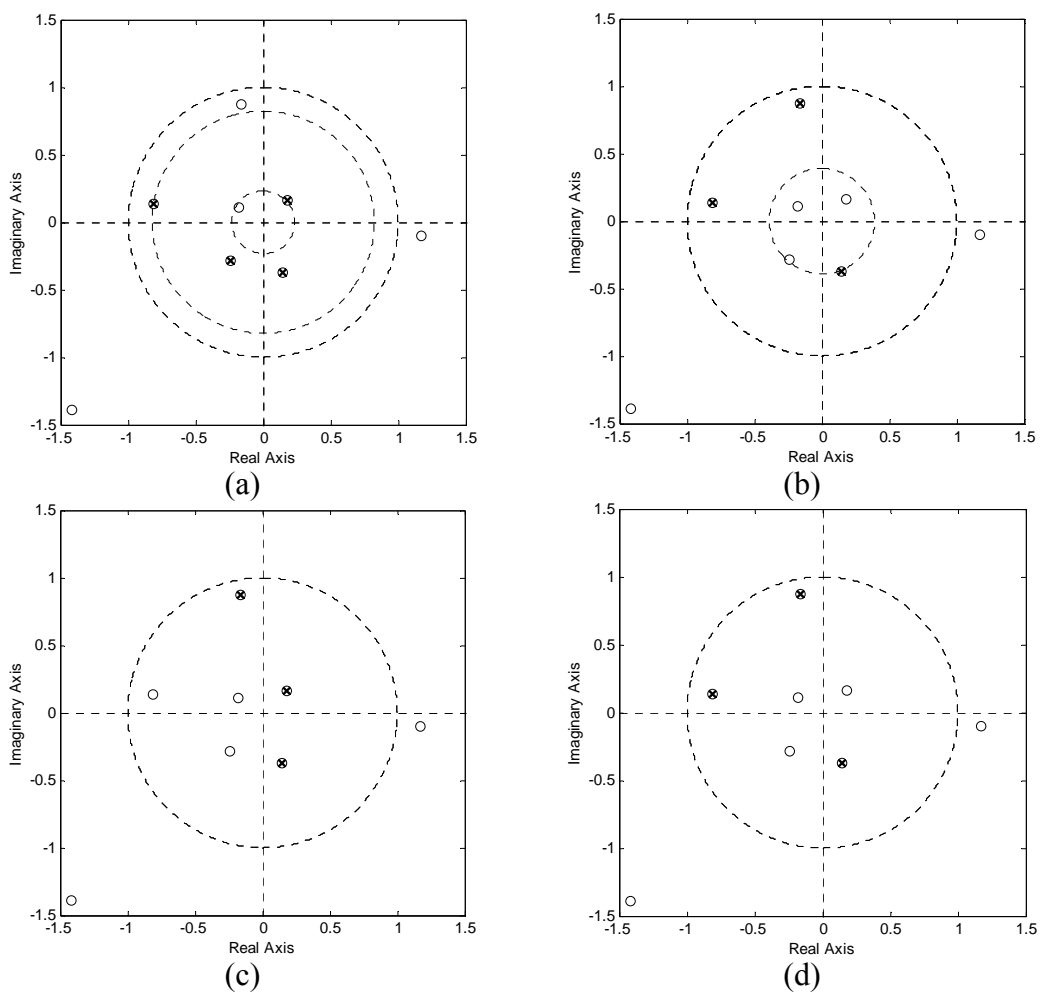


Figure 3.2 The pole-zero plots of FIR-IIR inverse filter. (a) ring-based for SNR=0 dB, (b) ring-based for SNR=20 dB, (c) optimum-partitioning for SNR=0 dB, (d) optimum-partitioning for SNR=20 dB. o represents channel zero and x represents pole of inverse filter.

At low SNR the channel zeros close to the unit circle can not be selected to construct the IIR part because of the large noise amplification, although it is the optimum selection in noiseless case. When SNR increases, the effect of noise amplification on the overall performance decreases and the channel zeros close to the unit circle are placed in the ring region to improve the LSE performance. But it should be note that, while these channel zeros enter the ring region, some channel zeros close to the origin are taken out from the ring region because of the FIR part length consideration. Optimum-partitioning works in a similar manner with a more freedom to select the channel zeros than ring-based approach. As a result, a tradeoff between output noise power and LSE should be performed for the inverse filter design for noisy observations.

3.2 MSE Optimum Statistical Inverse Filters

Statistical inverse filters use autocorrelation functions of input and noise sequences to minimize the MSE unlike the deterministic filters which use input and noise data itself. Statistical inverse filters have been widely investigated. In general, IIR Wiener filters are used for the MSE optimum deconvolution. Main disadvantage of this filter is that it is either noncausal or unstable. When the IIR Wiener filter is implemented in the frequency domain, it requires long FFT data sequences and therefore it is not very suitable for sample based and real-time applications. FIR Wiener filters are proposed in order to deconvolve the blurred images [21] for real-time implementations. In this section, we will start with the best delay MSE optimum FIR deconvolution filter formulation and present the MSE optimum FIR-IIR deconvolution filters [20]. In the last section we will review the IIR Wiener inverse filters.

3.2.1 MSE Optimum Best Delay FIR Deconvolution Filters

In this section, we will derive the MSE optimum best delay FIR deconvolution filter. In this case, we are trying to design an inverse filter $h_{inv}^{FIR}(n)$ with length N to have the minimum MSE when all the possible convolution delays are considered. Let $\hat{\mathbf{x}}$ be the vector form of the deconvolution output, then

$$\hat{\mathbf{x}} = \mathbf{X}\mathbf{H}\mathbf{h}_{inv}^{FIR} + \mathbf{W}\mathbf{h}_{inv}^{FIR} \quad (35)$$

where \mathbf{H} , \mathbf{X} , and \mathbf{W} are all full Toeplitz matrices. \mathbf{H} , \mathbf{X} , and \mathbf{W} are $(N+L) \times N$, $(N+L+M-1) \times (N+L)$, and $(N+L+M-1) \times N$ matrices respectively. We will define the error as,

$$\mathbf{e} = \mathbf{x} - \mathbf{C}\hat{\mathbf{x}} \quad (36)$$

where \mathbf{C} is a matrix to introduce the convolution delay and window the output sequence so that error is computed only at those samples where \mathbf{x} exists, namely,

$$\mathbf{C} = \begin{bmatrix} 0 & \cdots & 0 & 1 & 0 & \cdots & 0 \\ 0 & \cdots & 0 & 0 & 1 & \cdots & 0 \\ \vdots & \vdots & \vdots & \vdots & \vdots & \vdots & \vdots \\ 0 & \cdots & 0 & 0 & 0 & \cdots & 1 \end{bmatrix} \quad (37)$$

Then the MSE for the deconvolution can be written as,

$$\begin{aligned} E_{MSE} &= E\{\mathbf{e}^H \mathbf{e}\} \\ &= E\left\{\left(\mathbf{x} - \mathbf{C}\left[\mathbf{X}\mathbf{H}\mathbf{h}_{inv}^{FIR} + \mathbf{W}\mathbf{h}_{inv}^{FIR}\right]\right)^H \left(\mathbf{x} - \mathbf{C}\left[\mathbf{X}\mathbf{H}\mathbf{h}_{inv}^{FIR} + \mathbf{W}\mathbf{h}_{inv}^{FIR}\right]\right)\right\} \end{aligned} \quad (38)$$

In order to find the optimum filter, we will take the derivative of the MSE error with respect to the deconvolution filter. At this instant, we will assume that input, \mathbf{x} and noise, \mathbf{w} are uncorrelated. Then,

$$\frac{dE_{MSE}}{d(\mathbf{h}_{inv}^{FIR})^H} = E\left\{-\mathbf{H}^H \mathbf{X}^H \mathbf{C}^H \mathbf{x} + \mathbf{H}^H \mathbf{X}^H \mathbf{C}^H \mathbf{C} \mathbf{X} \mathbf{H} \mathbf{h}_{inv}^{FIR} + \mathbf{W}^H \mathbf{C}^H \mathbf{C} \mathbf{W} \mathbf{h}_{inv}^{FIR}\right\} = \mathbf{0} \quad (39)$$

We will define

$$\begin{aligned}
E\{\mathbf{X}^H \mathbf{C}^H \mathbf{x}\} &= \mathbf{r}_x^{(k)} \\
E\{\mathbf{X}^H \mathbf{C}^H \mathbf{C} \mathbf{X}\} &= \mathbf{R}_x^{(k)} \\
E\{\mathbf{W}^H \mathbf{C}^H \mathbf{C} \mathbf{W}\} &= \mathbf{R}_w^{(k)}
\end{aligned} \tag{40}$$

where $\mathbf{R}_x^{(k)}$ and $\mathbf{R}_w^{(k)}$ are the correlation matrices of input and noise with a delay of k . In general, $\mathbf{R}_x^{(k)}$ is different from \mathbf{R}_x and the two are same when \mathbf{x} is identically distributed. If we consider (39) and (40), we can write the inverse filter as,

$$\mathbf{h}_{inv}^{FIR} = \left(\mathbf{R}_w^{(k)} + \mathbf{H}^H \mathbf{R}_x^{(k)} \mathbf{H} \right)^{-1} \mathbf{H}^H \mathbf{r}_x^{(k)} \tag{41}$$

Given the above deconvolution filter, the next problem is the choice of the best delay k in a MSE optimum manner. To this end, we will consider the equation (38) and rewrite it as,

$$\begin{aligned}
E_{MSE} &= \mathbf{r}_x(0) + \left(\mathbf{h}_{inv}^{FIR} \right)^H \mathbf{H}^H \mathbf{R}_x^{(k)} \mathbf{H} \mathbf{h}_{inv}^{FIR} + \left(\mathbf{h}_{inv}^{FIR} \right)^H \mathbf{R}_w^{(k)} \mathbf{h}_{inv}^{FIR} \\
&\quad - \left(\mathbf{h}_{inv}^{FIR} \right)^H \mathbf{H}^H \mathbf{r}_x^{(k)} - \left(\mathbf{r}_x^{(k)} \right)^H \mathbf{H} \mathbf{h}_{inv}^{FIR}
\end{aligned} \tag{42}$$

For simplicity, we will assume that the input signal is white with a variance of σ_x^2 and noise which is uncorrelated with the input, is also white with a variance of σ_w^2 . Then we have the following expression for the inverse filter,

$$\mathbf{h}_{inv}^{FIR} = \left(\sigma_w^2 \mathbf{I} + \sigma_x^2 \mathbf{H}^H \mathbf{H} \right)^{-1} \mathbf{H}^H \mathbf{d} \sigma_x^2 \tag{43}$$

where we have taken $\mathbf{r}_x^{(k)} = \sigma_x^2 \mathbf{d}$ and $\mathbf{d} = [0 \ 0 \ \dots \ 0 \ 1 \ 0 \ \dots \ 0]^T$. We will denote the inverse matrix as,

$$\mathbf{S} = \left(\sigma_w^2 \mathbf{I} + \sigma_x^2 \mathbf{H}^H \mathbf{H} \right)^{-1} \tag{44}$$

Then we can write the MSE expression as,

$$\begin{aligned}
E_{MSE} &= \sigma_x^2 + \sigma_x^6 \mathbf{d}^H \mathbf{H} \mathbf{S}^H \mathbf{H}^H \mathbf{H} \mathbf{S} \mathbf{H}^H \mathbf{d} + \sigma_w^2 \sigma_x^4 \mathbf{d}^H \mathbf{H} \mathbf{S}^H \mathbf{S} \mathbf{H}^H \mathbf{d} \\
&\quad - 2 \sigma_x^4 \mathbf{d}^H \mathbf{H} \mathbf{S}^H \mathbf{H}^H \mathbf{d}
\end{aligned} \tag{45}$$

We will use the following notation,

$$\begin{aligned}
\mathbf{A} &= \mathbf{H} \mathbf{S}^H \mathbf{H}^H \\
\mathbf{B} &= \mathbf{H} \mathbf{S}^H
\end{aligned} \tag{46}$$

Then the MSE expression becomes

$$E_{MSE} = \sigma_x^2 + \sigma_x^6 \mathbf{d}^H \mathbf{A} \mathbf{A}^H \mathbf{d} + \sigma_w^2 \sigma_x^4 \mathbf{d}^H \mathbf{B} \mathbf{B}^H \mathbf{d} - 2\sigma_x^4 \mathbf{d}^H \mathbf{A} \mathbf{d} \quad (47)$$

When we consider that \mathbf{d} is a vector with all zeros except its k^{th} element, we find a simple expression for the MSE evaluation, namely,

$$E_{MSE} = \sigma_x^2 + \sigma_x^6 \sum_i |a(k, i)|^2 + \sigma_w^2 \sigma_x^4 \sum_i |b(k, i)|^2 - 2\sigma_x^4 |a(k, k)| \quad (48)$$

Therefore optimum delay k_{opt} is the value of k which minimizes (48),

$$k_{opt} = \arg \min_k (E_{MSE}) \quad (49)$$

When the input and noise statistics are not known, we need to use (41), (42) and (49) to find the MSE optimum FIR deconvolution filter. If the signal and noise have known statistics, then (43) and (48) can be used conveniently.

3.2.2 Best Delay FIR-IIR Partition-Based Deconvolution Filters

MSE performance of the FIR deconvolution filters can be improved by considering the partition-based FIR-IIR filters similar to their LSE counterparts. In the partition-based design, we will again consider the two alternatives, namely the optimum-partitioning and the ring-based design. At this point, it is important to clarify the MSE optimum partition-based FIR-IIR filter definition that we have employed in this thesis. Our target is to design the MSE optimum best delay FIR deconvolution filter for the group of channel zeros which are outside the selected partition, while the zeros inside the partition are handled by the all-pole IIR inverse filter. This IIR filter is the LSE optimum inverse filter and its LSE is zero since the channel zeros are completely compensated by the IIR inverse filter. However, MSE due to noise filtering is not zero for the IIR part. In our case, we design the IIR filter by selecting the zero grouping which returns the minimum MSE. In the optimum-partitioning case, we consider all the possible zero combinations inside the unit circle. When the ring-based partitioning is used, inner and outer ring radiuses are

jointly found to have the minimum MSE. Furthermore, the FIR part of the FIR-IIR inverse filter takes the IIR filtering into account to minimize the MSE.

Therefore the MSE optimum FIR-IIR deconvolution filter, $H_{MSE}^{FIR}(z)$, for a channel $H(z)=H_1(z)H_2(z)$ is,

$$H_{MSE}^{FIR}(z) = (H_1(z))^{-1} H_{2,inv}^{FIR}(z) = H_a(z)H_{2,inv}^{FIR}(z) \quad (50)$$

where $H_{2,inv}^{FIR}(z)$ is the FIR MSE best delay inverse filter of $H_2(z)$. We will consider $H_a(z)$ as the FIR equivalent of the $(H_1(z))^{-1}$ filter where the zeros of the $H_1(z)$ are determined by considering the optimum partitioning or ring-based approach. $H_a(z)$ can be found by impulse response truncation or by using the optimal H^∞ approximation [22].

The output for the partition-based FIR-IIR deconvolution filter can be written in vector form as,

$$\hat{\mathbf{x}} = \mathbf{X}\mathbf{H}_2\mathbf{h}_{2,inv}^{FIR} + \mathbf{W}\mathbf{H}_a\mathbf{h}_{2,inv}^{FIR} \quad (51)$$

where \mathbf{H}_2 is the Toeplitz convolution matrix for the reduced channel filter. We will define the error as,

$$\mathbf{e} = \mathbf{x} - \mathbf{C}\hat{\mathbf{x}} \quad (52)$$

and the MSE can be obtained as,

$$E_{MSE} = E\{\mathbf{e}^H\mathbf{e}\} = E\left\{\left(\mathbf{x} - \mathbf{C}\left[\mathbf{X}\mathbf{H}_2\mathbf{h}_{2,inv}^{FIR} + \mathbf{W}\mathbf{H}_a\mathbf{h}_{2,inv}^{FIR}\right]\right)^H \left(\mathbf{x} - \mathbf{C}\left[\mathbf{X}\mathbf{H}_2\mathbf{h}_{2,inv}^{FIR} + \mathbf{W}\mathbf{H}_a\mathbf{h}_{2,inv}^{FIR}\right]\right)\right\} \quad (53)$$

where we assumed that the input and noise are uncorrelated. We can take the derivative of the MSE with respect to the inverse filter vector in order to find the optimum filter, i.e.,

$$\frac{dE_{MSE}}{d(\mathbf{h}_{2,inv}^{FIR})^H} = E\left\{-\mathbf{H}_2^H\mathbf{X}^H\mathbf{C}^H\mathbf{x} + \mathbf{H}_2^H\mathbf{X}^H\mathbf{C}^H\mathbf{C}\mathbf{X}\mathbf{H}_2\mathbf{h}_{2,inv}^{FIR} + \mathbf{H}_a^H\mathbf{W}^H\mathbf{C}^H\mathbf{C}\mathbf{W}\mathbf{H}_a\mathbf{h}_{2,inv}^{FIR}\right\} = \mathbf{0} \quad (54)$$

From the above expression, FIR part of the FIR-IIR deconvolution filter is obtained as,

$$\mathbf{h}_{2,inv}^{FIR} = \left(\mathbf{H}_a^H \mathbf{R}_w^{(k)} \mathbf{H}_a + \mathbf{H}_2^H \mathbf{R}_x^{(k)} \mathbf{H}_2 \right)^{-1} \mathbf{H}_2^H \mathbf{r}_x^{(k)} \quad (55)$$

Then the FIR-IIR deconvolution filter, $H_{MSE}^{FIR}(z)$, can be written as in equation (50). It is possible to find the best delay for the FIR part of the FIR-IIR deconvolution filter similar to the previous case. We can write the MSE as,

$$\begin{aligned} E_{MSE} = & \mathbf{r}_x(0) - \left(\mathbf{r}_x^{(k)} \right)^H \mathbf{H}_2 \mathbf{h}_{2,inv}^{FIR} + \left(\mathbf{h}_{2,inv}^{FIR} \right)^H \mathbf{H}_a^H \mathbf{R}_w^{(k)} \mathbf{H}_a \mathbf{h}_{2,inv}^{FIR} \\ & - \left(\mathbf{h}_{2,inv}^{FIR} \right)^H \mathbf{H}_2^H \mathbf{r}_x^{(k)} + \left(\mathbf{h}_{2,inv}^{FIR} \right)^H \mathbf{H}_2^H \mathbf{R}_x^{(k)} \mathbf{H}_2 \mathbf{h}_{2,inv}^{FIR} \end{aligned} \quad (56)$$

We can assume that input and noise are white with variances σ_x^2 and σ_w^2 respectively. Then the inverse filter can be expressed as,

$$\mathbf{h}_{2,inv}^{FIR} = \left(\sigma_w^2 \mathbf{H}_a^H \mathbf{H}_a + \sigma_x^2 \mathbf{H}_2^H \mathbf{H}_2 \right)^{-1} \mathbf{H}_2^H \mathbf{d} \sigma_x^2 = \mathbf{S} \mathbf{H}_2^H \mathbf{d} \sigma_x^2 \quad (57)$$

where we have taken $\mathbf{r}_x^{(k)} = \sigma_x^2 \mathbf{d}$ similar to the previous part. If we use the inverse filter in the MSE expression, we can write the MSE as,

$$\begin{aligned} E_{MSE} = & \sigma_x^2 + \sigma_x^6 \mathbf{d}^H \mathbf{H}_2 \mathbf{S}^H \mathbf{H}_2^H \mathbf{H}_2 \mathbf{S} \mathbf{H}_2^H \mathbf{d} + \sigma_w^2 \sigma_x^4 \mathbf{d}^H \mathbf{H}_2 \mathbf{S}^H \mathbf{H}_a^H \mathbf{H}_a \mathbf{S} \mathbf{H}_2^H \mathbf{d} \\ & - 2 \sigma_x^4 \mathbf{d}^H \mathbf{H}_2 \mathbf{S}^H \mathbf{H}_2^H \mathbf{d} \end{aligned} \quad (58)$$

We will use the following notation,

$$\begin{aligned} \mathbf{A} &= \mathbf{H}_2 \mathbf{S}^H \mathbf{H}_2^H \\ \mathbf{B} &= \mathbf{H}_2 \mathbf{S}^H \mathbf{H}_a^H \end{aligned} \quad (59)$$

Then the MSE expression becomes

$$E_{MSE} = \sigma_x^2 + \sigma_x^6 \mathbf{d}^H \mathbf{A} \mathbf{A}^H \mathbf{d} + \sigma_w^2 \sigma_x^4 \mathbf{d}^H \mathbf{B} \mathbf{B}^H \mathbf{d} - 2 \sigma_x^4 \mathbf{d}^H \mathbf{A} \mathbf{d} \quad (60)$$

which is exactly the same expression as in the FIR case except now \mathbf{A} and \mathbf{B} are defined as in (59). A simple expression for the MSE evaluation is,

$$E_{MSE} = \sigma_x^2 + \sigma_x^6 \sum_i |a(k, i)|^2 + \sigma_w^2 \sigma_x^4 \sum_i |b(k, i)|^2 - 2 \sigma_x^4 |a(k, k)| \quad (61)$$

which is similar to the FIR case. Then the optimum delay k_{opt} is found as,

$$k_{opt} = \arg \min_k (E_{MSE}) \quad (62)$$

When the input and noise statistics are not known, we can use the expressions in (55), (56) and (62) in order to find the FIR-IIR deconvolution filter. If the input and noise are assumed to be white, then (57) and (61) can be employed for this purpose. During the design of the FIR-IIR deconvolution filters, we consider all the possible channel zero partitions and find the minimum MSE for each. Then, optimum FIR-IIR deconvolution filter is found as the one which returns the minimum MSE of all.

3.2.3 IIR Wiener Filters

IIR Wiener deconvolution filters are MSE optimum filters and they are used extensively in a variety of different fields. These filters are noncausal and therefore not very suitable for real-time applications. In general, input and noise statistics should be estimated before the design of the IIR Wiener filter. It is known that these filters are sensitive to the accuracy of the estimation. In [16] and [23], this point is elaborated and robust methods are proposed for a better Wiener performance. We will compare the FIR-IIR partition based MSE optimum filters with the IIR Wiener filters in two cases, namely, when the required statistics are estimated and when the true statistics are used.

In the following part, we will review the IIR Wiener formulation as proposed in [8]. As it is seen in Figure 3.1, the noisy observation can be written as,

$$y(n) = x(n) * h(n) + w(n) \quad (63)$$

then the estimated signal at the receiver output can be written as,

$$\hat{x}(n) = y(n) * h_{inv}(n) = \sum_{l=-\infty}^{\infty} h_{inv}(l)y(n-l) \quad (64)$$

Note that we are assuming that the filter is noncausal. The filter coefficients $h_{inv}(n)$ that minimize the mean square error,

$$MSE = E \left\{ |x(n) - \hat{x}(n)|^2 \right\} \quad (65)$$

are the solution to the Wiener-Hopf equations, which, in the frequency domain, becomes

$$H(e^{j\omega}) = \frac{S_{xy}(e^{j\omega})}{S_y(e^{j\omega})} \quad (66)$$

Therefore, all that needs to be done in the design of $H(e^{j\omega})$ is to find the power spectral densities $S_{xy}(e^{j\omega})$ and $S_y(e^{j\omega})$. Since $w(n)$ is assumed to be uncorrelated with $x(n)$, then $w(n)$ will also be uncorrelated with $x(n)*h(n)$. As a result, the power spectral density of $y(n)$ is the sum of the power spectrum of $x(n)*h(n)$ and the power spectrum of $w(n)$,

$$S_y(e^{j\omega}) = S_x(e^{j\omega})|H(e^{j\omega})|^2 + S_w(e^{j\omega}) \quad (67)$$

In addition, the cross-power spectral density $S_{xy}(e^{j\omega})$ is

$$S_{xy}(e^{j\omega}) = S_x(e^{j\omega})H^*(e^{j\omega}) \quad (68)$$

Therefore, substituting equations (67) and (68) into equation (66) we find that the optimum Wiener filter for deconvolution is given by

$$H_{inv}^{IIR}(e^{j\omega}) = \frac{S_x(e^{j\omega})H^*(e^{j\omega})}{S_x(e^{j\omega})|H(e^{j\omega})|^2 + S_w(e^{j\omega})} \quad (69)$$

We can compare the IIR Wiener filter in (69) with the FIR Wiener deconvolution filter with best delay in (41). If we consider the Fourier domain expression for (41), we obtain a similar form like (69). They are different in the sense that (41) represents a FIR and causal filter and it uses the MSE optimum convolution delay. These factors make a significant difference between the performances of two deconvolution filters when we use the estimates for $S_x(e^{j\omega})$ and $S_w(e^{j\omega})$. This is especially the case when there are only finite number of samples for the estimation. It turns out that FIR and FIR-IIR filters are much less sensitive to the estimation errors.

CHAPTER 4

PERFORMANCE EVALUATIONS

In this chapter, we will investigate the performances of inverse filters described in the previous chapters for more general channels with Monte Carlo trials. Since the error performances of inverse filters depend on channel zero distribution, channel models affect the performances. Throughout this chapter we will use two channel models, namely Uniform and Gaussian distributed, for the trials.

Uniform distributed channels are created from the zeros uniformly distributed in the interval of $[0, 2]$ radius. But locating channel zeros on the z -plane is done in a special manner to obtain better uniform distribution. The z -plane is divided into nonoverlapping subrings in the range of $[0, 2]$ radius and the uniformly distributed random channel zeros are located inside each subring. The number of subrings depends on channel order and the type of channel coefficients, namely real or complex. For the complex channels the number of subrings is chosen as L , while it is either $L/2$ or $(L-1)/2$ depending on whether the channel order is even or odd for the real case.

Gaussian distributed channels are created in a simpler manner. The Gaussian distributed zeros are located on the z -plane without any limitation.

In this chapter, the real and complex channel coefficients will be used for these distributions. Note that, Gaussian distributed complex channel is also known as Rayleigh fading channel, which is the most commonly used channel model.

In this chapter, we will investigate the performances of deterministic and statistical inverse filters. Deterministic filters will be investigated for noiseless and noisy observations. For the noisy observations LSE optimum and noise considered solutions will be given. The performances of statistical inverse filters will be

investigated in two cases. In the first case, we estimate the correlation functions for the input and noise from the available data. In the second case, we use the true correlation functions in the inverse filter design.

4.1 Deterministic Inverse Filters

In this section, we will investigate the effect of delay selection and the error performance of deterministic inverse filters for noiseless and noisy observations.

4.1.1 Noiseless Observations

As it was seen in section 2.1, system delay is an important parameter in FIR inverse filter design. We showed the effect of delay selection on LSE performance in Table 2.1. In order to show the delay selection effect for general channels we have prepared the following example.

Example 4.1: In most applications the system delay is chosen as $(N+L)/2$, which is the midpoint of the cascaded channel and inverse filter structure length. This is a simple procedure and mostly performs well, but it is not the optimum solution. Best delay can be found by the procedure described in section 2.1. Uniform and Gaussian distributed channels with real and complex coefficients are used to compare these selection procedures. The order of the channels are selected as $L=8$. For all channel models, 100 trials are done with different channel coefficients and the LSE corresponding to the best delay and $(N+L)/2$ delay designs are found. The average of the LSE is shown in Figure 4.1. As it is seen, best delay design is always better than $(N+L)/2$ delay design by about 1-2 dB depending on the channel characteristics.

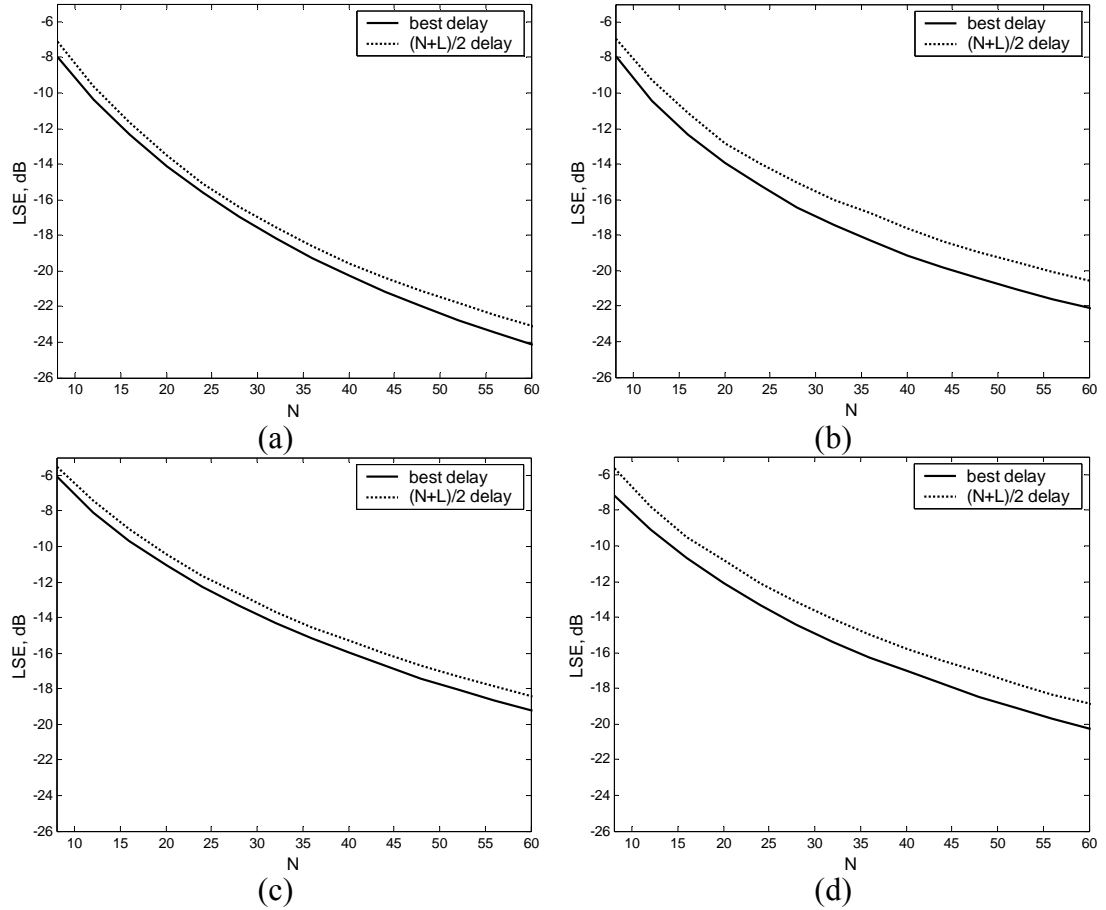


Figure 4.1 LSE performance of best and $(N+L)/2$ delay FIR inverse filters when $L=8$. (a) Uniform distributed complex channel, (b) Uniform distributed real channel, (c) Gaussian distributed complex channel, (d) Gaussian distributed real channel.

After a delay consideration, the LSE performances of inverse filters with best delay for different channel models have been investigated and the following example has been prepared.

Example 4.2: We have chosen Uniform and Gaussian distributed channels with real and complex coefficients. Channels are normalized and their order is selected as $L=12$. The system structure shown in Figure 1.1 is used and for each channel types 100 trials are done with different channel coefficients. At each case, optimum ring radiuses and optimum-partitioning are found. Figure 4.2 shows the LSE performances of FIR, FIR-IIR unit circle, FIR-IIR ring-based and FIR-IIR optimum-partitioning filters for different channel models. The average of the selected inner and outer ring radiuses is shown in Figure 4.3.

As it is seen from Figure 4.2, the LSE decreases with increasing inverse filter length, N , as expected. Two basic differences can be seen when uniform and Gaussian distributed channel models are compared. The first one is that, Gaussian distributed channel model causes larger LSE than normal distributed channel model especially for large N . The other one is about FIR-IIR unit circle inverse filter performance. At normal distributed channel model, it can be seen that for some N values FIR inverse filter performs better than FIR-IIR unit circle, while there is no such N value at Gaussian distributed channel model.

The explanation for these observations is related with the characteristics of channel model. While uniform distributed channel puts its zeros all over the defined region with equal probability, Gaussian distributed channel locates most of its zeros around the unit circle. Since the error contribution of the channel zeros close to the unit circle is large, Gaussian distributed channel zeros cause larger LSE. This fact can also explain the performance difference of FIR-IIR unit circle for these channel models. Since there are more channel zeros close to the origin and the error contribution of these zeros is small, FIR-IIR unit circle produces larger LSE for uniform distributed channel model especially when N is small because of unnecessary usage of poles. It can also be seen from Figure 4.3 that, Gaussian distributed channel model has larger ring region, which states that there is a small difference between FIR-IIR unit circle and ring-based design.

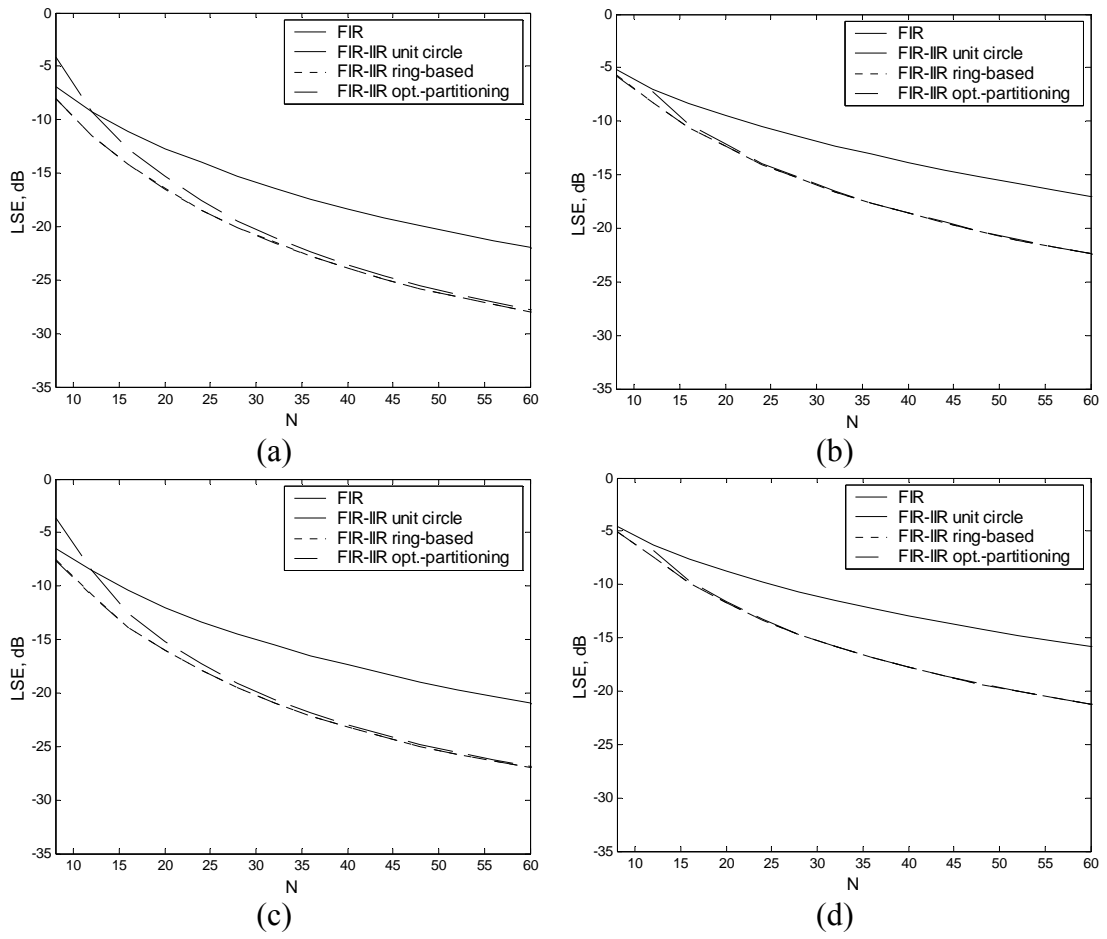


Figure 4.2 LSE performances of the inverse filters for different channel types, (a) uniform distributed real, (b) Gaussian distributed real, (c) uniform distributed complex, (d) Gaussian distributed complex channel.

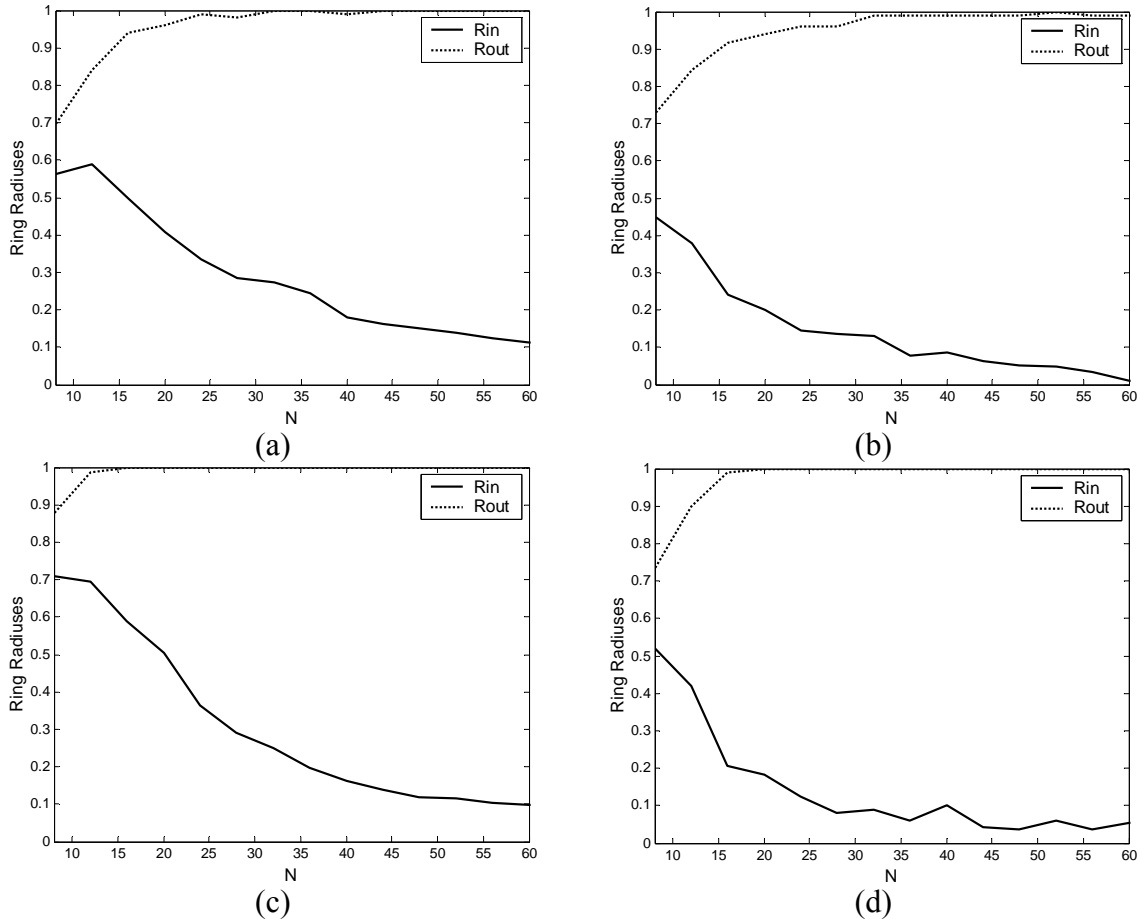


Figure 4.3 Inner and outer ring radiuses of ring-based FIR-IIR inverse filter for different channel types, (a) uniform distributed real, (b) Gaussian distributed real, (c) uniform distributed complex, (d) Gaussian distributed complex channel.

4.1.2 Noisy Observations

In this section, we will investigate the effectiveness of delay selection and the error performances of deterministic inverse filters when there is a system noise. Two design methods will be investigated, namely LSE optimum and noise considered. In LSE optimum design, there is no operation on noise data, while best delay selection and partitioning is performed by taking into account the noise data in noise considered design.

In the following example, we will compare the noise considered FIR inverse filter design with and without best delay property.

Example 4.3: We have considered a real, zero mean, Gaussian input signal with a variance $\sigma_x^2 = 1$. Four different channel models as in Example 4.2 with unit norm are used. The channel order and the inverse filter length are selected as $L=8$ and $N=32$, respectively. 100 trials are done with different input, channel and noise signals. Figure 4.4 shows the MSE performance of FIR inverse filter designed with noise considered deterministic approach for optimum and arbitrary delay cases. The delays are chosen as $k=0, 20$ and 32 respectively for the arbitrary delay designs. As it is seen from this figure, best delay FIR inverse filter performs significantly better than the other filters. The FIR inverse filter design with delay of 20 is closest to the best delay performance especially for high SNR. This delay value corresponds to the $(N+L)/2$ delay, which is used in most of applications. In low SNR, the closest one is 0 delay case. The MSE difference between best delay and arbitrary delay cases is changing with channel models. This difference is larger for real channels.

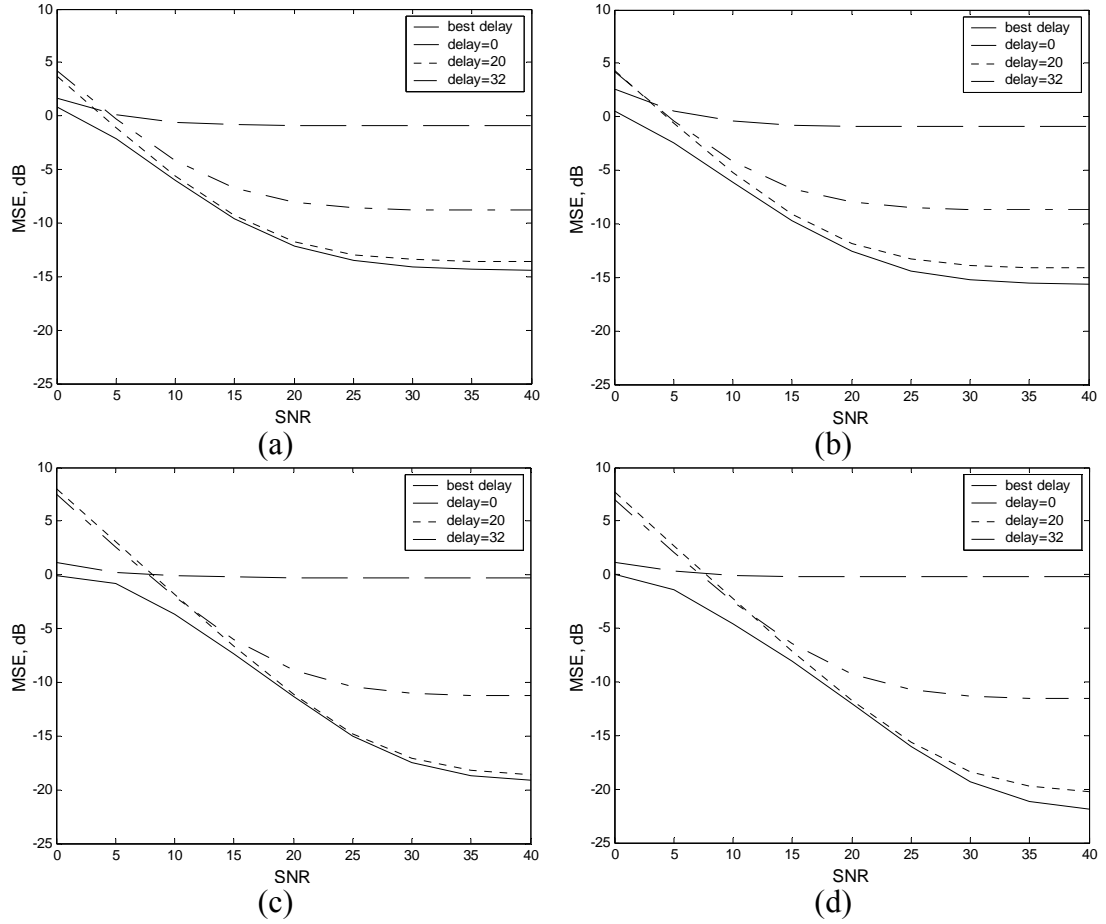


Figure 4.4 MSE performance of best and arbitrary delay FIR inverse filters designed with deterministic approach when $L=8$ and $N=32$. (a) Gaussian distributed complex channel, (b) Gaussian distributed real channel, (c) Uniform distributed complex channel, (d) Uniform distributed real channel.

In the following example, we will investigate the MSE performances of deterministic inverse filters for the LSE optimum and the noise considered design methods.

Example 4.4: We have considered a real, zero mean, Gaussian input signal with a variance $\sigma_x^2 = 1$. Noise and channel are also real sequences. Channel is selected as Gaussian distributed with unit norm. 100 trials are done with different input, channel and noise signals for channel orders of $L=8$, $L=12$ and the inverse filter length is selected as $N=24$. Figure 4.5 and Figure 4.6 show the MSE performances of inverse filters designed by LSE optimum and noise considered deterministic methods respectively. The average of selected inner and outer radiuses

of ring-based FIR-IIR inverse filter is shown in Figure 4.7 and Figure 4.8 for LSE optimum and noise considered deterministic methods respectively.

As it is seen from Figure 4.5, LSE optimum FIR-IIR inverse filters have approximately the same performances and they perform worse than the FIR inverse filter at low SNR. As the SNR increases FIR-IIR filters become better than the FIR filter. This result is obvious since there is no consideration about noise in LSE optimum design. The best delay selection and partitioning is performed to minimize the LSE but MSE is a function of LSE and output noise power. At low SNR, the output noise power is more effective on the MSE and as the SNR increases the LSE becomes more dominant. Therefore to minimize the MSE, a tradeoff should be made between LSE and output noise power. This is the case in noise considered deterministic inverse filters.

When the noise considered design is performed, at low SNR the performances of all the inverse filters become better compared with LSE optimum design. In this case, FIR-IIR ring-based and optimum-partitioning filters have similar performances. Their MSE response is approximately the same as the FIR inverse filter at low SNR and 5 dB better than the FIR response at high SNR. When channel order increases the performance difference decreases. It is also important to note that at low SNR, FIR-IIR unit circle has the worst performance while its performance is better than FIR inverse filter at high SNR similar to the performances of LSE optimum design. This fact can be explained by investigating Figure 4.7 and Figure 4.8. Since in LSE optimum deterministic design, ring region is obtained without considering the noise, inner and outer radiuses do not change with SNR; they are constant as can be seen in Figure 4.7. On the other hand as it is seen in Figure 4.6, outer ring radius changes significantly with respect to SNR, while inner radius changes slightly. For noise considered design, at low SNR, channel zeros close to the unit circle are not selected for the IIR part because of the large noise amplification of the poles used to cancel the effects of these zeros. They can be selected when the effect of output noise power on MSE performance decreases. Therefore FIR-IIR inverse filters based on LSE optimum design and noise considered FIR-IIR unit circle inverse filter have large output noise power at low SNR and their MSE performances are worse than the other inverse filters.

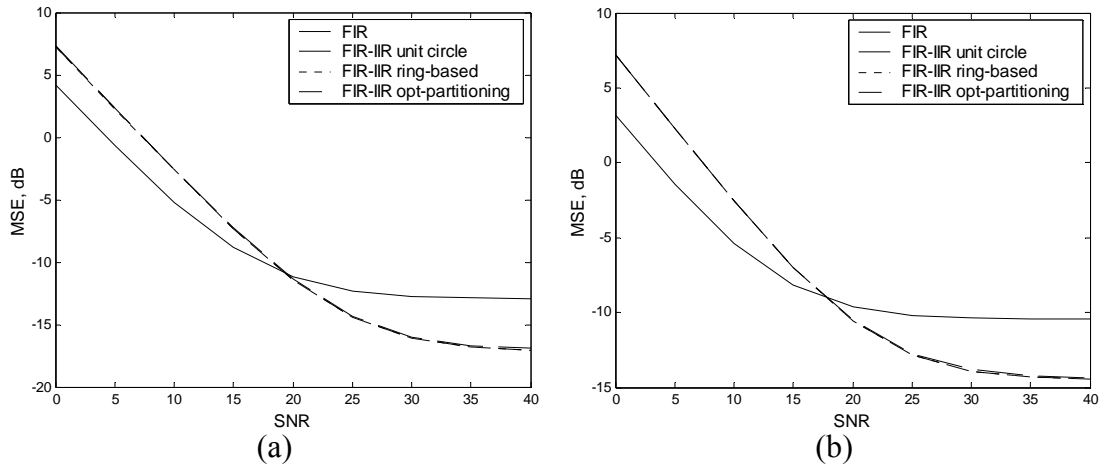


Figure 4.5 MSE performances of LSE optimum deterministic inverse filters when $N=24$, (a) $L=8$, (b) $L=12$.

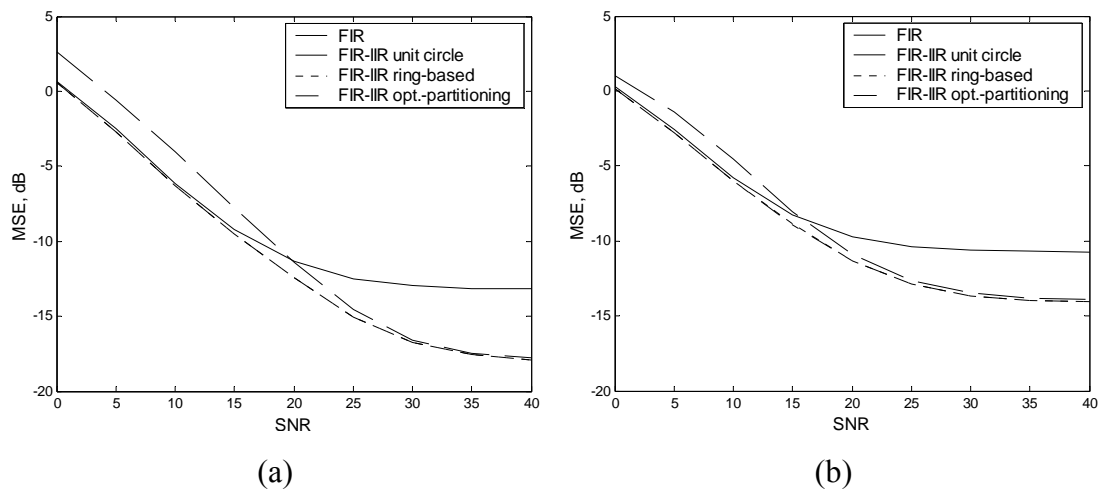


Figure 4.6 MSE performances of noise considered deterministic inverse filters when $N=24$, (a) $L=8$, (b) $L=12$.

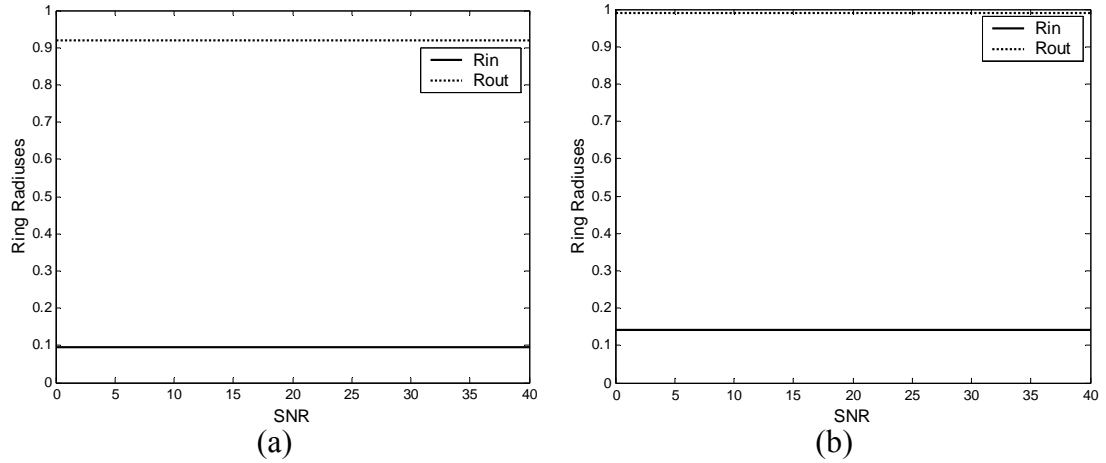


Figure 4.7 Inner and outer radiuses of ring-based FIR-IIR inverse filter for LSE optimum deterministic method when $N=24$, (a) $L=8$, (b) $L=12$.

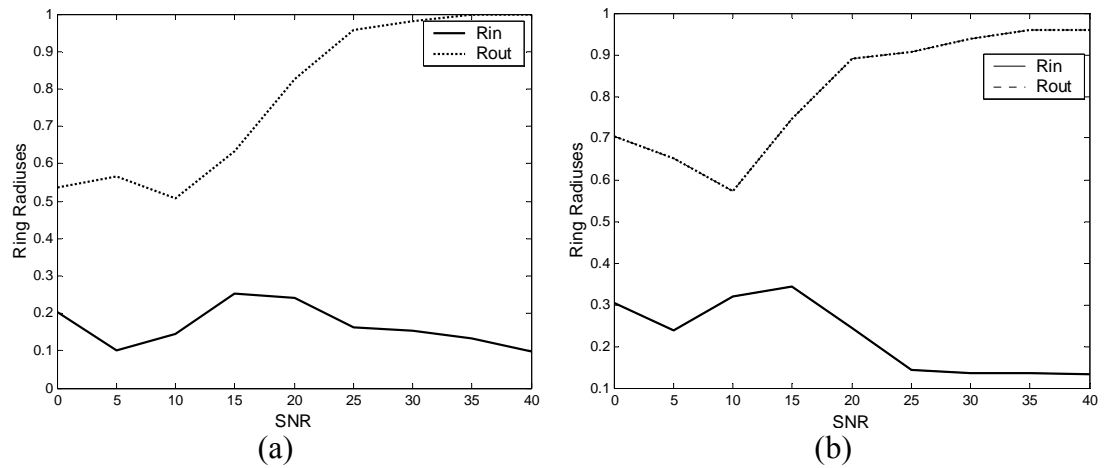


Figure 4.8 Inner and outer radiuses of ring-based FIR-IIR inverse filter for noise considered deterministic method when $N=24$, (a) $L=8$, (b) $L=12$.

4.2 Statistical Inverse Filters

In this section, we will investigate the performances of inverse filters based on statistical design method [20]. IIR Wiener filter performance will also be investigated in addition to the filters in deterministic design method. The performances will be investigated in two cases. In the first case, we will estimate the

correlation functions for the input and noise from the available data and equations (41) and (55) will be used for finding the FIR and FIR-IIR filters respectively. In the second case, we will use the true correlation functions in the inverse filter design.

Delay selection is an important part of the statistical FIR inverse filter design as it is in deterministic design. The MSE performance of FIR inverse filter designed with statistical approach for optimum and arbitrary delay cases are obtained by using the same parameters in Example 4.3. The results are shown in Figure 4.9. Again best delay FIR inverse filter performs significantly better than the other filters especially for Gaussian distributed channels. For uniform distributed channels, the difference between MSE performance of the best delay and the delay of 20 case is very small while it is approximately 1-2 dB for Gaussian distributed channels.

MSE performances of statistical inverse filters are compared by using the same parameters in Example 4.4. Figure 4.10 shows the performance of five filters for $L=8$ and $L=12$ respectively when the estimated correlation functions are used. It is seen from Figure 4.10 that IIR Wiener filter performance is almost independent from the channel order. FIR-IIR ring-based and optimum-partitioning filters have similar performances. Their MSE response is the same as the FIR MSE optimum inverse filter at low SNR and more than 5 dB better than the FIR response at high SNR. FIR-IIR unit circle filter performance is almost the same as the FIR-IIR ring-based and optimum-partitioning. These four filters perform better than the IIR Wiener filter at low SNR. As the SNR increases IIR Wiener filter eventually becomes better than these filters.

Figure 4.12 shows the results of the inverse filters when the true correlation functions are used. In this case, we used the expressions in (43) and (57) for the FIR and FIR-IIR filters respectively. When compared with Figure 4.10, it can be seen that, IIR Wiener filter is seriously affected by the estimation of the input and noise power spectral densities. The performances of FIR and FIR-IIR ring-based filters are similar to the case when the estimates are used. Therefore, they are more robust to the estimation errors. IIR Wiener filter has the best performance when the true correlation functions are used. It is followed by the FIR-IIR and FIR inverse filters respectively. We did not plot the FIR-IIR optimum-partitioning filter response in this figure since its performance is almost the same as the FIR-IIR ring-based filter.

Figure 4.11 and Figure 4.13 show the average of the inner and outer ring radiuses found during estimated and true correlation functions usage respectively. As the SNR increases inner radius gets closer to zero while outer radius goes to one. For low SNR, ring radiuses are close to each other indicating that FIR part is favoured over the IIR part in constructing the FIR-IIR inverse filter.

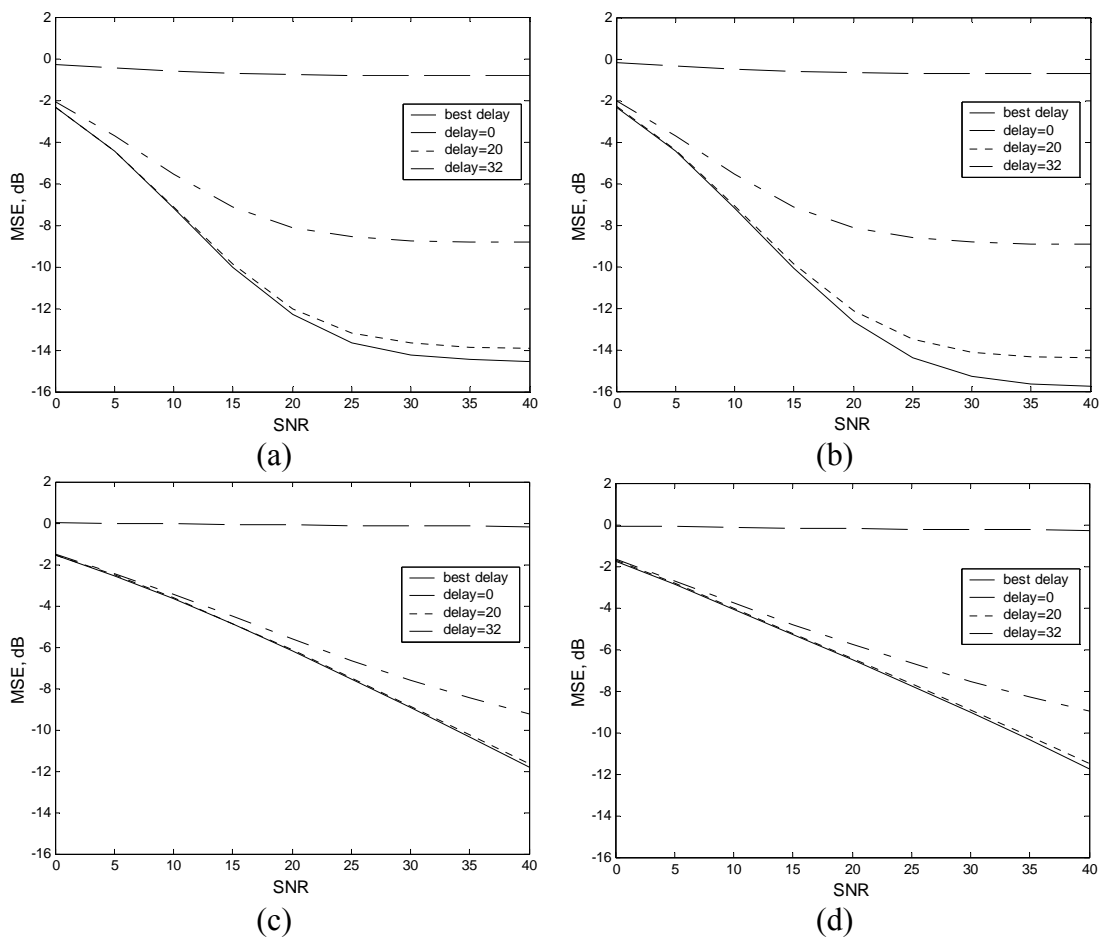


Figure 4.9 MSE performance of best and arbitrary delay FIR inverse filters designed with statistical approach when $L=8$ and $N=32$. (a) Gaussian distributed complex channel, (b) Gaussian distributed real channel, (c) Uniform distributed complex channel, (d) Uniform distributed real channel.

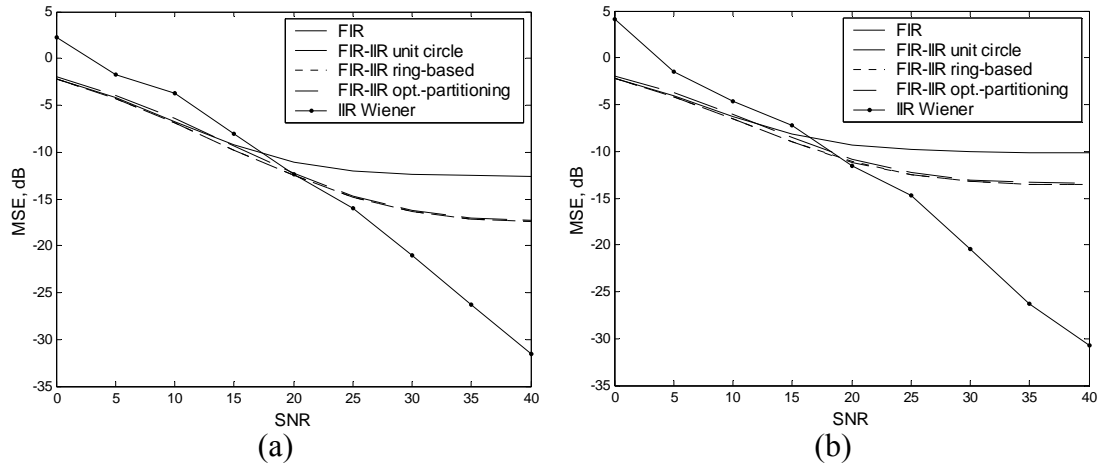


Figure 4.10 MSE performances of inverse filters for statistical method when the correlation estimates are used. $N=24$, (a) $L=8$, (b) $L=12$.

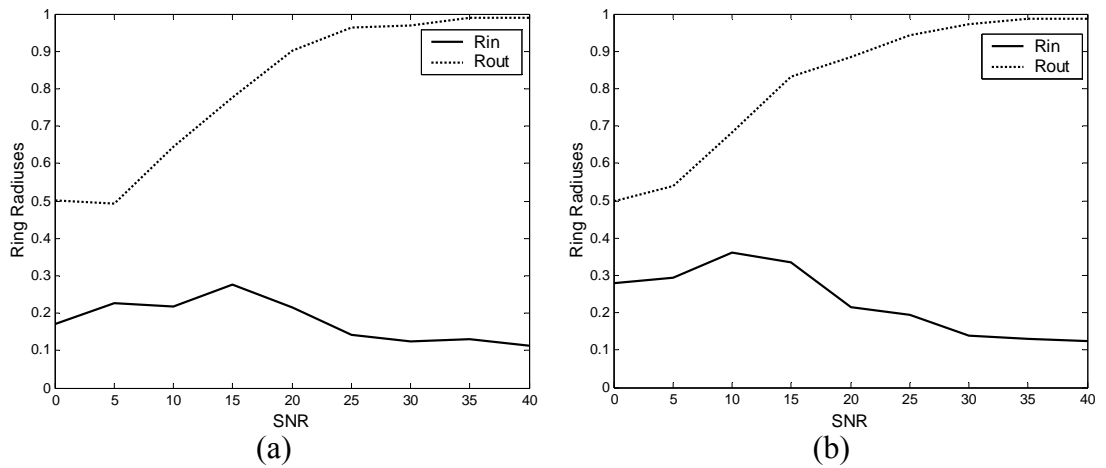


Figure 4.11 Inner and outer radiuses of ring-based FIR-IIR inverse filter for statistical method when the correlation estimates are used. $N=24$, (a) $L=8$, (b) $L=12$.

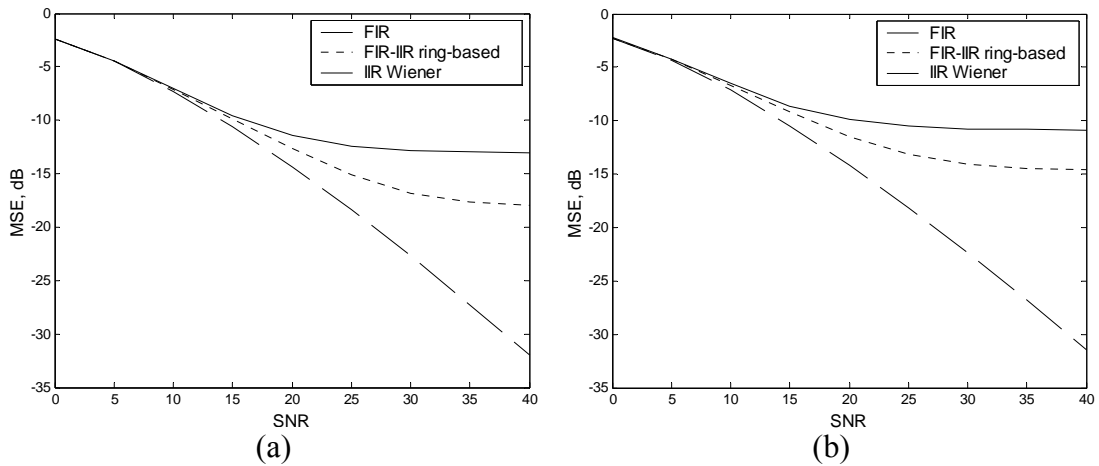


Figure 4.12 MSE performances of inverse filters for statistical method when true correlations are used. $N=24$, (a) $L=8$, (b) $L=12$.

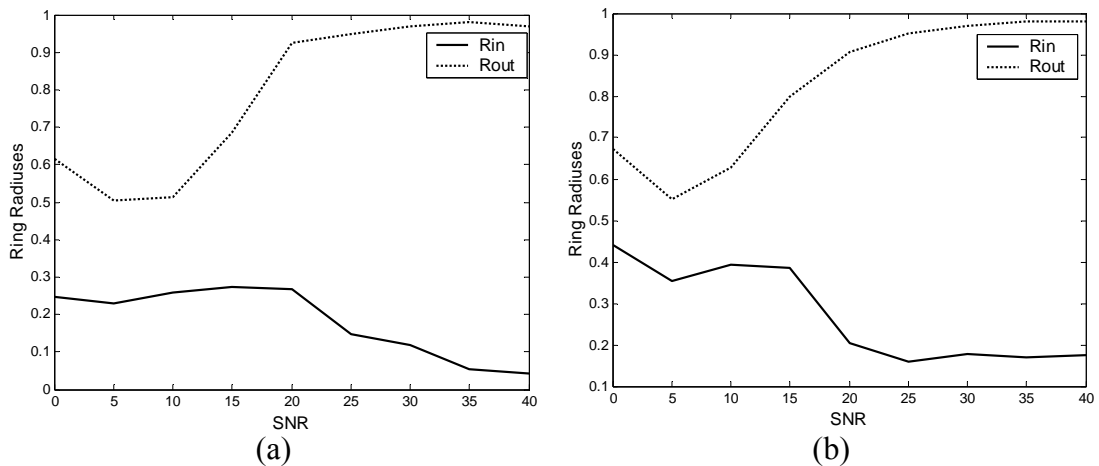


Figure 4.13 Inner and outer radiuses of ring-based FIR-IIR inverse filter for statistical method when the true correlations are used. $N=24$, (a) $L=8$, (b) $L=12$.

4.3 Noise Considered Deterministic versus Statistical Inverse Filters

In the following example, we have compared the performances of inverse filters for noise considered deterministic and MSE optimum statistical design methods.

Example 4.5: We have considered a real, zero mean, Gaussian input signal with a variance $\sigma_x^2 = 1$. Noise and channel are complex sequences and channel has unit norm with Gaussian distributed. 100 trials are done with different input, channel and noise signals for channel orders of $L=8$, $L=12$ and the inverse filter length is selected as $N=24$. For each trial, FIR and FIR-IIR optimum-partitioning inverse filters are designed by using noise considered deterministic and statistical methods with true correlation functions. Figure 4.14 shows the results. As it is seen, statistical method performs better than the noise considered deterministic method for both inverse filters at low SNR by about 1-2 dB. They are close to each other for the SNR values of 10-15 dB. For higher SNR, deterministic method performs better than the statistical method by about 0.5-1 dB. When the channel order increases, the characteristic does not change but the MSE of all filters increases, as expected. These results are reasonable. Because, statistical method uses complete information about noise data, while this is not the case for deterministic method. Therefore minimizing output noise power can be realized in statistical method more effectively. As the SNR increases since the effect of noise on MSE decreases, LSE becomes more dominant and deterministic method performs better. This is due to the fact that MSE optimum approach has certain assumptions which might not be valid at all times.

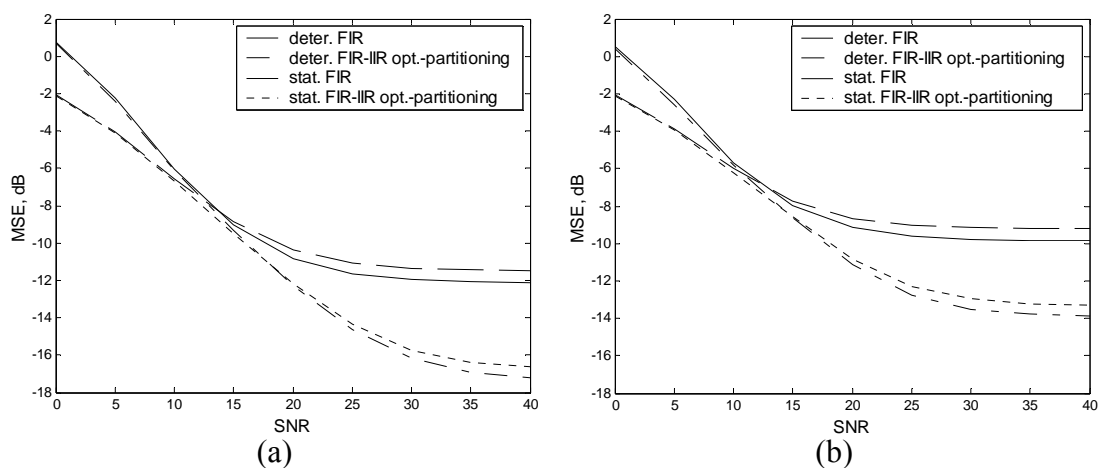


Figure 4.14 MSE performances of FIR, FIR-IIR optimum-partitioning inverse filters for statistical and deterministic methods when $N=24$, (a) $L=8$, (b) $L=12$.

CHAPTER 5

CONCLUSION

In this thesis, deconvolution problem is investigated. It is a problem of recovering the original source signal from the observed signal at the receiver. It is a major problem in many areas such as telecommunication, radar and sonar systems, astrophysics, seismology and so on. An effective solution for this problem is the inverse filter design. Many design procedures have been considered in the previous works. In this thesis, we have proposed a new inverse filtering method which is called partition-based FIR-IIR filters. In general, FIR-IIR inverse filters are hybrid filters composed of best delay FIR inverse filter and the all pole IIR inverse filter.

We have started with the inverse filter design for noiseless observation and reviewed the FIR inverse filters. It turns out that delay selection seriously affects the LSE. We have presented an efficient way of finding the best delay for the FIR inverse filter as proposed in [19]. Then we have investigated the factors that affect the LSE of the best delay FIR inverse filters. These factors are inverse filter length, N , channel order, L and the distribution of channel zeros on the z -plane. Also we have derived closed form LSE expressions as a function of channel coefficients for small channel order to effectively show the effect of these factors. It turns out that, increasing inverse filter length decreases the LSE, while LSE increases with the channel order. Channel zero positions also affect the LSE. LSE increases as the channel zero gets closer to the unit circle and it decreases when the zero is away from the unit circle. In addition, when two channel zeros come closer to each other, LSE increases. In order to understand these facts more clearly, we have looked the inverse filtering procedure of FIR inverse filter and seen that the overall system (cascaded channel and inverse filter) zeros are located uniformly on the z -plane to minimize the LSE.

We have also reviewed the IIR inverse filters. IIR filters are perfect inverse filter with no error for minimum-phase channels but for nonminimum-phase channels they have stability problems. On the other hand although FIR inverse filters always produce nonzero error, they have no such limitation. Therefore the idea of proposing FIR-IIR inverse filter is to combine the advantages of both FIR and IIR inverse filters in deconvolution problem. It should be note that for the fair comparison FIR-IIR inverse filter is designed in such a way that its complexity is equal to the complexity of the FIR inverse filter. The order of the FIR-IIR inverse filter is defined as the summation of the FIR part and IIR part orders. Therefore, we decrease the length of the FIR part of the FIR-IIR inverse filter by one for every pole in IIR part.

The most critical point in FIR-IIR inverse filter design is the selection of FIR and IIR parts or in other words partitioning the channel zeros into two regions. The channel zeros inside these regions are used to design the FIR and IIR parts of the FIR-IIR inverse filter. It is important to note that, the region used for IIR part design should not contain any channel zero outside the unit circle because of the stability problem. In this thesis, we have proposed three types of partitioning approaches, namely unit circle-based, ring-based and optimum-partitioning. In unit circle-based partitioning IIR part is constructed by the minimum-phase part of the channel, while maximum-phase part is used to obtain the FIR part. Ring-based partitioning divides the z-plane into two parts by a ring inside the unit circle. The ring is defined by the inner and outer radiuses. In optimum-partitioning IIR part is obtained by considering all the possible channel zero combinations inside the unit circle. So the region corresponding to the IIR part can be in any shape.

Unit circle-based partitioning does not take into account the factors that affect the LSE. Although IIR part produces no error, it may decrease the FIR part length so much that the LSE of the FIR-IIR inverse filter exceeds the LSE of the purely FIR inverse filter. Therefore, although unit circle-based partitioning is simple, its performance is not always better than FIR inverse filter. Ring-based partitioning uses a tradeoff between FIR part length and the error contribution of channel zeros inside the unit circle. It tries to use poles to eliminate the effect of channel zeros with a large error contribution inside the unit circle and leaves the channel zeros with a

small error contribution to the FIR part in order not to decrease the FIR part length so much. Thus it has a better solution than the unit circle based partitioning. Optimum-partitioning has more freedom to select the FIR and IIR parts than ring-based partitioning. The difference between these two approaches is very small and can be observed for special channels such as there are channel zeros on the same radius or close to each other. Therefore ring-based partitioning is suboptimum compared to the optimum-partitioning, but ring-based partitioning is always more efficient in the design procedure.

After investigating the inverse filter designs for noiseless observations, we have extended them to the noisy observations. In this case, inverse filter design has been investigated for the deterministic and statistical methods. For the noisy observations the overall error (MSE) is a function of LSE for noiseless observations and the output noise power and the inverse filters should be designed to minimize this error. Therefore inverse filters should use a tradeoff between LSE and the output noise power. Especially for low SNR, output noise power plays an important role on the performances. The effect of output noise power has been shown by comparing LSE optimum deterministic inverse filter with noise considered one. It turns out that, delay selection and partitioning procedures should consider the noise power to minimize the MSE.

For the statistical method, we have started with MSE optimum best delay FIR inverse filter formulations and extended it for the partition-based FIR-IIR inverse filter design. We have also reviewed the IIR Wiener filter, which is known as the MSE optimum inverse filter. The main disadvantage of IIR Wiener filter is it is either noncausal or unstable. It turns out that MSE optimum FIR-IIR inverse filters are better than FIR Wiener filters. When the true correlations are used IIR Wiener inverse filter is the best. On the other hand if the correlations are estimated, the performance of the IIR Wiener filter degrades significantly, while the FIR-IIR does not. Therefore, FIR-IIR filter is more robust to the estimation error than IIR Wiener filter.

From the comparison of deterministic and statistical methods, it has been seen that for low SNR statistical method has better performance by about 1-2 dB, while deterministic method performs better for high SNR by about 0.5-1 dB.

REFERENCES

- [1] T. Engin Tuncer, "A New Method For D-Dimensional Exact Deconvolution," *IEEE Trans. on Signal Processing*, vol. 47, No.5, pp. 1324-1334, May. 1999.
- [2] D.Zazula, L.Gyergyek "Direct frequency-domain deconvolution when the signals have no spectral inverse," *IEEE trans. on Signal Processing*, vol. 41, pp. 977-981, Feb. 1993.
- [3] P.L. Dragotti, M. Vetterli, "Deconvolution with wavelet footprints for ill-posed inverse problems " *IEEE Int. Conf. on ASSP*, pp.1257-1260, ICASSP-2002, May 2002.
- [4] J. Fan, J. Koo, "Wavelet Deconvolution," *IEEE Trans. on Information Theory*, Vol.48, pp. 734-747, March 2002.
- [5] C. Podilchuck, "Signal recovery from partial information," *Digital Signal Processing Handbook*, Boca Raton: CRC Press LLC, 1999.
- [6] Pratt, W.K and Davarian, F., "Fast computational techniques for pseudoinverse and Wiener image restoration", *IEEE Tans. Comp.*, 26, 571-580, 1977.
- [7] S. Haykin, *Adaptive Filter Theory*, Prentice Hall, Inc., 3rd edition, 1996.
- [8] Monson H. Hayes, *Statistical Signal Processing and Modelling*, John Wiley & Sons, Inc., New York, 1996.
- [9] T. Daboczi, T. B. Bako, "Inverse filtering of optical images," *IEEE Trans. on Inst. and Measurement.*, Vol.50, pp. 991-994, Aug. 2001.

- [10] Twomey, S., "On the numerical solution of fredholm integral equations of the first kind by the inversion of the linear system produced by quadrature", *J. assoc. Comp. Mach.*, 10, 97-101, 1963.
- [11] Tikonov, A.N., "Regularization of incorrectly posed problems", *Soviet Math.*, 4, 1624-1627, 1963.
- [12] Phillips, D.L., "A technique for the numerical solution of certain integral equations of the first kind", *J. Assoc. Comput. Mach.*, 9, 84-97, 1964.
- [13] C. W. Therrien, "Discrete Random Signals And Statistical Signal Processing," Prentice Hall, 1992.
- [14] John F. Doherty, "Channel Equalization as a Regularized Inverse Problem", *Digital Signal Processing Handbook*, Boca Raton: CRC Press LLC, 1999
- [15] Petre Stoica and Randolph L. Moses, *Introduction to Spectral Analysis*, Prentice Hall, New Jersey, 1997
- [16] H. Vincent Poor, "On robust Wiener filtering " *IEEE Trans. on Automatic Control*, Vol. 25, pp.531-536, June 1980.
- [17] T. Engin Tuncer, "Causal and stable FIR-IIRWiener Filters " *IEEE Workshop on Statistical Sig. Proc.*, St. Louis, USA, Sep. 28, 2003.
- [18] M. Miyoshi, Y. Kaneda, "Inverse Filtering of Room Acousics," *IEEE Trans. on ASSP.*, Vol. 36, No.2, pp. 145-152, Feb. 1988.
- [19] T. Engin Tuncer, "Deconvolution and Preequalization With Best Delay LS Inverse Filters", *Elsevier Science*, to be published on *Signal Processing*.
- [20] T. Engin Tuncer, Metin Aktaş "LSE and MSE Optimum Partition-based FIR-IIR Deconvolution Filters With Best Delay", submitted to *IEEE Trans. On Signal Processing*.
- [21] A. Jain, S. Ranganath, "Image restoration and edge extraction based on 2-D stochastic models " *Int. Conf. on Acoustics Speech and Signal Proc.*, ICASSP-1982, Vol.7, pp.1520-1523, May 1982.

[22] Y. Yamamoto, B.D.O. Anderson, M. Nagahara, Y. Koyanagi “Optimizing FIR approximation for discrete-time IIR filters ” *IEEE Signal Proc. Letters*, Vol. 10, pp.273-276, Sep. 2003.

[23] P. Comon, J.L. Lacoume, “Noise reduction for an estimated Wiener filter using noise references ” *IEEE Trans. on Inf. Theory*, Vol. 32, pp.310-313, March 1986.

[24] D.G. Manolakis, N. Kalouptsidis, G. Carayannis, “Fast algorithms for discrete-time wiener filters with optimum lag, ” *IEEE Tr. ASSP*, Vol.31, pp.168-179, Feb. 1983.

[25] I. Koltracht, T. Kailath, “Linear complexity parallel algorithm for discrete-time Wiener filters with optimum lag, ” *IEEE Tr. on ASSP*, Vol.36, pp.1680-81, Oct. 1988.

[26] Metin Aktas, T.Engin Tuncer, “Ring Based FIR-IIR Best Delay LS Inverse Filters ” *Int. Conf. on Acoustics Speech and Signal Proc.*, ICASSP-2004, Montreal, Canada, May 17, 2004.

APPENDIX A

This part includes the derivation of equation (25). Since LSE depends on inverse filter length, we will use N as a sub-index to determine the parameters at a specific inverse filter length.

First of all 7 properties of matrix \mathbf{B}_N , which is given in equation (21), will be represented and each of these properties will be proved. Then equation (25) will be obtained by using these properties with iterative manner.

A.i Properties of \mathbf{B}_N

Property 1

\mathbf{B}_N is idempotent matrix for all N values, which means that,

$$\mathbf{B}_N^2 = \mathbf{B}_N \quad \forall N$$

Proof:

$$\begin{aligned} \mathbf{B}_N^2 &= \mathbf{I} - \mathbf{H}_N \mathbf{H}_N^\dagger - \mathbf{H}_N \mathbf{H}_N^\dagger + \mathbf{H}_N \mathbf{H}_N^\dagger \mathbf{H}_N \mathbf{H}_N^\dagger \\ &= \mathbf{I} - \mathbf{H}_N \mathbf{H}_N^\dagger - \mathbf{H}_N \mathbf{H}_N^\dagger + \mathbf{H}_N \mathbf{I} \mathbf{H}_N^\dagger \\ &= \mathbf{I} - \mathbf{H}_N \mathbf{H}_N^\dagger \end{aligned}$$

$$\mathbf{B}_N^2 = \mathbf{B}_N \quad (\text{A.1})$$

Property 2

$$\mathbf{B}_N = \hat{\mathbf{B}}_{N-1} \mathbf{B}_N \quad \forall N$$

where,

$$\hat{\mathbf{B}}_{N-1} = \begin{bmatrix} \mathbf{B}_{N-1} & \mathbf{0} \\ \mathbf{0} & 1 \end{bmatrix}_{(N+L) \times (N+L)} \quad (\text{A.S1})$$

or,

$$\tilde{\mathbf{B}}_N = \mathbf{B}_{N-1} \tilde{\mathbf{B}}_N \quad \forall N$$

where,

$$\mathbf{B}_N = \begin{bmatrix} \tilde{\mathbf{B}}_N & \bar{\mathbf{b}}_N \\ \bar{\mathbf{b}}_N^H & b_N \end{bmatrix}_{(N+L) \times (N+L)} \quad (\text{A.S2})$$

$\bar{\mathbf{b}}_N$ is $(N+L-1) \times 1$ vector and b_N is scalar.

Proof:

The Toeplitz channel matrix \mathbf{H}_N can be rearranged as follows:

$$\mathbf{H}_N = [\mathbf{H} \quad \mathbf{P}]$$

where \mathbf{P} is $(N+L) \times 1$ vector and \mathbf{H} is $(N+L) \times (N-1)$ matrix such as,

$$\mathbf{H} = \begin{bmatrix} \mathbf{H}_{N-1} \\ \mathbf{0}_{1 \times (N-1)} \end{bmatrix}_{(N+L) \times (N-1)}$$

where \mathbf{H}_{N-1} is Toeplitz channel matrix with inverse filter length of $N-1$. Then pseudoinverse of \mathbf{H}_N can be written as,

$$\begin{aligned} \mathbf{H}_N^\dagger &= (\mathbf{H}_N^H \mathbf{H}_N)^{-1} \mathbf{H}_N^H \\ &= \left(\begin{bmatrix} \mathbf{H}^H \\ \mathbf{P}^H \end{bmatrix} [\mathbf{H} \quad \mathbf{P}] \right)^{-1} \begin{bmatrix} \mathbf{H}^H \\ \mathbf{P}^H \end{bmatrix} \\ &= \begin{bmatrix} \mathbf{H}^H \mathbf{H} & \mathbf{H}^H \mathbf{P} \\ \mathbf{P}^H \mathbf{H} & \mathbf{P}^H \mathbf{P} \end{bmatrix}^{-1} \begin{bmatrix} \mathbf{H}^H \\ \mathbf{P}^H \end{bmatrix} \end{aligned}$$

Let,

$$\begin{bmatrix} \mathbf{H}^H \mathbf{H} & \mathbf{H}^H \mathbf{P} \\ \mathbf{P}^H \mathbf{H} & \mathbf{P}^H \mathbf{P} \end{bmatrix}^{-1} = \begin{bmatrix} \mathbf{X} & \mathbf{Y} \\ \mathbf{Z} & \mathbf{W} \end{bmatrix} \quad (\text{A.2})$$

To find the unknowns \mathbf{X} , \mathbf{Y} , \mathbf{Z} , \mathbf{W} as a function of matrix \mathbf{H} and vector \mathbf{P} , multiply equation (A.2) with

$$\begin{bmatrix} \mathbf{H}^H \mathbf{H} & \mathbf{H}^H \mathbf{P} \\ \mathbf{P}^H \mathbf{H} & \mathbf{P}^H \mathbf{P} \end{bmatrix}$$

by left and right, then equalize it to identity. After that, the unknowns can be found by solving the equations obtained from matrix multiplications.

Let,

$$\mathbf{P}^H \mathbf{P} = k \quad (\text{A.3})$$

and,

$$\mathbf{U} = \mathbf{I} - \frac{1}{k} \mathbf{P} \mathbf{P}^H \quad (\text{A.4})$$

then the unknowns are:

$$\mathbf{X} = [\mathbf{H}^H \mathbf{U} \mathbf{H}]^{-1} \quad (\text{A.5})$$

$$\mathbf{Y} = -\frac{1}{k} \mathbf{X} \mathbf{H}^H \mathbf{P} \quad (\text{A.6})$$

$$\mathbf{Z} = -\frac{1}{k} \mathbf{P}^H \mathbf{H} \mathbf{X} \quad (\text{A.7})$$

$$\mathbf{W} = \frac{1}{k} \left(1 + \frac{1}{k} \mathbf{P}^H \mathbf{H} \mathbf{X} \mathbf{H}^H \mathbf{P} \right) \quad (\text{A.8})$$

Then, the pseudoinverse of \mathbf{H}_N can be written as,

$$\mathbf{H}_N^\dagger = \begin{bmatrix} \mathbf{X} & \mathbf{Y} \\ \mathbf{Z} & \mathbf{W} \end{bmatrix} \begin{bmatrix} \mathbf{H}^H \\ \mathbf{P}^H \end{bmatrix} = \begin{bmatrix} \mathbf{X} \mathbf{H}^H + \mathbf{Y} \mathbf{P}^H \\ \mathbf{Z} \mathbf{H}^H + \mathbf{W} \mathbf{P}^H \end{bmatrix} \quad (\text{A.9})$$

Finally, \mathbf{B}_N matrix can be written by using (21), (A.4), (A.6), (A.7), (A.8) and (A.9) as,

$$\begin{aligned} \mathbf{B}_N &= \mathbf{I} - [\mathbf{H} \quad \mathbf{P}] \begin{bmatrix} \mathbf{X} \mathbf{H}^H + \mathbf{Y} \mathbf{P}^H \\ \mathbf{Z} \mathbf{H}^H + \mathbf{W} \mathbf{P}^H \end{bmatrix} \\ \mathbf{B}_N &= \mathbf{I} - (\mathbf{H} \mathbf{X} \mathbf{H}^H + \mathbf{H} \mathbf{Y} \mathbf{P}^H + \mathbf{P} \mathbf{Z} \mathbf{H}^H + \mathbf{P} \mathbf{W} \mathbf{P}^H) \\ \mathbf{B}_N &= \mathbf{U} (\mathbf{I} - \mathbf{H} \mathbf{X} \mathbf{H}^H \mathbf{U}) \end{aligned} \quad (\text{A.10})$$

To complete the proof, the relation between $\hat{\mathbf{B}}_{N-1}$ and \mathbf{B}_N should be found. Like in equation (21), \mathbf{B}_{N-1} can be written as,

$$\mathbf{B}_{N-1} = \mathbf{I} - \mathbf{H}_{N-1} (\mathbf{H}_{N-1}^H \mathbf{H}_{N-1})^{-1} \mathbf{H}_{N-1}^H \quad (\text{A.11})$$

To be able to define $\hat{\mathbf{B}}_{N-1}$, let us investigate the following equations,

$$\begin{aligned} \mathbf{I} - \mathbf{H} (\mathbf{H}^H \mathbf{H})^{-1} \mathbf{H}^H &= \mathbf{I} - \begin{bmatrix} \mathbf{H}_{N-1} \\ \mathbf{0} \end{bmatrix} \left(\begin{bmatrix} \mathbf{H}_{N-1}^H & \mathbf{0} \end{bmatrix} \begin{bmatrix} \mathbf{H}_{N-1} \\ \mathbf{0} \end{bmatrix} \right)^{-1} \begin{bmatrix} \mathbf{H}_{N-1}^H & \mathbf{0} \end{bmatrix} \\ &= \begin{bmatrix} \mathbf{I} - \mathbf{H}_{N-1} (\mathbf{H}_{N-1}^H \mathbf{H}_{N-1})^{-1} \mathbf{H}_{N-1}^H & \mathbf{0} \\ \mathbf{0} & 1 \end{bmatrix} \\ \mathbf{I} - \mathbf{H} (\mathbf{H}^H \mathbf{H})^{-1} \mathbf{H}^H &= \begin{bmatrix} \mathbf{B}_{N-1} & \mathbf{0} \\ \mathbf{0} & 1 \end{bmatrix} \\ \Rightarrow \hat{\mathbf{B}}_{N-1} &= \mathbf{I} - \mathbf{H} (\mathbf{H}^H \mathbf{H})^{-1} \mathbf{H}^H \end{aligned} \quad (\text{A.12})$$

Let us rearrange the matrix \mathbf{U} in equation (A.4) as,

$$\mathbf{U} = \mathbf{I} + \mathbf{M} \quad (\text{A.13})$$

where

$$\mathbf{M} = -\frac{1}{k} \mathbf{P} \mathbf{P}^H \quad (\text{A.14})$$

then, equation (A.5) becomes,

$$\mathbf{X} = \left[\mathbf{H}^H (\mathbf{I} + \mathbf{M}) \mathbf{H} \right]^{-1} = \left[\mathbf{H}^H \mathbf{H} + \mathbf{H}^H \mathbf{M} \mathbf{H} \right]^{-1} \quad (\text{A.15})$$

To represent the matrix \mathbf{B}_N as a function of matrix $\hat{\mathbf{B}}_{N-1}$, matrix inversion lemma [7] is used,

$$[\mathbf{A} + \mathbf{BCD}]^{-1} = \mathbf{A}^{-1} - \mathbf{A}^{-1} \mathbf{B} [\mathbf{DA}^{-1} \mathbf{B} + \mathbf{C}^{-1}]^{-1} \mathbf{DA}^{-1}$$

In our case;

$$\mathbf{A} = \mathbf{H}^H \mathbf{H}; \quad \mathbf{B} = \mathbf{H}^H \mathbf{M} \mathbf{H}; \quad \mathbf{C} = \mathbf{I}; \quad \mathbf{D} = \mathbf{I}$$

So equation (A.15) can be rewritten as,

$$\mathbf{X} = (\mathbf{H}^H \mathbf{H})^{-1} - (\mathbf{H}^H \mathbf{H})^{-1} \mathbf{H}^H \mathbf{M} \mathbf{H} \left[(\mathbf{H}^H \mathbf{H})^{-1} \mathbf{H}^H \mathbf{M} \mathbf{H} + \mathbf{I} \right]^{-1} (\mathbf{H}^H \mathbf{H})^{-1} \quad (\text{A.16})$$

By using equations (A.10), (A.12), (A.13) and (A.16), \mathbf{B}_N can be found as,

$$\mathbf{B}_N = \mathbf{U} - \mathbf{U}^2 + \mathbf{U}\hat{\mathbf{B}}_{N-1}\mathbf{U} + \left(\mathbf{U}^2 - \mathbf{U} - \mathbf{U}\hat{\mathbf{B}}_{N-1}\mathbf{U} + \mathbf{U}\hat{\mathbf{B}}_{N-1}\right)\mathbf{H}\left[\mathbf{H}^H\mathbf{U}\mathbf{H}\right]^{-1}\mathbf{H}^H\mathbf{U} \quad (\text{A.17})$$

Let us investigate \mathbf{U}^2 matrix,

$$\begin{aligned} \mathbf{U}^2 &= \mathbf{I} - \frac{1}{k}\mathbf{P}\mathbf{P}^H - \frac{1}{k}\mathbf{P}\mathbf{P}^H + \frac{1}{k^2}\mathbf{P}\mathbf{P}^H\mathbf{P}\mathbf{P}^H \\ &= \mathbf{I} - \frac{1}{k}\mathbf{P}\mathbf{P}^H - \frac{1}{k}\mathbf{P}\mathbf{P}^H + \frac{1}{k^2}\mathbf{P}k\mathbf{P}^H \\ &= \mathbf{I} - \frac{1}{k}\mathbf{P}\mathbf{P}^H \\ \mathbf{U}^2 &= \mathbf{U} \end{aligned}$$

So, \mathbf{B}_N in equation (A.17) becomes,

$$\begin{aligned} \mathbf{B}_N &= \mathbf{U}\hat{\mathbf{B}}_{N-1}\mathbf{U} + \left(-\mathbf{U}\hat{\mathbf{B}}_{N-1}\mathbf{U} + \mathbf{U}\hat{\mathbf{B}}_{N-1}\right)\mathbf{H}\left[\left(\mathbf{H}^H\mathbf{H}\right)^{-1}\mathbf{H}^H\mathbf{U}\mathbf{H}\right]^{-1}\left(\mathbf{H}^H\mathbf{H}\right)^{-1}\mathbf{H}^H\mathbf{U} \\ \mathbf{B}_N &= \mathbf{U}\hat{\mathbf{B}}_{N-1}\mathbf{U} + \left(-\mathbf{U}\hat{\mathbf{B}}_{N-1}\mathbf{U} + \mathbf{U}\hat{\mathbf{B}}_{N-1}\right)\mathbf{H}\left(\mathbf{H}^H\mathbf{U}\mathbf{H}\right)^{-1}\left(\mathbf{H}^H\mathbf{H}\right)^{-1}\mathbf{H}^H\mathbf{U} \\ \mathbf{B}_N &= \mathbf{U}\hat{\mathbf{B}}_{N-1}\mathbf{U}\left[\mathbf{I} - \mathbf{H}\left(\mathbf{H}^H\mathbf{U}\mathbf{H}\right)^{-1}\mathbf{H}^H\mathbf{U}\right] + \mathbf{U}\hat{\mathbf{B}}_{N-1}\mathbf{H}\left(\mathbf{H}^H\mathbf{U}\mathbf{H}\right)^{-1}\mathbf{H}^H\mathbf{U} \end{aligned} \quad (\text{A.18})$$

The second term on right hand side of equation (A.18) vanishes. This can be seen by multiplying equation (A.12) with \mathbf{H} by right,

$$\hat{\mathbf{B}}_{N-1}\mathbf{H} = \mathbf{H} - \mathbf{H}\left(\mathbf{H}^H\mathbf{H}\right)^{-1}\mathbf{H}^H\mathbf{H} = \mathbf{0} \quad (\text{A.19})$$

So equation (A.18) reduces to,

$$\mathbf{B}_N = \mathbf{U}\hat{\mathbf{B}}_{N-1}\mathbf{U}\left[\mathbf{I} - \mathbf{H}\mathbf{X}\mathbf{H}^H\mathbf{U}\right] \quad (\text{A.20})$$

Substitute equation (A.10) into equation (A.20)

$$\mathbf{B}_N = \mathbf{U}\hat{\mathbf{B}}_{N-1}\mathbf{B}_N \quad (\text{A.21})$$

Equation (A.21) can be rewritten by using (A.10), (A.12) and (A.13) as,

$$\mathbf{B}_N = \hat{\mathbf{B}}_{N-1}\mathbf{B}_N + \mathbf{M}\mathbf{U}\left[\mathbf{I} - \mathbf{H}\mathbf{X}\mathbf{H}^H\mathbf{U}\right] \quad (\text{A.22})$$

The second term on the right hand side of (A.22) vanishes, because,

$$\begin{aligned} \mathbf{M}\mathbf{U} &= \mathbf{M}(\mathbf{I} + \mathbf{M}) \\ &= -\frac{1}{k}\mathbf{P}\mathbf{P}^H + \frac{1}{k^2}\mathbf{P}\mathbf{P}^H\mathbf{P}\mathbf{P}^H \end{aligned}$$

$$= -\frac{1}{k} \mathbf{P} \mathbf{P}^H + \frac{1}{k^2} \mathbf{P} k \mathbf{P}^H$$

$$\mathbf{M} \mathbf{U} = \mathbf{0}$$

So equation (A.22) becomes,

$$\mathbf{B}_N = \hat{\mathbf{B}}_{N-1} \mathbf{B}_N \quad (\text{A.23})$$

Because of the definitions of $\hat{\mathbf{B}}_{N-1}$, $\tilde{\mathbf{B}}_N$ and equation (A.23) the following equation is also valid,

$$\tilde{\mathbf{B}}_N = \mathbf{B}_{N-1} \tilde{\mathbf{B}}_N \quad (\text{A.24})$$

Property 3:

$$\mathbf{B}_N^H = \mathbf{B}_N \quad \forall N$$

Proof:

$$\begin{aligned} \mathbf{B}_N^H &= (\mathbf{I} - \mathbf{H}_N \mathbf{H}_N^\dagger)^H \\ &= \left(\mathbf{I} - \mathbf{H}_N (\mathbf{H}_N^H \mathbf{H}_N)^{-1} \mathbf{H}_N^H \right)^H \\ &= \left(\mathbf{I} - \mathbf{H}_N \left[(\mathbf{H}_N^H \mathbf{H}_N)^H \right]^{-1} \mathbf{H}_N^H \right) \\ &= \left(\mathbf{I} - \mathbf{H}_N (\mathbf{H}_N^H \mathbf{H}_N)^{-1} \mathbf{H}_N^H \right) \\ &= (\mathbf{I} - \mathbf{H}_N \mathbf{H}_N^\dagger) \\ \mathbf{B}_N^H &= \mathbf{B}_N \end{aligned}$$

Property 4:

$$\det(\mathbf{B}_N) = 0 \quad \forall N$$

Proof:

Since \mathbf{B}_N is idempotent matrix (Property 1), it should be singular, because, if it is nonsingular, then the only solution is identity matrix; but \mathbf{B}_N can be different from identity.

$$\mathbf{B}_N \mathbf{B}_N = \mathbf{B}_N$$

If \mathbf{B}_N is nonsingular,

$$\begin{aligned}\mathbf{B}_N^{-1}\mathbf{B}_N\mathbf{B}_N &= \mathbf{B}_N^{-1}\mathbf{B}_N \\ \Rightarrow \mathbf{B}_N &= \mathbf{I}\end{aligned}$$

So \mathbf{B}_N must be singular matrix.

Property 5:

For $L=1$

$$\text{rank}(\mathbf{B}_N) = 1 \quad \forall N$$

Proof:

From Property 2

$$\tilde{\mathbf{B}}_N = \mathbf{B}_{N-1}\tilde{\mathbf{B}}_N$$

for $N=2$;

$$\tilde{\mathbf{B}}_2 = \mathbf{B}_1\tilde{\mathbf{B}}_2$$

where \mathbf{B}_1 is 2×2 matrix and from Property 4 $\det(\mathbf{B}_1)=0$. So rank of this matrix is equal to 1. From the multiplication relation of \mathbf{B}_1 and $\tilde{\mathbf{B}}_2$, rank of $\tilde{\mathbf{B}}_2$ is also 1. This can be seen by Sylvester's inequality as,

$$\begin{aligned}\mathbf{A}_{m \times k}\mathbf{B}_{k \times n} &= \mathbf{C}_{m \times n} \\ \Rightarrow \text{rank}(\mathbf{A}) + \text{rank}(\mathbf{B}) - k &\leq \text{rank}(\mathbf{C}) \leq \min(\text{rank}(\mathbf{A}), \text{rank}(\mathbf{B}))\end{aligned}$$

In our case $m=n=k=2$, $\mathbf{A} = \mathbf{B}_1$ and $\mathbf{B} = \mathbf{C} = \tilde{\mathbf{B}}_2$. Then

$$1 + \text{rank}(\tilde{\mathbf{B}}) - 2 \leq \text{rank}(\tilde{\mathbf{B}}_2) \leq \min(1, \text{rank}(\tilde{\mathbf{B}}_2))$$

$\tilde{\mathbf{B}}_2$ is 2×2 matrix, so its rank should be 1 or 2.

$$\begin{aligned}\text{if } \text{rank}(\tilde{\mathbf{B}}_2) &= 2; \\ 1 + 2 - 2 &\leq 2 \leq \min(1, 2) \\ 1 &\leq 2 \leq 1 \\ \Rightarrow \text{rank}(\tilde{\mathbf{B}}_2) &\neq 2\end{aligned}$$

$$\begin{aligned}
& \text{if } \text{rank}(\tilde{\mathbf{B}}_2) = 1; \\
& 1+1-2 \leq 1 \leq \min(1,1) \\
& 0 \leq 1 \leq 1 \\
& \Rightarrow \text{rank}(\tilde{\mathbf{B}}_2) = 1
\end{aligned}$$

From the relation between $\tilde{\mathbf{B}}_2$ and \mathbf{B}_2 in Property 2, it can be seen that rank of \mathbf{B}_2 is also equal to 1. If this iterative procedure continues rank of \mathbf{B}_N is found to be 1 for all values of N .

Property 6:

For $L=1$,

$$\tilde{\mathbf{B}}_N = \alpha_N \mathbf{B}_{N-1} \quad \forall N$$

where α_N is scalar

Proof:

From Property 5 the matrix $\tilde{\mathbf{B}}_N$ and \mathbf{B}_{N-1} can be rewritten as,

$$\begin{aligned}
\mathbf{B}_{N-1} &= [\beta_0 \mathbf{b}_{N-1} \quad \beta_1 \mathbf{b}_{N-1} \quad \cdots \quad \beta_{N-1} \mathbf{b}_{N-1}] = \mathbf{b}_{N-1} [\beta_0 \quad \beta_1 \quad \cdots \quad \beta_{N-1}]_{1 \times N} \\
\tilde{\mathbf{B}}_N &= [\gamma_0 \tilde{\mathbf{b}}_N \quad \gamma_1 \tilde{\mathbf{b}}_N \quad \cdots \quad \gamma_{N-1} \tilde{\mathbf{b}}_N] = \tilde{\mathbf{b}}_N [\gamma_0 \quad \gamma_1 \quad \cdots \quad \gamma_{N-1}]_{1 \times N}
\end{aligned} \tag{A.25}$$

\mathbf{b}_{N-1} and $\tilde{\mathbf{b}}_N$ are $N \times 1$ basis vectors for \mathbf{B}_{N-1} and $\tilde{\mathbf{B}}_N$ respectively. Let,

$$[\beta_0 \quad \beta_1 \quad \cdots \quad \beta_{N-1}]_{1 \times N} = \bar{\beta}$$

$$[\gamma_0 \quad \gamma_1 \quad \cdots \quad \gamma_{N-1}]_{1 \times N} = \bar{\gamma}$$

The relationship between \mathbf{b}_{N-1} and $\tilde{\mathbf{b}}_N$ can be obtained by using Property 2 such as,

$$\begin{aligned}
\mathbf{B}_{N-1} \tilde{\mathbf{B}}_N &= \tilde{\mathbf{B}}_N \\
\mathbf{b}_{N-1} \bar{\beta} \tilde{\mathbf{b}}_N \bar{\gamma} &= \tilde{\mathbf{b}}_N \bar{\gamma} \\
\theta \mathbf{b}_{N-1} \bar{\gamma} &= \tilde{\mathbf{b}}_N \bar{\gamma}
\end{aligned} \tag{A.26}$$

where,

$$\theta_{1 \times 1} = \bar{\beta} \tilde{\mathbf{b}}_N \tag{A.27}$$

Multiply both sides of (A.26) with $\bar{\gamma}^H$ by right.

$$\begin{aligned}
\theta \mathbf{b}_{N-1} \|\bar{\gamma}\|^2 &= \tilde{\mathbf{b}}_N \|\bar{\gamma}\|^2 \\
\theta \mathbf{b}_{N-1} &= \tilde{\mathbf{b}}_N
\end{aligned} \tag{A.28}$$

Since matrix $\tilde{\mathbf{B}}_N$ is hermitian (Property 3), then the following equations can be written by the help of Property 2,

$$\begin{aligned}
\mathbf{B}_{N-1} \tilde{\mathbf{B}}_N^H &= \tilde{\mathbf{B}}_N \\
\mathbf{b}_{N-1} \bar{\beta} \bar{\gamma}^H \tilde{\mathbf{b}}_N^H &= \tilde{\mathbf{b}}_N \bar{\gamma} \\
\varphi \mathbf{b}_{N-1} \tilde{\mathbf{b}}_N^H &= \tilde{\mathbf{b}}_N \bar{\gamma}
\end{aligned} \tag{A.29}$$

where,

$$\varphi_{1 \times 1} = \bar{\beta} \bar{\gamma}^H$$

Substitute equation (A.28) into equation (A.29)

$$\varphi \theta^* \mathbf{b}_{N-1} \mathbf{b}_{N-1}^H = \theta \mathbf{b}_{N-1} \bar{\gamma} \tag{A.30}$$

Multiply both sides of (A.30) with \mathbf{b}_{N-1}^H by left.

$$\begin{aligned}
\varphi \theta^* \|\mathbf{b}_{N-1}\|^2 \mathbf{b}_{N-1}^H &= \theta \|\mathbf{b}_{N-1}\|^2 \bar{\gamma} \\
\varphi \theta^* \mathbf{b}_{N-1}^H &= \theta \bar{\gamma} \\
\mathbf{b}_{N-1}^H &= \frac{\theta}{\varphi \theta^*} \bar{\gamma}
\end{aligned} \tag{A.31}$$

From Property 1 and 3,

$$\begin{aligned}
\mathbf{B}_{N-1} \mathbf{B}_{N-1}^H &= \mathbf{B}_{N-1} \\
\mathbf{b}_{N-1} \bar{\beta} \bar{\beta}^H \mathbf{b}_{N-1}^H &= \mathbf{b}_{N-1} \bar{\beta} \\
\mathbf{b}_{N-1} \|\bar{\beta}\|^2 \mathbf{b}_{N-1}^H &= \mathbf{b}_{N-1} \bar{\beta}
\end{aligned} \tag{A.32}$$

Multiply both sides of (A.32) with \mathbf{b}_{N-1}^H by left

$$\begin{aligned}
\|\bar{\beta}\|^2 \|\mathbf{b}_{N-1}\|^2 \mathbf{b}_{N-1}^H &= \|\mathbf{b}_{N-1}\|^2 \bar{\beta} \\
\mathbf{b}_{N-1}^H &= \frac{1}{\|\bar{\beta}\|^2} \bar{\beta}
\end{aligned} \tag{A.33}$$

Combining (A.24), (A.25), (A.27), (A.31) and (A.33), proves the property.

$$\begin{aligned}
\tilde{\mathbf{B}}_N &= \theta \mathbf{b}_{N-1} \frac{\varphi \theta^*}{\theta} \mathbf{b}_{N-1}^H \\
&= \varphi \theta^* \mathbf{b}_{N-1} \mathbf{b}_{N-1}^H \\
&= \varphi \theta^* \mathbf{b}_{N-1} \frac{1}{\|\bar{\beta}\|^2} \bar{\beta} \\
&= \frac{\varphi \theta^*}{\|\bar{\beta}\|^2} \mathbf{B}_{N-1} \\
\tilde{\mathbf{B}}_N &= \alpha_N \mathbf{B}_{N-1}
\end{aligned} \tag{A.34}$$

Property 7:

For $L=1$,

$$\|\mathbf{B}_N\| = \sum_{i=1}^{N+L} \sum_{j=1}^{N+L} |b_{i,j}|^2 = 1 \quad \forall N$$

Proof:

By using equations (A.27) and (A.28), the followings can be written,

$$\begin{aligned}
\theta_{1 \times 1} &= \bar{\beta} \theta \mathbf{b}_{N-1} \\
\bar{\beta} \mathbf{b}_{N-1} &= 1
\end{aligned} \tag{A.35}$$

If we multiply both sides of equation (A.33) with \mathbf{b}_{N-1} by right, the following one is obtained,

$$\|\mathbf{b}_{N-1}\|^2 = \frac{1}{\|\bar{\beta}\|^2} \bar{\beta} \mathbf{b}_{N-1} \tag{A.36}$$

If we substitute equation (A.35) into equation (A.36), the following equation is obtained,

$$\|\mathbf{b}_{N-1}\|^2 \|\bar{\beta}\|^2 = 1 \tag{A.37}$$

From equation (A.25), the norm of \mathbf{B}_{N-1} can be written as,

$$\begin{aligned}
\|\mathbf{B}_{N-1}\|^2 &= |\beta_0|^2 \|\mathbf{b}_{N-1}\|^2 + |\beta_1|^2 \|\mathbf{b}_{N-1}\|^2 + \cdots + |\beta_{N-1}|^2 \|\mathbf{b}_{N-1}\|^2 \\
&= \|\mathbf{b}_{N-1}\|^2 \sum_{i=1}^N |\beta_i|^2
\end{aligned}$$

$$\|\mathbf{B}_{N-1}\|^2 = \|\mathbf{b}_{N-1}\|^2 \|\bar{\beta}\|^2 \quad (\text{A.38})$$

Substitute equation (A.37) into equation (A.38),

$$\|\mathbf{B}_{N-1}\|^2 = 1 \quad (\text{A.39})$$

This equation is valid for all value of N .

A.ii Iterative Procedure

By using these properties LSE for first order channel filter can be found iteratively. From Property 7,

$$\|\mathbf{B}_N\|^2 = 1$$

By using structure in (A.S2), this equation can be rewritten as,

$$\|\tilde{\mathbf{B}}_N\|^2 + 2\|\bar{\mathbf{b}}_N\|^2 + |b_N|^2 = 1 \quad (\text{A.40})$$

Since \mathbf{B}_N is hermitian (Property 3) b_N is real. Property 1 helps us to rewrite the second and third terms of right hand side of (A.40) as a function of b_N only.

$$\begin{aligned} \mathbf{B}_N^2 &= \mathbf{B}_N \\ \begin{bmatrix} \tilde{\mathbf{B}}_N & \bar{\mathbf{b}}_N \\ \bar{\mathbf{b}}_N^H & b_N \end{bmatrix} \begin{bmatrix} \tilde{\mathbf{B}}_N & \bar{\mathbf{b}}_N \\ \bar{\mathbf{b}}_N^H & b_N \end{bmatrix} &= \begin{bmatrix} \tilde{\mathbf{B}}_N & \bar{\mathbf{b}}_N \\ \bar{\mathbf{b}}_N^H & b_N \end{bmatrix} \\ \Rightarrow \begin{bmatrix} \bar{\mathbf{b}}_N^H & b_N \end{bmatrix} \begin{bmatrix} \bar{\mathbf{b}}_N \\ b_N \end{bmatrix} &= b_N \\ \|\bar{\mathbf{b}}_N\|^2 + b_N^2 &= b_N \\ 2\|\bar{\mathbf{b}}_N\|^2 + b_N^2 &= 2b_N - b_N^2 \end{aligned} \quad (\text{A.41})$$

So equation (A.41) becomes,

$$\|\tilde{\mathbf{B}}_N\|^2 + 2b_N - b_N^2 = 1 \quad (\text{A.42})$$

By using Property 6 and 7, (A.42) can be rewritten as,

$$|\alpha_N|^2 + 2b_N - b_N^2 = 1 \quad (\text{A.43})$$

From Property 6 and the definition of $\tilde{\mathbf{B}}_N$ in structure (A.S2), the first row and first column element of matrices \mathbf{B}_N and \mathbf{B}_{N-1} is related as,

$$\begin{aligned}\mathbf{B}_N(1,1) &= \alpha_N \mathbf{B}_{N-1}(1,1) \\ \alpha_N &= \frac{\mathbf{B}_N(1,1)}{\mathbf{B}_{N-1}(1,1)}\end{aligned}\quad (\text{A.44})$$

Since matrix \mathbf{B}_N is hermitian (Property 3), both $\mathbf{B}_N(1,1)$ and $\mathbf{B}_{N-1}(1,1)$ are real. So α_N is also real. By using these facts (A.43) can be written as,

$$\frac{[\mathbf{B}_N(1,1)]^2}{[\mathbf{B}_{N-1}(1,1)]^2} + 2b_N - b_N^2 = 1 \quad (\text{A.45})$$

Since channel filter order is 1, the channel must be either minimum phase or maximum phase. For minimum phase channel, optimum delay for LS inverse filter is 0, and for maximum phase channel, optimum delay is N. So LSE can be either first element or last element of diagonal of matrix \mathbf{B}_N , depending on channel characteristic (min or max phase).

Let a be the root of channel filter. The minimum or maximum phase depends on magnitude of a .

$$|a| < 1 \rightarrow \text{minimum phase} \rightarrow \text{LSE} = \mathbf{B}_N(1,1)$$

$$|a| > 1 \rightarrow \text{maximum phase} \rightarrow \text{LSE} = b_N = \mathbf{B}_N(N+1, N+1)$$

But these relations can also be written as,

$$1/|a| < 1 \rightarrow \text{maximum phase}$$

$$1/|a| > 1 \rightarrow \text{minimum phase}$$

So the first and last diagonal element of matrix \mathbf{B} can be written as,

$$\begin{aligned}\mathbf{B}_N(1,1) &= f(|a|) \\ b_N = \mathbf{B}_N(N+1, N+1) &= f(|a|^{-1})\end{aligned}\quad (\text{A.46})$$

and

$$\begin{aligned}\mathbf{B}_{N-1}(1,1) &= g(|a|) \\ \mathbf{B}_{N-1}(N, N) &= g(|a|^{-1})\end{aligned}\quad (\text{A.47})$$

So (A.45) can be rewritten as,

$$\frac{f^2(|a|)}{g^2(|a|)} + 2f(|a|^{-1}) - f^2(|a|^{-1}) = 1 \quad (\text{A.48})$$

If $|a|$ is replaced with $1/|a|$, then equation (A.48) becomes,

$$\frac{f^2(|a|^{-1})}{g^2(|a|^{-1})} + 2f(|a|) - f^2(|a|) = 1 \quad (\text{A.49})$$

By using (A.48) and (A.49), LSE can be found as follows:

Substitute (A.48) into (A.49),

$$\begin{aligned} f^2(|a|) \left[\frac{1}{g^2(|a|)} - g^2(|a|^{-1}) \right] + 2f(|a|) \left[g^2(|a|^{-1}) - g(|a|^{-1}) \right] \\ + 2g(|a|^{-1}) - g^2(|a|^{-1}) - 1 = 0 \end{aligned} \quad (\text{A.50})$$

Equation (A.50) is simply a second order equation and it can be solved easily as,

$$\begin{aligned} f_1(|a|) &= \frac{\left[1 - g(|a|^{-1}) \right] \left[g(|a|^{-1}) - \frac{1}{g(|a|)} \right]}{\left[\frac{1}{g(|a|)} - g(|a|^{-1}) \right] \left[\frac{1}{g(|a|)} + g(|a|^{-1}) \right]} = -\frac{1 - g(|a|^{-1})}{\frac{1}{g(|a|)} + g(|a|^{-1})} < 0 \\ f_2(|a|) &= \frac{\left[1 - g(|a|^{-1}) \right] \left[g(|a|^{-1}) + \frac{1}{g(|a|)} \right]}{\left[\frac{1}{g(|a|)} - g(|a|^{-1}) \right] \left[\frac{1}{g(|a|)} + g(|a|^{-1}) \right]} = \frac{1 - g(|a|^{-1})}{\frac{1}{g(|a|)} - g(|a|^{-1})} > 0 \end{aligned}$$

Since LSE should be positive, the second one is the correct results,

$$f(|a|) = \frac{1 - g(|a|^{-1})}{\frac{1}{g(|a|)} - g(|a|^{-1})} \quad (\text{A.51})$$

Note that since $\|\mathbf{B}_N\|$ is equal to 1, then the entries of \mathbf{B}_N should be smaller than 1. So, iterative LSE formulation for $L=1$, can be written as,

$$\begin{aligned}
LSE_N^{(1)} &= \frac{1 - LSE_{N-1}^{(2)}}{\frac{1}{LSE_{N-1}^{(1)}} - LSE_{N-1}^{(2)}} \\
LSE_N^{(2)} &= \frac{1 - LSE_{N-1}^{(1)}}{\frac{1}{LSE_{N-1}^{(2)}} - LSE_{N-1}^{(1)}}
\end{aligned} \tag{A.52}$$

where,

$$\begin{aligned}
LSE_N^{(1)} &= f(|a|) \\
LSE_N^{(2)} &= f(|a|^{-1}) \\
LSE_{N-1}^{(1)} &= g(|a|) \\
LSE_{N-1}^{(2)} &= g(|a|^{-1})
\end{aligned}$$

The final LSE formula for $L=1$, and inverse filter length N is:

$$LSE_N = \min(LSE_N^{(1)}, LSE_N^{(2)}) \tag{A.53}$$

Initialization:

$$\begin{aligned}
LSE_1^{(1)} &= \mathbf{B}_1(1,1) \\
LSE_1^{(2)} &= \mathbf{B}_1(2,2) \\
\mathbf{B}_1 &= \mathbf{I} - \mathbf{H}_1 (\mathbf{H}_1^H \mathbf{H}_1)^{-1} \mathbf{H}_1^H \\
\mathbf{B}_1 &= \begin{bmatrix} 1 & 0 \\ 0 & 1 \end{bmatrix} - \begin{bmatrix} 1 \\ a \end{bmatrix} \left(\begin{bmatrix} 1 & a^* \\ 1 & a \end{bmatrix} \right)^{-1} \begin{bmatrix} 1 & a^* \end{bmatrix} \\
\mathbf{B}_1 &= \frac{1}{1+|a|^2} \begin{bmatrix} |a|^2 & -a^* \\ -a & 1 \end{bmatrix} \\
LSE_1^{(1)} &= \frac{|a|^2}{1+|a|^2} \\
LSE_1^{(2)} &= \frac{1}{1+|a|^2}
\end{aligned} \tag{A.54}$$

The general LSE as a function of channel root a and inverse filter length N can be found by induction method:

From equations (A.52) and (A.54),

$$\begin{aligned}
LSE_2^{(1)} &= \frac{1 - \frac{1}{1+|a|^2}}{\frac{1+|a|^2}{|a|^2} - \frac{1}{1+|a|^2}} = \frac{1+|a|^2-1}{1+|a|^2} \frac{(1+|a|^2)|a|^2}{(1+|a|^2)^2 - |a|^2} \\
&= \frac{|a|^2|a|^2}{1+2|a|^2+|a|^4-|a|^2} = \frac{|a|^4}{1+|a|^2+|a|^4} \\
LSE_2^{(2)} &= \frac{1 - \frac{|a|^2}{1+|a|^2}}{(1+|a|^2) - \frac{|a|^2}{1+|a|^2}} = \frac{1+|a|^2-|a|^2}{1+|a|^2} \frac{1+|a|^2}{(1+|a|^2)^2 - |a|^2} \\
&= \frac{1}{1+2|a|^2+|a|^4-|a|^2} = \frac{1}{1+|a|^2+|a|^4}
\end{aligned} \tag{A.55}$$

And let us assume that,

$$\begin{aligned}
LSE_{N-1}^{(1)} &= \frac{|a|^{2(N-1)}}{1+|a|^2+\dots+|a|^{2(N-1)}} \\
LSE_{N-1}^{(2)} &= \frac{1}{1+|a|^2+\dots+|a|^{2(N-1)}}
\end{aligned} \tag{A.56}$$

then we should show that,

$$\begin{aligned}
LSE_N^{(1)} &= \frac{|a|^{2N}}{1+|a|^2+\dots+|a|^{2N}} \\
LSE_N^{(2)} &= \frac{1}{1+|a|^2+\dots+|a|^{2N}}
\end{aligned}$$

To do this use equation (A.52) and (A.56),

$$\begin{aligned}
LSE_N^{(1)} &= \frac{1 - \frac{1}{1 + |a|^2 + \dots + |a|^{2(N-1)}}}{\frac{1 + |a|^2 + \dots + |a|^{2(N-1)}}{|a|^{2(N-1)}}} = \frac{|a|^{2N}}{1 + |a|^2 + \dots + |a|^{2N}} \\
LSE_N^{(2)} &= \frac{\frac{1}{|a|^{2N}}}{1 + \frac{1}{|a|^2} + \dots + \frac{1}{|a|^{2N}}} = \frac{1}{|a|^{2N}} \frac{|a|^{2N}}{|a|^{2N} + |a|^{2(N-1)} + \dots + |a|^2 + 1} \\
&= \frac{1}{|a|^{2N} + |a|^{2(N-1)} + \dots + |a|^2 + 1}
\end{aligned}$$

So the general LSE function of first order channel filter and inverse filter with length N is:

$$LSE_N = \min \left[\frac{|a|^{2N}}{1 + |a|^2 + \dots + |a|^{2N}}, \frac{1}{1 + |a|^2 + \dots + |a|^{2N}} \right] \quad (\text{A.57})$$

APPENDIX B

For the channel filter with order two the Toeplitz channel matrix is modeled as,

$$\mathbf{H}_2 = \begin{bmatrix} 1 & 0 & \cdots & 0 \\ a & 1 & \cdots & 0 \\ b & a & \cdots & \vdots \\ 0 & b & \cdots & 1 \\ \vdots & \vdots & \cdots & a \\ 0 & 0 & \cdots & b \end{bmatrix}_{(N+2) \times N}$$

where a and b is the channel coefficients. The channel zeros, z_1 and z_2 , are related with these coefficients as,

$$\begin{aligned} a &= -(z_1 + z_2) \\ b &= z_1 z_2 \end{aligned}$$

Then LSE formulas for $N=2$ and $N=3$ are found as,

For $N=2$,

$$LSE_{k=0} = \left[1 - \frac{P}{K} \right]^2 + \left| -a \frac{P}{K} + \frac{a+a^*b}{K} \right|^2 + \left| -b \frac{P}{K} + a \frac{a+a^*b}{K} \right|^2 + \frac{|a+a^*b|^2}{(K)^2} |b|^2$$

$$\begin{aligned} LSE_{k=1} &= \left| -a \frac{P}{K} + \frac{a+a^*b}{K} \right|^2 + \left\{ 1 - \left[a \frac{P}{K} - \frac{a+a^*b}{K} \right] a^* + a \frac{a^*+b^*a}{K} - \frac{P}{K} \right\}^2 \\ &+ \left| \left[a \frac{P}{K} - \frac{a+a^*b}{K} \right] b^* - \left[-a \frac{a^*+b^*a}{K} + \frac{P}{K} \right] a^* \right|^2 + \left| -ab^* \frac{a^*+b^*a}{K} + b^* \frac{P}{K} \right|^2 \end{aligned}$$

$$\begin{aligned}
LSE_{k=2} &= \left| -b \frac{P}{K} + a \frac{a+a^*b}{K} \right|^2 + \left\{ 1 - \left[b \frac{P}{K} - a \frac{a+a^*b}{K} \right] b^* - \left[-b \frac{a^*+b^*a}{K} + a \frac{P}{K} \right] a^* \right\}^2 \\
&\quad + \left| - \left[b \frac{P}{K} - a \frac{a+a^*b}{K} \right] a^* + b \frac{a^*+b^*a}{K} - a \frac{P}{K} \right|^2 + \left| b \right|^2 \left| \frac{a+a^*b}{K} - a^*b \frac{P}{K} \right|^2 \\
LSE_{k=3} &= \frac{|a^*+b^*a|^2}{K^2} |b|^2 + \left| a^*b \frac{a+a^*b}{K} - b \frac{P}{K} \right|^2 + \left| b \right|^2 \left| \frac{a+a^*b}{K} - a^*b \frac{P}{K} \right|^2 + \left[1 - b \frac{P}{K} b^* \right]^2
\end{aligned}$$

where,

$$\begin{aligned}
K &= 1 + |a|^2 + 2|b|^2 + |a|^4 + |a|^2|b|^2 + |b|^4 - (a^*)^2 b - b^* a^2 \\
P &= 1 + |a|^2 + |b|^2
\end{aligned}$$

For N=3,

$$\begin{aligned}
LSE_{k=0} &= \left[1 - \frac{K}{R} \right]^2 + \left| -a^* \frac{K}{R} + \frac{S}{R} \right|^2 + \left| -b \frac{K}{R} + a \frac{S^*}{R} - \frac{M}{R} \right|^2 + \left| b \frac{S^*}{R} - a \frac{M}{R} \right|^2 + \left| b \frac{M}{R} \right|^2 \\
LSE_{k=1} &= \left\{ 1 - \left[a \frac{K}{R} - \frac{S^*}{R} \right] a^* + a \frac{S}{R} - \frac{V}{R} \right\}^2 + \left| - \left[b \frac{K}{R} - a \frac{S^*}{R} + \frac{M}{R} \right] a^* + b \frac{S}{R} - a \frac{V}{R} + \frac{S^*}{R} \right|^2 \\
&\quad + \left| -a^* \frac{K}{R} + \frac{S}{R} \right|^2 + \left| - \left[-b \frac{S^*}{R} + a \frac{M}{R} \right] a^* - b \frac{V}{R} + a \frac{S^*}{R} \right|^2 + \left| -a^*b \frac{M}{R} + b \frac{S^*}{R} \right|^2 \\
LSE_{k=2} &= \left| -b \frac{K}{R} + a \frac{S^*}{R} - \frac{M}{R} \right|^2 + \left| - \left[b \frac{K}{R} - a \frac{S^*}{R} + \frac{M}{R} \right] a^* + b \frac{S}{R} - a \frac{V}{R} + \frac{S^*}{R} \right|^2 \\
&\quad + \left\{ 1 - \left[b \frac{K}{R} - a \frac{S^*}{R} + \frac{M}{R} \right] b^* - \left[-b \frac{S}{R} + a \frac{V}{R} - \frac{S^*}{R} \right] a^* - b \frac{M^*}{R} + a \frac{S}{R} - \frac{K}{R} \right\}^2 \\
&\quad + \left| - \left[-b \frac{S}{R} + a \frac{V}{R} - \frac{S^*}{R} \right] b^* - \left[b \frac{M^*}{R} - a \frac{S}{R} + \frac{K}{R} \right] a^* \right|^2 + \left| b \right|^2 \left| \frac{M^*}{R} - ab^* \frac{S}{R} + b^* \frac{K}{R} \right|^2 \\
LSE_{k=3} &= \left| b \frac{S^*}{R} - a \frac{M}{R} \right|^2 + \left| - \left[-a \frac{S}{R} + \frac{V}{R} \right] b^* - \left[a \frac{M^*}{R} - \frac{S}{R} \right] a^* \right|^2 \\
&\quad + \left| - \left[-b \frac{S}{R} + a \frac{V}{R} - \frac{S^*}{R} \right] b^* - \left[b \frac{M^*}{R} - a \frac{S}{R} + \frac{K}{R} \right] a^* \right|^2
\end{aligned}$$

$$\begin{aligned}
& + \left\{ 1 - \left[b \frac{V}{R} - a \frac{S^*}{R} \right] b^* - \left[-b \frac{S}{R} + a \frac{K}{R} \right] a^* \right\}^2 + \left| -|b|^2 \frac{S}{R} + ab^* \frac{K}{R} \right|^2 \\
LSE_{k=4} & = |b|^2 \frac{|M^2|}{(R)^2} + \left| -a^* b \frac{M}{R} + b \frac{S^*}{R} \right|^2 + \left| -|b|^2 \frac{M}{R} + a^* b \frac{S^*}{R} - b \frac{K}{R} \right|^2 \\
& + \left| -|b|^2 \frac{S}{R} + ab^* \frac{K}{R} \right|^2 + \left[1 - |b|^2 \frac{K}{R} \right]^2
\end{aligned}$$

where,

$$K = 1 + |a|^2 + 2|b|^2 + |a|^4 + |a|^2|b|^2 + |b|^4 - (a^*)^2 b - b^* a^2$$

$$\begin{aligned}
R & = 1 - 2a^* a^3 b^* - 2(a^*)^3 ab + |a|^2 + 2|b|^2 + |a|^4 + 2|b|^4 - (a^*)^2 b - b^* a^2 - b^* b^2 (a^*)^2 \\
& - (b^*)^2 ba^2 + 5|a|^2|b|^2 + |a|^4|b|^2 + |a|^2|b|^4 + |a|^6 + |b|^6
\end{aligned}$$

$$S = a^* + (a^*)^2 a + b^* a^2 a^* + (b^*)^2 ab$$

$$M = a^2 + |a|^2 b + (a^*)^2 b^2 - b - b^* b^2$$

$$V = 1 + 2|a|^2 + |b|^2 + |a|^4 + 2|a|^2|b|^2 + |b|^4$$